AD_____

CONTRACT NO.

DAMD 17-93-C-3036

TITLE:

The Effects of Ricin on the Heart and Coronary Arteries

PRINCIPAL INVESTIGATOR:

Casey P. Robinson, Ph.D.

CONTRACTING ORGANIZATION:

University of Oklahoma, HSC
College of Pharmacy
1110 N. Stonewall, Oklahoma City, OK 73190

REPORT DATE:

1 Feb 95

TYPE OF REPORT:

Final

PREPARED FOR: U.S. Army Medical Research and Materiel Command
Fort Detrick
Frederick, Maryland 21702-5012

DISTRIBUTION STATEMENT: Approved for public release;
distribution unlimited

REPORT DOCUMENTATION PAGE

Form Approved
OMB No. 0704-0188

1. AGENCY USE ONLY (Leave blank)	2. REPORT DATE	3. REPORT TYPE AND DATES COVERED
	1 Feb 95	Final

4. TITLE AND SUBTITLE
The Effects of Ricin on the Heart and Coronary Arteries

5. FUNDING NUMBERS
DAMD 17-93-C-3036

6. AUTHOR(S)
Casey P. Robinson, C.-H. Hsu, Lin Zhang, and Lianmin Ma

7. PERFORMING ORGANIZATION NAME(S) AND ADDRESS(ES)
University of Oklahoma, HSC
College of Pharmacy
1110 N. Stonewall
Oklahoma City, OK 73190

8. PERFORMING ORGANIZATION REPORT NUMBER

9. SPONSORING/MONITORING AGENCY NAME(S) AND ADDRESS(ES)
U.S. Army Medical Research and Materiel Command
Ft Detrick, MD 21702-5012

10. SPONSORING/MONITORING AGENCY REPORT NUMBER

11. SUPPLEMENTARY NOTES

12a. DISTRIBUTION/AVAILABILITY STATEMENT
Approved for public release;
distribution unlimited

12b. DISTRIBUTION CODE

13. ABSTRACT *(Maximum 200 words)*

14. SUBJECT TERMS
Ricin, effects on rabbit heart; Ricin, effects on coronary arteries; Ricin, effects on calcium flux; Ricin, effects on signal transduction

15. NUMBER OF PAGES

16. PRICE CODE

17. SECURITY CLASSIFICATION OF REPORT	18. SECURITY CLASSIFICATION OF THIS PAGE	19. SECURITY CLASSIFICATION OF ABSTRACT	20. LIMITATION OF ABSTRACT
Unclassified	Unclassified	Unclassified	UL

Effects of ricin on rabbit heart, coronary arteries, and distribution of blood flow to various organs and tissues were investigated. Ricin increased cardiac output, and blood flow to most organs/tissues. Ricin was given 0.22 μg/kg and 48 hours later changes were determined. Ricin decreased sensitivities of coronary arteries to 5-HT- and histamine contractions, increased sensitivity to NE relaxations, increased maximal contractions, but did not alter ACh-induced relaxations. Ricin increased basal IP_3 levels, but histamine stimulated IP_3 levels and basal hydrolysis rates from IP_2 to IP_1 were depressed. In myocardium, ricin depressed cAMP and cGMP accumulation but not phosphoinositide hydrolysis. Heart rate, bipolar electrocardiograms, action potentials and *beta* adrenergic receptor number or affinity were not altered. Ricin reduced left ventricular compliance and decreased left ventricular developed pressure per balloon volume. Ricin depressed calcium influx into papillary muscle and microsomes, increased intracellular calcium concentration and depressed NE-stimulated calcium efflux from papillary muscle. Thus, ricin increased cardiac output and increased blood flow to most tissues and reduced left ventricular compliance. It altered responses of coronary arteries to vasoactive agents, altered intracellular concentrations of cyclic nucleotides and inositol phosphate, and altered calcium handling in isolated tissues and organelles.

FOREWORD

Opinions, interpretations, conclusions and recommendations are those of the author and are not necessarily endorsed by the US Army.

____ Where copyrighted material is quoted, permission has been obtained to use such material.

____ Where material from documents designated for limited distribution is quoted, permission has been obtained to use the material.

____ Citations of commercial organizations and trade names in this report do not constitute an official Department of Army endorsement or approval of the products or services of these organizations.

__X__ In conducting research using animals, the investigator(s) adhered to the "Guide for the Care and Use of Laboratory Animals," prepared by the Committee on Care and Use of Laboratory Animals of the Institute of Laboratory Resources, National Research Council (NIH Publication No. 86-23, Revised 1985).

____ For the protection of human subjects, the investigator(s) adhered to policies of applicable Federal Law 45 CFR 46.

____ In conducting research utilizing recombinant DNA technology, the investigator(s) adhered to current guidelines promulgated by the National Institutes of Health.

____ In the conduct of research utilizing recombinant DNA, the investigator(s) adhered to the NIH Guidelines for Research Involving Recombinant DNA Molecules.

____ In the conduct of research involving hazardous organisms, the investigator(s) adhered to the CDC-NIH Guide for Biosafety in Microbiological and Biomedical Laboratories.

Casey Robinson, Ph.D. 1 Feb 95

PI Signature Date

AD_____

COOPERATIVE AGREEMENT NO:

DAMD 17-93-C-3036

TITLE:

Effects of Ricin on the Rabbit's Heart and Coronary Arteries.

PRINCIPAL INVESTIGATOR:

Casey P. Robinson, Ph.D.

CONTRACTING ORGANIZATION:

University of Oklahoma, HSC
College of Pharmacy
1110 N. Stonewall, Oklahoma City, OK 73190

REPORT DATE:

1 Feb 95

TYPE OF REPORT:

Final

PREPARED FOR: U.S. Army Medical Research and Materiel Command
Fort Detrick
Frederick, Maryland 21702-5012

TABLE OF CONTENTS

I. Introduction.....1

II. Methods.....31

III. Results 57

IV. Discussion 139

V. Conclusions 160

VI. Acknowledgments 163

VII. References 165

I. INTRODUCTION

Ricin, a toxic protein component of the castor bean (*Ricinus communis*), is the fifth most poisonous substance known (Middlebrook, 1989). It has wide-ranging biological effects on higher organisms. Ricin exists in slightly different forms in beans of different origin. Ricin, like all other plant toxins, is a glycoprotein. Ricin consists of two polypeptide chains, A and B, with a total molecular weight of about 62,000 Da. The toxic effect resides in the A chain. The A chain alone is non-toxic to an intact cell, because it can not get into the cell. The A-chain has enzymatic activity and the B-chain has lectin-like properties and binds the toxin to cell surface receptors containing terminal galactose residues (Nicolson and Blaustein, 1972). Besides the role in binding, the B-chain is thought to facilitate the entrance of the A-chain into the cell cytoplasm. This appears to be an obligatory step in the intoxication of the cell (Olsnes *et al.*, 1974, and 1976). In the entry process the disulfide bond is broken and the free A-chain blocks protein synthesis by interaction with the 60S ribosomal subunit (Olsnes *et al.*, 1976). The extreme toxicity of ricin is due to the fact that the liberated A-chain is an enzyme and a single A-chain in the cell may be sufficient to kill the cell (Eiklid *et al.*, 1980). Even though ricin is toxic to all nucleated mammalian cells tested (Olsnes and Pihl, 1982), it appears that it is more toxic to certain cells (Fodstad and Pihl, 1978).

Ricin has been subjected to detailed studies using various biochemical and morphological approaches (Olsnes *et al.*, 1982, 1983, 1985, 1987, Gonatas *et al.*, 1975; Hickey *et al.*, 1983; van Deurs *et al.*, 1985, 1986, 1987, 1988; Sandvig *et al.*, 1987). There are several reasons for the increased interest in ricin. One is, ricin serves as a valuable tool for elucidating intracellular pathways of internalized ligands and membrane molecules in general, and also represents, together with several other toxins, an interesting model for studying post-translational translocation of proteins across membrane (Olsnes *et al.*, 1987). Also, ricin is frequently used in the construction of immunotoxins designed to

kill specific target cells, such as cancer cells with the purpose of developing potential anticancer drugs (Vitetta *et al*, 1983; 1984; Pastan *et al.*, 1986). Also, because of ricin's toxicity, solubility and stability in water, and its easy portability, it could readily be used in chemical warfare. It is, therefore, important that information on ricin's toxicity should be obtained.

A. *Ricinus Communis* and the Early Findings with Ricin.

The earliest record of the castor bean being used as a medicine was in Ebers Papyrus in 1550 B.C. which described its laxative properties and the use of oil from castor beans to treat skin irritation and stimulate hair growth (Anderson, 1977). Similar applications can also be found in the medicinal history of China and India. At present, *Ricinus communis* is mainly cultivated as a source of oil.

The "toxic component of the castor oil seed" was first noticed by Ritthausen in 1878 and further studied and named "ricin" by Stillmark (1888) 10 years later. Dixon (1887) was the first to find its extreme toxicity and to find that it is a protein. He carried out the initial toxicological experiments with ricin on animals. More detailed experiments on ricin were conducted by Derselbe (1899), Cruz (1898), Cushny (1898) and Muller (1899) in the next 20 years, during which it was further established that ricin is a protein. It was the most toxic material known at that time. Muller (1899) first described in detail the clinical symptoms of poisoning with castor bean seeds. He also stated that ricin is resistant to the action of pepsin. Kobert (1900) later demonstrated that trypsin does not decrease the toxicity of ricin.

Research on the chemical, pharmacological and immunological properties of ricin did not start until the beginning of this century when the first method for extracting ricin was described by Osborne (1905), marking the beginning of a new era for ricin research.

B. Chemistry of Ricin.

Ricin is a toxic heterodimeric lectin. It, together with the closely related lectin, *Ricinus communis* agglutinin make up 5% of the total protein in mature castor seeds. There are several isoforms of ricin in seeds of different origin. Ricin D is isolated from large-grain seeds of castor beans grown in Thailand (Ishiguro *et al.*, 1964). Ricin E comes from small-grain seeds of castor beans cultivated in Japan (Mise *et al.*, 1989). The two kinds of ricin are similar in molecular weight, toxicity to mice and agglutinating activity but differ in isoelectric point, affinity to Sepharose 4B and toxicity toward cultured cells (Mise, *et al.*, 1987). Generally, ricin refers to Ricin D or RCA_{II}(*Ricinus Communis* Agglutinin II).

Ricin can be purified by affinity chromatography on Sepharose 4B which contains ß-galactose residues binding the ricin and ricinus agglutinin (RCA_I). The two components can be separated by N-acetyl-galactosamine which elutes only the ricin and further elution with galactose which removes the RCA_I (Nicolson *et al.*, 1974).

C. Ricin Biochemistry

Ricin is synthesized as a single polypeptide in maturing castor beans, where it accumulates in the storage granules of the seeds (Youle *et al.*, 1976). After synthesis, the toxin is rapidly cleaved into two S-S linked polypeptides, termed the A- and the B-chain (Olsnes *et al.*, 1982; Lord, 1985; Harley *et al.*, 1985). The molecular weights of the two chains are 30,6235 and 31,431 kDa, respectively.

The three-dimensional structure of ricin has been resolved by X-ray crystallography (Montfort *et al.*, 1987; Wei and Koh, 1978) and refined to 2.5 Å resolution (Rutenber *et al.*, 1991). A low resolution study (4 Å) revealed that ricin B-chain has a bi-lobal structure with each domain being able to bind a galactose residue (Villafranca and Robertus, 1981). This model allowed for an accurate and detailed description of both the A-chain and the B-

chain. A further refinement of the structure of recombinant ricin A-chain has been done to 2.3 Å resolution (Mlsna *et al.*, 1993). The amino acid sequence and carbohydrate composition of both ricin A- and B-chains have been determined. The enzymatic A-chain is a globular protein with eight *alpha* helices (A-H) and eight strands of *beta* sheets (a-h), while the B-chain lectin is composed of two separate folding domains with somewhat different affinity for lactose (Zentz *et al.*, 1978). These sites are responsible for the binding of the toxin to carbohydrates at the cell surface. The enzyme active sites for ricin A-chain have been identified; these include Tyr 80, Tyr 123, Glu 177, Arg 180, and Trp 211. They serve as binding sites for polynucleotide substrates or maintain the active site conformation (Monzingo, 1992).

The sequence of the B-chain was redetermined and revised in 1985 by Araki and Funatsu. There are 4 internal disulfide bridges in the B-chain, but none in the A-chain. There are no reactive sulfhydryl groups on the intact toxin. However, in the presence of sodium dodecyl sulfate (Cawley and Houston, 1979) and 6 M guanidine chloride (Yoshitake *et al.*, 1978) a buried sulfhydryl group can be uncovered in position 171 of the A chain.

The neutral A chain in native ricin can be observed as a doublet when analyzed by polyacrylamide gel electrophoresis. These have been designated as an A_1 component (64%) with a molecular weight of approximately 30,000 and an A_2 component (36%) with a molecular weight of 32,000. This higher molecular weight component contains an additional second mannose-rich oligosaccharide (Foxwell *et al.*, 1985). The A-chain has 265 amino acid residues with sequences consisting of both hydrophilic and hydrophobic sections, and has a helical content estimated at 0.3% (Funatsu *et al.*, 1973).

The acidic B-chain has 262 amino acid residues with a molecular weight of 31,557 (Araki and Funatsu, 1987) and has a helical content of 10% (Funatsu *et al.*, 1979). The B-chain has four internal disulfide bridges linking cysteine residues at positions 20 to 39, 63 to 80, 151 to 164 and 190 to 207 (Araki and Funatsu, 1985). Even though weak

interactions would hold the chains together, the presence of the intact disulfide bridge linking the two appears to be necessary for ricin's toxic effect. However this link must be reversible in order to release the free A-chain into the cell. When a covalent interchain crossing of ricin is made with N, N'-*O*-phenylenedimaleimide, a non-toxic product results. Similar treatment of the free A-chain did not alter toxicity (Oda and Funatsu, 1979). The A-chain of ricin D and ricin E is identical. The amino acid sequence for the B-chain of ricin E was determined by Araki and Funatsu (1987). The B-chain of ricin E contains 262 amino acid residues and is composed of the N-terminal half of ricin D and the C-terminal half of *Ricinus communis* agglutinin, another toxic lectin found in the castor bean (Araki *et al.*, 1986).

Ricin B-chain has two homologous domains, each containing 4 subunits. Each subunit consists of a 17-residue linking peptide, lambda, and three homologous units. These may arise from multiplication and fusion of DNA encoding an ancient galactose binding peptide (Mlsna *et al.*, 1993). There are six potential galactose binding sites. Site-directed mutagenesis experiments have demonstrated that Asn 46 and Gln 256 residues are very important for galactose binding (Vitetta and Yen, 1990; Wales *et al.*, 1991). Other sites including Trp 37, Tyr 248, Asp 22, Asp 234 Gln 47 and Gln 256 are also involved in galactose binding. The X-ray diffraction structure of substrate binding to ricin A-chain with the adenosine analog, formycin monophosphate and dinucleotide ApG, has shown that the binding sites are two invariant tyrosines, Tyr 80 and Tyr 123 (Monzingo and Robertus, 1992).

Both of the constituent polypeptide chains in ricin are glycoproteins (Olsnes *et al.*, 1982). Most of the carbohydrate is carried by the B-chain. These carbohydrates may play a role in binding of the toxin to certain cells containing mannose receptors. Funatsu *et al.* (1971) and Nanno *et al.* (1975) found one oligosaccharide chain on the A-chain consisting of $(GlcNAc)_2(Man)_4$. Foxwell *et al.* (1985) found one oligosaccharide chain on the A_1 component of the composition $(GlcNAc)_2(Xyl)_1(Fuc)_1(Man)_{3-4}$ and evidence for another

oligosaccharide chain on the A_2-chain consisting of only GlcNAc and mannose. Funatsu *et al.* (1971) found two carbohydrate chains on the B-chain consisting of $(GlcNAc)_2(Man)_6$ and $(GlcNAc)_2(Man)_7$. These oligosaccharide chains are each attached to asparagine residues. In addition, ricin binds to concanavalin A indicating that the mannose residues are exposed. Crystallization studies of ricin have been carried out. These show only one ricin molecule per asymmetric unit. A low resolution study (4 Å) showed a bilobal structure for ricin B chain with each domain being able to bind a galactose residue (Villafranca and Robertus, 1981).

D. Detection of Ricin.

Several immunoassays, enzyme-linked immunosorbent assays (ELISA), radioimmunoassays, and immunocytochemical procedures have been developed to detect ricin in biological fluids and tissues (Koja *et al.*, 1980; Godal *et al.*, 1983; Cmiech *et al.*, 1985; Kopferschmitt *et al.*, 1983; Griffiths *et al.*, 1986a; 1986b; 1989a; 1989b; Leith *et al.*, 1988).

Wannemacher and his co-workers (1992) made a comparison among bioassay, immunoassays, and chemistry assays of ricin. The results of their assays of the ricin content in a castor bean meal extract in their laboratories showed good agreement among the methods. The ricin content was found to be as follows: Mouse bioassay, from the median effective dose, 4.1 mg/ml; Mouse bioassay, from the mean time to death, 3.7 mg/ml; Vero cell cytotoxicity, 4.9 mg/ml; ELISA, 1.8 mg/ml; HPLC, 3.3 mg/ml; SDS-PAGE, 2.9 mg/ml; and capillary electrophoresis, 3.3 mg/ml. They also indicated that the goat polyclonal anti-ricin antibody was highly specific for the ricin molecule and only reacted with its own A and B chains.

E. Mechanism of Action.

1. Function of Ricin A-Chain.

Ricin toxin A-chain is delivered into cells via receptor-mediated endocytosis. Following uptake via the mannose receptor, ricin A-chain is rapidly cleaved by endosomal proteases. A recent study (Fiani *et al.*, 1993) showed that the activation or membrane translocation of ricin A-chain is dependent upon the action of specific proteases. The A-chain of ricin is responsible for the potent toxic activity of ricin. Ricin toxin A-chain is a potent catalytic enzyme that inhibits protein synthesis by inactivating 60S ribosomes of eukaryotic cells. The ricin toxin A-chain probably acts as a specific N-glycosidase to remove adenine from rRNA (Endo *et al.*, 1987). These experiments indicated that ricin toxin A-chain inactivated eukaryotic ribosomes by a specific modification of the adenine^{4324} residue of 28S rRNA. Ricin toxin A-chain probably acts as a specific N-glycosidase to remove adenine from rRNA (Endo *et al.*, 1987). Endo and Tsurugi (1987) quantitated the amount of adenine liberated per mole of ribosomes treated with ricin. They concluded that the ricin A-chain removes the adenine residue by hydrolysis and does not act as a phosphorolytic enzyme. They further concluded that ricin A-chain has RNA N-glycosidase activity cleaving the N-glycosidic bond of a single adenine residue (A^{4324}) of the 28S rRNA in a hydrolytic fashion, leaving the phosphoribose backbone intact. This missing adenine rendered the fragment susceptible to digestion by nucleases. The nucleotide sequence around position 4324 is part of a highly conserved sequence. Olsnes *et al.* (1975) demonstrated in kinetic experiments that ricin A-chain in simple buffer solution inactivated salt-washed ribosomes at a rate of about 1500 ribosomes per minute per molecule of ricin A-chain. The Q_{10} was about 1.8 and the K_m about 1-2 X 10^{-7}M. The inactivation of ribosomes could be halted at any time by adding specific anti-A chain antibodies. Several plant toxins have similar structure and action to ricin. Two of these, abrin and modeccin also remove adenine from A^{4324} (Endo *et al.*, 1987).

The enzymatic activity of ricin was demonstrated in a kinetic experiment by Olsnes and co-workers who showed that pure ricin A-chain chains inactivated salt-washed ribosomes in simple buffer solutions at a rate of about 1500 ribosomes per minute per ricin A-chain (1975). The Q_{10} and K_m were 1.8 and 1.2 X 10^{-7}M respectively. Since no cofactors were required, it was speculated that ricin has endonuclease activity. After many attempts to prove this failed, Endo and co-workers (1987) found the 28S rRNA of the 60S subunit caused an almost undetectable reduction in its electrophoretic migration rate after ricin treatment. This was caused by a 550-nucleotide fragment derived from the 3' end of 28S rRNA. Further sequence analysis of the fragment revealed a missing adenine at position 4324 in ricin treated-ribosomes. They also demonstrated that A_{4324} is the sole site of action. The region in which A_{4324} lies is strongly conserved between species. Since only ribosomes of eukaryotic cells are sensitive and ricin A-chain dose not affect bacterial ribosomes (Olsnes *et al.*, 1973; Greco *et al.*, 1974), apparently, ricin A-chain recognizes the three-dimensional structure around A_{4324}. By virtue of site-directed mutagenesis several active sites on ricin A-chain identified by X-ray analysis have been well investigated. Conversions of Arg 180 or Glu 177 to Gln reduce activity by approximately 2000 or 200-fold respectively (Frankel *et al.*, 1990). Arg 180 and Glu 177 are not responsible for substrate binding but are necessary for stabilizing the transition state of the catalytic reaction. Mutations at these two sites primarily affect K_{cat} with little effect on K_m in kinetic analysis (Ready *et al.*, 1990). Monzingo and Robertus (1992) demonstrated that Tyr 80 and Tyr 123 were the binding sites in a study of the structure of the ricin with formycin, an adenosine analog.

From the information from the structural and kinetic analysis studies, a mechanism of ricin A-chain action has been proposed by Lord (1994). The substrate binds in the cleft and adenine is sandwiched between tyrosines 80 and 123 in a stacking interaction. The leaving group adenine is protonated by Arg 180, promoting breakage of the C1'-N9 bond and thereby forming an oxycarbonium moiety on the ribose. This transition state structure

is stabilized by ion pairing with Glu 177. A water molecule, in the crystal structure, lies on the opposite side of the sugar ring from adenosine. It is polarized by Arg 180 to a hydroxide moiety that rapidly attacks the sugar carbonium, completing the reaction.

2. *Function of Ricin B-Chain.*

Ricin toxin B-chain has two functional roles in the intoxication process, binding to cell surface galactose residues and facilitating ricin toxin A-chain translocation into the cell cytosol. Baenziger and Fiete (1979) studied the specificity of this binding by measuring the association constant (K_a) of ricin with a series of glycopeptides of known composition. They concluded that ß-1, 4-linked galactose residues are primarily responsible for binding. The oligosaccharides which bind ricin can be found on a variety of glycoproteins and glycolipids. Therefore, the toxin can bind to several different molecular species. Binding studies have shown that HeLa cells possess 3×10^7 binding sites for ricin. Hatakeyama *et al.* (1989, 1990) reported two binding sites on the B chain, a high affinity binding site and a low affinity site. The ethoxyformylation of histidine residues in ricin E abolishes the saccharide binding capability of the high affinity binding site, indicating that one of the three histidine residues must be present at the high affinity binding site. Structural studies with ricin-gold conjugates or enzyme bound ricin have shown that ricin is bound all over the cell surface (van Deurs *et al.*, 1989; Sandvig *et al.*, 1991). After combining at the cell surface the B chain facilitates the entry of the A-chain into the cell where it interacts with the 60S ribosomal subunit and interferes with protein synthesis (Olsnes *et al.*, 1974). In addition to a role in binding, a translocation-enhancing effect has been reported for ricin B-chain (Youle *et al.*, 1982). Goldmacher and co-workers (1992) presented evidence that the membrane binding and A-chain translocation activities of ricin cannot be separated. The addition of purified ricin B-chain can accelerate the cytotoxic activity of A-chain immunotoxin without increasing the amount of A-chain bound to cells. The presence of B-

chain somehow increases the rate of A-chain transport to the ribosomes and augments the toxicity of ricin toxin A-chain.

3. Endocytosis.

One of the fundamental properties of living cells is their ability to sense and respond to their external environment. This is accomplished, in part, by endocytosis. Ricin is transported into the cell complexed to the receptor in a process called receptor-mediated endocytosis. It is then stored in endosomes until it is released into the cytosol (Olsnes and Sandvig, 1983). According to work done by Moya and co-workers (1985), ricin entry into the cell is not dependent on coated pits. Hypotonic shock and incubation in K^+-free media arrests clathrin coated pit formation in cells (Larkin *et al.*, 1983). After this treatment ricin still retained the original amount of cell toxicity. Immunoelectron microscopy has shown that a portion of the endocytosed ricin is transported via endosomes to the *trans*-Golgi network, suggesting that ricin toxin A-chain translocation takes place from the *trans*-Golgi network or a post-*trans*-Golgi network compartment (van Deurs *et al.*, 1988). Gonatas *et al.* (1975; 1980) labeled ricin with horseradish peroxidase to study its uptake. When incubation was at 4° C, a continuous rim of the plasma membrane was stained. However, when cells were washed and incubated at 37° C, the plasma membrane became patchy. After 30 min, various degrees of staining appeared in vesicles. Clusters of stained vesicles were found adjacent to the cisternae of the Golgi. After 1 hour, vesicles were found near the *trans*-Golgi network, and at the edges of the cisternae. Even after 3 hours at 37° C, some small patches of staining remained at the cell surface. However, most of the label was found in intracellular compartments, particularly in the Golgi cisternae. The intracellular role of ricin toxin B-chain in ricin cytotoxicity may be to ensure delivery of ricin toxin A-chain to a translocationally competent compartment.

Ricin variants require at least one of the two ricin toxin B-chain galactose-binding sites to remain functional for cytotoxicity, even when the toxin binds to an alternative

surface receptor such as the mannose receptor of macrophages (Newton *et al.*, 1992). This suggests that ricin may change binding sites from the surface mannose receptor to an intracellular galactosylated receptor during intracellular transport, and that this change is essential for cytotoxicity.

Calcium in the media and its influx into the cell are not required for entry of ricin into the cell. A deprivation of Ca^{2+} in the media provided only partial protection against ricin intoxication. Verapamil, a calcium channel antagonist, afforded moderate protection against intoxication. This partial protection by Ca^{2+} deprivation and a calcium channel blocker along with the increased toxicity at higher pH where Ca^{2+} influx is increased seems to indicate that ricin is internalized by two mechanisms, one of which is Ca^{2+} dependent and another which is Ca^{2+} independent (Sandvig and Olsnes, 1982). Sodium deprivation afforded no protection against ricin toxicity. The presence of trivalent cations of the lanthanide series provided strong protection against intoxication. These cations markedly inhibit Ca^{2+} uptake by cells. However Fe^{3+}, which does not affect calcium flux, also provides good protection against ricin intoxication, so the protection afforded by the lanthanides may come from another mechanism and not from their effects on calcium flux. These treatments do not affect the ability of the ricin A-chain to inactivate ribosomes in cell-free systems. Therefore, all of these protective effects are due to the inability of the toxin to enter the cytosol and gain access to the ribosomes.

After toxin is taken up by endocytosis, it may be transported to different compartments of the vesicular and tubular system in the cell before it eventually crosses the limiting membrane to gain access to the ribosomes. Internalized ricin appears to be able to enter the cytosol for hours after endocytosis (Sandvig *et al.*, 1982). Ricin is accumulated only to a low degree in lysosomes, and is degraded very slowly. Sandvig and co-workers (1978) showed that even after 2 hours, about 90% of internalized ricin remained active. Internalization of the ricin toxins is a very slow process with only about 8% of cell-bound toxin internalized each 10 minutes at 37° C in Hep_2 cells with functional coated pits (Moya

et al., 1985). It had been suggested that ricin enters the cytosol by the rupture of endocytic vesicles (Nicholson, 1974; Nicholson *et al.*, 1975). However, in light of the work by Sandvig and Olsnes (1982) this unspecific vesicle rupture does not seem likely. They showed that low pH and an absence of Ca^{2+} protected well against the toxicity of ricin and the related toxins, abrin and modeccin, but not against diphtheria toxin in spite of the fact that all were endocytosed equally under these conditions. The transfer of endocytosed ricin to the Golgi complex appears to be necessary for intoxication (Sandvig *et al.*, 1986). Studies involving the labeling of ricin with a horseradish peroxidase (van Deurs *et al.*, 1986) found that ricin was routed through the vacuolar and tubulo-vesicular portions of the endosomal system on its way to the Golgi complex. With immunogold labeling, Hansen *et al.* (1989) demonstrated the localization of ricin in Golgi stacks and the associated *trans*-Golgi network. Evidence now shows that ricin is translocated to the cytoplasm from the *trans*-Golgi network. Van Deurs *et al.* (1990) presented a scheme for intracellular routing and sorting of ricin based on current knowledge and speculation. Ricin, bound to membrane glycoproteins and glycolipids, is internalized by both uncoated and coated pits and vesicles to reach endosomes. From the endosomes it may be rapidly recycled to the cell surface, transferred to lysosomes where it is slowly degraded, or delivered to the *trans*-Golgi network. From the *trans*-Golgi network it can be routed back to the cell surface or translocated into the cytosol where it can inhibit protein synthesis.

Treatment with brefeldin A, which can disrupt the *trans*-Golgi network, will protect cells against ricin intoxication, although it does not block endocytosis or the transportation of ricin to the *trans*-Golgi network (Yoshida *et al.*, 1991; Sandvig *et al.*, 1991). Hybridoma cells producing an anti-ricin antibody can not be intoxicated, possibly because the antibody blocks ricin in the *trans* Golgi network (Youle *et al.*, 1987). The cells are protected when intracellular ricin transport is inhibited at low temperature (<18°C)(van Deurs *et al.*, 1993). Thus, transport of the ricin into or through the Golgi stack is essential before toxicity can occur. The disulfide bond between the A- and B- chain is cleaved somewhere in the *trans* -

Golgi network and ricin A- chain is translocated to the cytoplasm from the *trans*-Golgi network (van Deurs *et al.*, 1990). Whether the *trans*-Golgi network is the exact location from which ricin is released is still controversial. Some speculation about the importance of the endoplasmic reticulum (ER) is based on the finding that a tetrapeptide (KDEL) increases the toxicity of the A chain. In eukaryotic cells KDEL plays an important role in the retrograde vesicular membrane flow through the trans Golgi network to the ER, which is a normal process. A receptor that is recycling between the two components can recognize the KDEL sequence present at the COOH-terminus of soluble ER proteins (Pelham et al, 1990). A bacterial toxin, Pseudomonas exotoxin A, contains a KDEL-like sequence that is essential for its cytotoxicity, suggesting ER may be the final point of distribution before entering the cytosol (Chaudhary *et al.*, 1990). However, ricin does not contain a KDEL like portion. This may explain the requirement of ricin B-chain galactose binding sites which somehow interact with proteins with this sequence. So far, there is no direct evidence of transport of ricin to ER. Alternative pathways are also being considered. For instance, ricin A-chain may translocate to the cytosol from a prelysosomal vesicle released from the *trans*-Golgi network.

4. Other effects of ricin.

In addition to protein synthesis inhibition, ricin also has other actions. In cultured macrophages, ricin induces the metabolism of arachidonic acid (Naseem and Pace, 1991). Ricin stimulates the release of tumor necrosis factor-A and interleukin-1 from alveolar macrophages (Bavari *et al.*, 1992). It also releases acid and alkaline phosphatases, lactic dehydrogenase and 5' nucleotidase (Creasia *et al.*, 1992) from lung tissue. Mitochondrial function is affected by ricin in alveolar macrophages indicating that oxygen consumption or the electron transport chain may be disturbed (Swauger *et al.*, 1992).

F. Toxicity.

Ricin is highly toxic to animals after parenteral administration, and it also causes intoxication after oral ingestion because it is resistant to the hydrolysis of pepsin and trypsin. Sensitivity of animals varies among different species and even among strains of the same species. On a weight basis, the horse is the most sensitive animal of those tested. The lethal dose of castor oil seed is 0.10 g/kg for horse and 0.90 g/kg for rabbit (Balint, 1974). The dose-lethality curves for ricin after iv injection are very steep in some animal experiments so the LD_{50} is hard to estimate, and the minimum lethal dose is a more meaningful indicator of its toxicity. The MLD is 2.40 μg/kg in B6D2 mice, 1.6-1.75 μg/kg in dogs and 0.44 μg/kg in rabbits (Aslak *et al.*, 1984; Fodstad *et al.*, 1979; Robinson *et al.*, 1992)

Ricin's distribution in the body following administration has been studied by many researchers. Following iv injection, the liver and spleen are the major organs of accumulation. A study with ^{125}I-labelled ricin in rats showed 46% of an injected dose accumulated in liver and 33% in spleen (Ramsden *et al.*, 1989). Godal and co-workers (1984) also found high levels in the bone marrow and adrenal cortex in mice. No activity was found in the brain.

There is always a latent period before intoxication following ricin administration even after i.v. administration. This period varies from a few hours to several days, with the survival time highly related to the dose (Fodstad *et al.*, 1976). With high doses, animals develop symptoms in a few hours and die after about 10 hours. Symptoms of acute intoxication include loss of appetite and body weight, slight fever, diarrhea, edema in the extremities and ascites. A fall in blood pressure was observed in rabbits 28 hours after i.v. ricin administration (Robinson *et al.*, 1992). Animals recovered completely after nonlethal doses.

Pathological examination of ricin-poisoned animals showed severe necrosis in liver and pancreas (Barbieri *et al.*, 1979). It is possible that reticulo-endothelial cells are

particularly sensitive to ricin. In rabbits, severe hemorrhage and mucosal erosion in stomach, severe congestion, edema and hemorrhage in lungs and severe hemorrhage in the myocardium were observed after i.v administration of ricin (Robinson *et al.*, 1992). A decrease in hematocrit and thrombocytes and an increase in leukocytes were also found. Bone marrow examination in dogs revealed a marked reduction in the number of erythroblasts but no change in myelopoiesis (Fodstad *et al.*, 1979). The pathology of intestine and lymphoid tissue have been investigated after an intramuscular dose of ricin. The severity of the cellular infiltration in intestines was similar to that found in a local immune response triggered by orally administered ricin (Leek *et al.* 1989). After intramuscular injection of ricin, there was a large-scale disruption with an apoptotic type of cell death observed in lymphoid tissue (Griffiths *et al.* 1987). Oral administration of ricin primarily affects the intestinal mucosa and impairs sugar absorption by the small intestine (Ishiguro *et al.*, 1983).

Ricin can also produce damage following local application. Pulmonary necrosis was observed after administration of ricin as an aerosol. This was not caused by protein synthesis inhibition, but rather by ricin-induced release of tumor necrosis factor A, interleukin-1 and various enzymes which indicate macrophage activation (Bavari *et al.* 1992).

Cell Culture and Cytotoxicity.

The toxicity of ricin to cultured cells was first reported by Lin and co-workers (1970 and 1971). The earliest toxic effect observed is inhibition of protein synthesis. Incorporation of amino acid into protein is inhibited (Ishiguro *et al.*, 1992). There is a lag time of 20 to 30 minutes before inhibition is observable even at high concentrations (Refsnes *et al.*, 1974). DNA and RNA synthesis are also decreased later. Energy metabolism and oxidative phosphorylation are not affected. Ricin is toxic in tissue culture at concentrations of about 1 ng/ml. This lag time can be reduced by increasing the

concentration of the toxin, but the lag time is always more than 20 to 30 minutes even at high concentrations (Refsnes *et al.*, 1974; Olsnes *et al.*, 1976).

The synthesis of proteins may be inhibited to different extents. For example, in a myeloma cell line, the synthesis of a myeloma protein (IgA) was more rapidly inhibited than bulk protein synthesis (Ko and Kaji, 1975). Different cell lines differ in sensitivity to ricin, but this sensitivity does not correlate well between animals and cell culture. Ricin D is much more toxic than ricin E in cultured cells (Koga *et al.*, 1979). Ricin has a cytostatic, and then a cytotoxic effect on cells in culture (Lungnier *et al.*, 1980) which are highly damaged (important membranous protrusions). After intoxication the cell undergoes early morphological changes. The cell surface becomes irregular, but the surface membrane remains functional even after all protein synthesis ceases. This was demonstrated by the cells continuing ability to exclude trypan blue (Nicholson *et al.*, 1975; Lin *et al.*, 1970). Griffiths *et al.* (1987) found large scale disruption in lymphoid tissue and intestine with an apoptotic type of cell death after an intramuscular dose of ricin. Later, they also observed that the apoptotic type of cell death also occurs in spleen and liver (Leek *et al.*, 1990). Different cell strains may show different sensitivities to ricin.

Malignant cells seems to be more sensitive than normal cells (Fodstad *et al.*, 1978). In a myeloma cell line, myeloma protein synthesis is more rapidly inhibited than bulk protein synthesis (Ko and Kaji, 1975). Some anti-inflammatory agents have a synergistic effect on ricin-induced protein synthesis inhibition (Syed and Judith, 1993). The inhibition of endosomal proteases such as cathepsin D will reduce ricin cytotoxicity while blockade of cathepsin B will enhance ricin toxicity (Maria *et al.*, 1993). Ricin D and ricin E are equally toxic in mice but in mouse cell culture ricin D is much more toxic than ricin E. Intoxicated cells first undergo morphological changes. The cell surface becomes irregular, but the cell membrane is still functional several hours after protein synthesis has ceased because the cell continues to exclude trypan blue for several hours (Nicolson *et al.*, 1975 and Lin *et al.*, 1970).

The mannose-terminal oligosaccharide of ricin A-chain acts as a ligand for the mannose receptor in macrophages *in vitro*, leading to intoxication of the cells (Dimmons *et al.*, 1986; Skilleter and Foxwell, 1986). This allows the toxin to be removed from the blood by the reticuloendothelial system and accounts for the high levels of the toxin found in the liver by Fodstad *et al.* (1976) and the severe damage which occurs in the hepatic sinusoids as reported by Derenzini *et al.* (1987).

Systemic toxicity.

Ricin is especially toxic after parenteral administration, but even after oral administration it still exhibits toxicity. The toxicity of ricin varies among species with the guinea pig more sensitive on a weight basis than the mouse and the horse being the most sensitive animal of those tested (Ehrlich, 1957; Balint, 1974). Laugnier *et al.* (1980) reported that the symptoms of ricin intoxication were established on mice which died from a dramatic hepatonephritic injury, but always after a lag period. Fodstad *et al.* (1976) determined an approximate LD_{50} in B6D2 mice of 55 to 65 ng/mouse (mice weighing 22-26 g). Christiansen *et al.* (1994) studied the effects of ricin on the cardiovascular system in rabbits after determining its LD_{50} and minimum lethal dose in rabbits by the Up and Down method, as a basis for dosing. The minimum lethal dose (0.44 μg/kg) of ricin caused a significant decrease in both systolic and diastolic pressures. Dogs given toxic doses of ricin showed weakness, anorexia, apathy, and moderate fever. No signs attributable to the central nervous system were observed (Fodstad *et al.* 1979). Dogs dying from intoxication expired after 15-40 hours. No evidence for specific liver damage or impairment of kidney function was obtained. Marrow examinations in dogs revealed no clear abnormality in myelopoiesis. With the highly sensitive enzyme-linked immunosorbent assay (ELISA) for determination of ricin in serum, Godal *et al.* (1984) found that IV-injected ricin disappeared from the plasma of mice and cancer patients according to first-order kinetics. When mice of different strains were given the same dose of ricin, ricin concentrations found in liver,

spleen, and kidneys were highest in the most sensitive mice. Whole-body autoradiography after IV injection of ^{125}I-labeled ricin showed the highest amount of radioactivity in liver, spleen, and adrenal cortex. Considerable amounts of radioactivity were also present in bone marrow. In cancer patients, toxicity appeared at about the same initial serum levels as in mice. These investigators felt that, with ricin, a minimum lethal dose (MLD) was a more meaningful parameter that an LD_{50}. The MLD in mice varied from 1.95 μg/kg for DBA mice to 2.40 μg/kg for B6D2 mice. Clinical symptoms of acute intoxication included loss of appetite and body weight, slight fever, edema in the extremities, and ascites. Pathological findings included an enlarged and congested spleen along with the reticuloendothelial cells of the liver and spleen showing increased phagocytic activity. Hematologic parameters were altered with a decrease in hematocrit and thrombocytes and an increase in leukocytes.

Retrograde transport of ricin in neurons has been demonstrated by Harper *et al.* (1980). Their experiments confirmed a retrograde transport of ricin from the submandibular gland of rats to neuronal bodies in the superior cervical ganglia. Morphologic changes in the neurons support the observations from biochemical studies that ricin interferes with ribosomal function and protein synthesis. A small number of the neurons are destroyed, but no phagocytosis occurs with the capsular cells remaining intact around empty spaces. In 1982, Wiley *et al.* confirmed this retrograde transport by dipping a transsected nerve into a ricin solution and then determining neuronal cell changes after 12 to 52 days. They found cell damage limited to those neurons which projected into the application site of the nerve. This damage included the disappearance of virtually all Nissl substance, pycnotic nuclei and a glial reaction. Helke *et al.* (1985) reported that the retrograde transport of ricin applies only to those nerves projecting into the periphery or located in the periphery, and not to those neurons residing entirely within the CNS.

Man. Most intoxications in man are caused by ingesting castor bean seeds, many times by children. Ingestion of one seed is enough to cause symptoms in adults, two seeds

can cause intoxication and three seeds may be fatal. According to previous reports, an often cited lethal dose of ricin for human is 1mg (Rauber and Heard, 1985). There is a latent period of 8 to 10 hours before the appearance of symptoms. The patient will completely recover if he has taken a sublethal dose of ricin (Crompton and Gall, 1980).

Balint (1974) reviewed about 700 human case histories, and reported the following signs and symptoms. Nausea, headache, general malaise, somnolence, loss of consciousness, convulsions, bloody diarrhea with tenesmus, dehydration, thirst, cyanosis, tachycardia, fall in blood pressure, changes in the electrocardiogram, asthmatic symptoms, exanthema, liver necrosis, nephritis, proteinuria, rise in excretion of non-protein nitrogen, conjunctivitis, optic nerve lesion, mydriasis, leukocytosis and changes in biological data. At post mortem the main changes noticed were bleeding in the serous membranes, hemorrhage in the stomach and intestines, degenerative changes in the heart as well as liver and kidneys, infiltrations of the lymph nodes and changes in the spleen, especially in its lymphoid elements. Specific references for each case are listed in the 1974 Balint paper.

Ricin is useful as a research tool despite its toxicity. In the work of Solis *et al.* (1993), ricin toxicity has been reduced by chemical modification of carboxyl groups using 1-ethyl-3-(3-dimethylaminopropyl) carbodiimide and [^{14}C]-glycine methyl ester. The modification did not substantially alter the strength and specificity of the carbohydrate-binding ability of the lectin, as observed by hemagglutination tests and by inhibition assays with different carbohydrate structures. However, the LD_{50} decreased 90-fold when the highest modification was achieved. Therefore, the modified lectin can be used more safely in the study of galactose-containing carbohydrates.

G. Treatment of Ricin Intoxication.

Studies are ongoing to screen numerous compounds for their ability to alter ricin toxicity *in vitro* and ricin lethality *in vivo*. Some compounds seem useful for reducing ricin intoxication, but no specific chemoprotective agents are available against ricin. Brefeldin A,

an antiviral macrolide antibiotic, inhibits the transport of proteins from the endoplasmic reticulum to the Golgi and causes disassembly of the Golgi stacks. Yoshida and his co-workers (1991) found that pretreatment with brefeldin A reduced ricin-induced protein synthesis inhibition in Vero cells and in a ricin-sensitive mutant Chinese hamster ovary cell line. They studied the cytotoxicity of ricin in cells treated with brefeldin A, which dramatically disrupts the structure of the Golgi apparatus causing the Golgi content and membranes to redistribute to the endoplasmic reticulum. Brefeldin A inhibits the cytotoxicity of ricin in Chinese hamster ovary, normal rat kidney, and Vero cells and abolishes the enhancement of ricin cytotoxicity by NH_4Cl, nigericin, swainsonine, and tunicamycin or by a mutation in endosomal acidification. The mechanism of brefeldin A protection is disassembly of the *trans*-Golgi network stacks which are the translocation site necessary for ricin cytotoxicity.

Zidovudine (3'-azido-3'-deoxythymidine) and 2',3'-dideoxycytidine were also found to be effective against ricin intoxication *in vitro* (Mereish and Fajer, 1993). Pace (1992) reported that zidovudine inhibited ricin toxicity in Vero cells, and this inhibition was not due to a block of ricin enzymatic activity. Wellner and his co-workers (1994) extended these findings and examined the effects of zidovudine treatment on the toxicities of ricin and other protein toxins in Chinese hamster ovary and Vero cell lines. Zidovudine treatment did not significantly alter the toxicity of modeccin or diphtheria toxin in either cell line, but it markedly reduced ricin toxicity in both cell lines. The ID_{50} values (concentration of toxin required to inhibit protein synthesis by 50%) for ricin in Chinese hamster ovary cells increased approximately 6.5-fold; while in Vero cells the ID_{50} values increased about 8.5-fold. As zidovudine did not block ricin enzymatic activity, they examined the effects of zidovudine on earlier steps in the ricin intoxication process. Zidovudine treatment did not inhibit cell-surface binding or internalization of [^{125}I]-ricin. Results of kinetic studies showed that when Zidovudine was incubated with cells at the time of ricin exposure, it caused no major change in the lag phase, during which ricin

reaches the site of translocation. However, it clearly reduced the subsequent first-order reduction in the rate of protein synthesis, suggesting an effect on translocation. Monensin, an ionophore that perturbs intracellular trafficking and increases the toxicities of ricin, reduced zidovudine protection against ricin. Nocodazole and colchicine, agents that disrupt microtubules and some routes of intracellular trafficking, reduced the ability of zidovudine to inhibit ricin toxicity (Pace, 1992).

Indomethacin, a non-steroidal anti-inflammatory agent, decreased ricin-induced protein synthesis inhibition in cultured macrophages by decreasing the binding and internalization of ricin. However, fluocinolone, an anti-inflammatory glucocorticoid, increased ricin-induced protein synthesis inhibition by increasing binding and internalization of ricin (Nassem and Pace, 1992).

Lactose and lactulose decrease ricin binding to cell surface receptors and increase the rate of dissociation from receptors and thereby decrease ricin-induced protein synthesis inhibition in cell culture. However, pretreatment with lactose or lactulose had no effect on survival rate or mean time to death in mice after an i.v. challenge with ricin (Wannemacher *et al.*, 1991).

Hewetson and his co-workers (1993) vaccinated mice subcutaneously with 25 μg/kg of ricin in the presence of Freund's complete adjuvant or Ribi adjuvant, followed by a boost 14 days later with 50 μg/kg ricin in Freund's incomplete adjuvant or Ribi adjuvant, respectively. Three subsequent boosts at 28-day intervals with 25 μg/kg ricin yielded high anti-ricin antibody titers as determined by ELISA. Vaccinated animals were exposed to an aerosolized LD_{99} dose of ricin. With the exception of one death not attributable to ricin intoxication, all vaccinated mice survived the lethal aerosol exposure. In addition, a passive protection regimen was evaluated in mice pretreated with 100 μg purified goat anti-ricin IgG administered intravenously, and then challenged with ricin intravenously. All were resistant to 125 μg/kg of ricin, a dose greater than 25 times the intravenous lethal dose. Mice injected intravenously with 5 mg of the same IgG were protected from a lethal

aerosol challenge. Their findings indicated that it is possible to protect animals from inhaled ricin by vaccination or passive administration of specific antibodies.

In this model pulmonary inflammation was reduced but not prevented fully (Walters *et al.*, 1993). Passive immunization to ricin has also been investigated. Avian anti-ricin antibodies proved to be superior to other polyclonal or monoclonal anti-ricin antibodies in neutralizing ricin toxicity when tested in several protection bioassays in mice (Thalley *et al.*, 1993).

H. Current Applications of Ricin.

The anti-tumor properties of ricin have been known for a long time. In 1951 an effect of ricin on sarcomas in rats was reported by Mosinger. Lin *et al.* (1970) found that mice could be cured by treatment with crystalline ricin as late as 5 days after intraperitoneal injection of Ehrlich ascites tumor cells. In the next two decades, there were a large number of reports regarding the antitumor activity of ricin both in *in vivo* and in *in vitro* models. Recently, with further understanding of ricin's chemistry and mechanism of toxicity as well as the appearance of monoclonal antibody techniques, ricin has become more interesting for clinical study. In order to avoid nonspecific binding to cells, only ricin A chains are used. Immunotoxins have shown potent, highly selective toxicity toward target cells *in vitro*. However, in *in vivo* studies, either on animals or humans, their antitumor effects have not been satisfactory (Vitetta and Thorpe, 1991).

Drug targeting is an attractive new approach to killing malignant cells, while leaving normal tissue unharmed. Ricin is prominent among a group of toxic proteins that have been used in attempts to selectively kill unwanted cells, in particular, malignant cells. Ricin has generally been linked to monoclonal antibodies by a disulfide bond, formed using hetero-bifunctional cross-linkers. These conjugates are called immunotoxins.

The first generation of immunotoxins (holotoxin conjugated to the antibody) produced impressive results *in vitro* but in most cases disappointing antitumor effects in

animals or humans (Gottstein *et al.*, 1994). By contrast, the second generation of immunotoxins, consisting only of the A-chain, have been demonstrated to have specific cytotoxicity toward their target cells and have been extremely effective in several animal models. Preliminary results of the current clinical trials suggest a possible clinical use for immunotoxins in leukemia and lymphoma patients (Amlot *et al.*, 1993; Winkler *et al.* 1994; Porro *et al*, 1993; Grossbard *et al.*, 1993).

Ricin toxin A chain-immunotoxins seems useful *in vitro* to purge bone marrow of unwanted cells prior to transplantation. In allogeneic bone marrow transplantation this has entailed using the immunotoxins to destroy T lymphocytes in the bone marrow taken from a histocompatible donor to reduce the incidence of graft-vs.-host disease (GVHD) in patients receiving the transplant (Vitetta *et al.*, 1991). Ricin toxin A chain-immunotoxins have generally proved more effective when the target cells are readily accessible to the blood-stream. In this regard, anti-T cell ricin toxin A chain-immunotoxins have been the most successful, particularly in the treatment of steroid-resistant, acute GVHD (Kerman *et al.*, 1988).

Ricin A chain-immunotoxins have been demonstrated to be more effective when target cells are easily accessible to the blood-stream. In 1988, Byers and her colleagues achieved very impressive results when using an H65 (CD5) ricin A chain immunotoxin to treat 15 patients who developed steroid-resistant GVHD after allogeneic bone marrow transplantation. Disease significantly decreased in twelve patients and completely remitted without any noticeable toxicity in 3 patients.

There are a considerable number of unsolved problems involved in the *in vivo* treatment of solid tumors. These include poor access of immunotoxins to the tumors, lack of immunotoxin specificity, tumor cell heterogeneity, antigen shedding, and breakdown or rapid clearance of the immunotoxins as well as dose-limiting side effects. Studies have been done to overcome these problems. For example, the ricin A-chain is naturally glycosylated with mannose- and fucose-containing oligosaccharides which bind to

mannose and fucose receptors which are in abundance on liver cells. This leads to a rapid hepatic clearance of immunotoxins (Blakey *et al.*, 1987, Bourrie *et al.*, 1986). Another approach, ricin A-chain is chemically deglycosylated prior to immunotoxin construction. A new coupling reagent, 4-succinimidyl-oxycarbonyl-a(2-pyridyldithio) toluene will hinder disulfide bonding between ricin A-chain and antibody and increase stability *in vivo* (Thorpe *et al.*, 1987). The results of treatment of solid cancers with intravenous immunotoxins are not impressive. However, they have been used successfully *in vivo* for local therapy, leading to the eradication of solid tumors by direct injection into the tumor (Kanellos, 1988).

Immunotoxins have also been used for treatment of rheumatoid arthritis. Rheumatoid arthritis is an autoimmune disease characterized by inflammation of synovial membranes and with increased numbers of active lymphocytes (80% T lymphocytes) in the synovium (Janossy *et al.*, 1981). Removing T cells resulted in clinical improvement in rheumatoid arthritis patients (Paulus *et al.*, 1977), since $CD4^+$ T-cells are the predominant T-cell population in the synovium of rheumatoid arthritis patients (Duke *et al.*, 1982). Anti-$CD4^+$ cell immunotoxins may be used to specifically remove the T cells involved in rheumatoid arthritis (Blakey and Thorpe, 1988). However, in order to prevent a general immune suppression, some specific antigens need to be found on the T cells responsible for rheumatoid arthritis. This treatment is still under investigation.

The last potential application of ricin to be discussed is the treatment of AIDS. The human immunodeficiency virus (HIV) envelope glycoprotein, gp120 is expressed on the surface of many HIV-infected cells and binds to $CD4^+$ on T cells. Soluble $CD4^+$ has been cloned (Fisher *et al.*, 1988). Recombinant $CD4^+$ has been coupled to ricin A chain and it was found that this conjugate kills the cells expressing the HIV-encoded gp120 (Till *et al.*, 1988). Also, ricin A chain-immunotoxins produced against another HIV protein, gp41 can also effectively destroy infected cells (Till *et al.*, 1989). A major limitation of this method

is that in the latent period of HIV infection, infected cells lack these molecules on their cell surface, and therefore they are not sensitive to immunotoxins.

I. Purposes of the Present Study.

This study was designed to investigate the effects of ricin on hemodynamics in the rabbits, including cardiac function, cardiac output, blood flow, blood distribution and on the contraction and relaxation of rabbit coronary arteries. Systemic hemodynamics can be simply described by an equation derived from Poiseuille's Law (Milnor, 1980): CO = BP / R, where CO = cardiac output, BP = blood pressure and R = peripheral resistance. These three factors are closely related to each other. A change in one factor must result in or from a corresponding change in another of the two factors.

Peripheral resistance is mainly regulated by small arterial vessels. These vessels can increase or decrease their vascular tone by contraction or relaxation of their smooth muscle in responses to a variety of external stimulations. Contractile stimuli cause vascular smooth muscle contraction by increasing the myoplasmic calcium concentration. The Ca^{2+} binds to calmodulin which activates myosin light chain kinase. Activated myosin light chain kinase phosphorylates the 20-kd myosin light chain and activates the myosin ATPase. The activation of myosin ATPase activity starts the cycling of cross-bridges between myosin and actin and, hence initiates contraction (Hathaway *et al.*,1991). Generally, there are two mechanisms for contractile stimuli to increase intracellular Ca^{2+}: 1) Membrane depolarization activates L-type Ca^{2+} channels, inducing Ca^{2+} influx. 2) Agonists bind to cell surface receptors and activate phospholipase C via G-proteins which increase 1,4,5-inositol triphosphate (IP_3) levels. The IP_3 releases Ca^{2+} from intracellular stores. Histamine and 5-HT contract coronary arteries via IP_3 pathway. Relaxing stimuli directly or indirectly increase cAMP or cGMP levels which enhance Ca^{2+} extrusion and sequestration (Rembold, 1992) in vascular smooth muscle and therefore decrease Ca^{2+} and induce relaxation. Furthermore, cAMP-dependent protein kinase will break cross-bridge

cycling via a phosphorylation of myosin light chain kinase which decreases myosin ATPase activity and facilitate relaxation (Conti and Adelstein, 1981). Norepinephrine induces relaxation of coronary arteries via a cAMP-dependent mechanism. Acetylcholine relaxes coronary artery by releasing endothelium derived relaxing factor which increases cGMP levels in vascular smooth muscle.

The coronary artery was used to determine whether ricin affects coronary artery contractility. Histamine and 5-HT were used to determine the ability of coronary arteries to respond to contracting agents, while NE and ACh were used to determine their ability to respond to relaxing agents (Griffith et al., 1984). Furthermore, the mechanisms of hemodynamic or vascular effects involved in second messenger systems including cAMP, cGMP and IP_3 were studied.

Several studies of the effects of ricin on performance of the isolated heart and papillary muscle were carried out, all in tissue from rabbits previously given ricin.

Studies on the effects of ricin on calcium flux in blood vessels, microsomes and mitochondria, and isolated myocyte, yielded information on the effects of ricin on calcium handling in blood vessels and the heart.

These studies provide important information for further understanding the changes in the cardiovascular system during ricin intoxication and the possible role of coronary arteries in lethality. Finally, this information would also be important for designing more effective therapy for ricin intoxication.

Hypothesis and Methods of Approach

1. Ricin alters cardiac output, blood distribution and blood flow to tissues and organs in rabbits.

Decreased blood pressure is a primary symptom both in human patients and in animals after ricin intoxication (Crompton and Gall, 1980; Robinson *et al.*, 1992). According to the hemodynamic rule, it is very likely that cardiac output and blood flow are changed during ricin intoxication. In order to investigate this, a radioactive microsphere technique was used. Microspheres of red blood cell size represented the circulation of red blood cells after injection into the rabbit heart. Blood flow changes provided information about the sensitivity to or the extent of damage to tissues or organs by ricin administration.

2. Ricin alters responses of coronary artery smooth muscle to some neuroeffectors.

In order to demonstrate whether or not ricin affects the function of rabbit coronary artery, contractions and relaxation of its smooth muscle to some endogenous vasoactive substances were evaluated. These agents participate in the maintenance or regulation of coronary artery tone *in vivo* and contract or relax coronary artery smooth muscle via receptor mediated mechanisms. The endothelium will be removed to avoid the influence of endothelium-derived relaxing factor (EDRF) and other contracting or relaxing factors. Histamine, serotonin and norepinephrine will be used in the experiment as they are endogenous vasoactive substances. The data will demonstrate whether there are any abnormalities in the related receptors and their coupling to effector systems.

3. Ricin damages the endothelium resulting in an altered ability to relax the artery smooth muscle by releasing EDRF.

The contractions of coronary arteries both with endothelium present and without endothelium to histamine and serotonin provided evidence for evaluation of endothelial

function, because these two artery preparations from normal animals have different responses (Griffith *et al.*, 1984) which may be altered in ricin-intoxicated arteries. Endothelial function also was evaluated by applying acetylcholine (ACh) to coronary artery preparations with an intact endothelium. The ACh relaxes coronary artery by directly stimulating the release of EDRF from endothelium (Angus *et al.*, 1984). An intact endothelium is necessary to prevent spontaneous coronary artery constriction (Lamping *et al.*, 1985).

4. *Ricin damages one or more pathways of intracellular signal transduction.*

Arterial vascular smooth muscle tone is directly regulated by the free intracellular calcium concentration which is raised or lowered by releasing or sequestering calcium by intracellular signal molecules. These molecules include cAMP, cGMP and inositol triphosphate (IP_3). The IP_3 opens calcium channels on intracellular stores (Berridge *et al.*, 1987), while cAMP and cGMP reduce the concentration of intracellular Ca^{2+} activating serial kinases. The EDRF-induced relaxation in artery smooth muscle is accomplished via a cGMP mechanism (Griffith *et al.*, 1985). So, any changes in the amount or the production rate of the above messengers will affect the function of coronary arteries. In the present study, cAMP, cGMP and the hydrolysis of inositol phosphate will be determined in rabbit coronary arteries.

5. *Ricin alters the activity of enzymes involved in the metabolism of endogenous neuroeffectors.*

There are two important enzymes in the initial steps of metabolic transformation of catecholamines and other biogenic amines (Axelrod, 1966), monoamine oxidase (MAO) and catechol-O-methyltransferase (COMT). Under physiological conditions, endogenous vasoactive amines are quickly deactivated after their release and receptor effects by MAO and COMT. Changes in the activities of these enzymes could alter the amount of some

endogenous amines available to their receptors on smooth muscle thereby altering contractile effects of these amines. Therefore the activities of MAO and COMT in the coronary artery were measured.

6. *Ricin alters cardiac function.*

Parameters measured included: heart rate, time to peak tension, contraction index, myocardial oxygen consumption, left intraventricular pressure and volume, effects of *alpha*- and *beta*-adrenergic receptor stimulation, and action potential of the myocardium.

7. *Ricin alters beta receptors, and signal transduction.*

Beta adrenergic receptor binding also were determined to help understand the effects of ricin on the *beta*-adrenergic receptor system. Effects of ricin on monoamine oxidase (MAO), catechol-*O*-methyltransferase (COMT), cyclic AMP, cyclic GMP, and phosphoinositide hydrolysis were also determined.

8. *Ricin alters calcium utilization.*

The effects of ricin on calcium uptake and release was studied in papillary muscle. Calcium uptake into mitochondria and microsomes was also examined. Effects on basal intracellular calcium concentrations in isolated myocytes was determined using Fura 2. The response of papillary muscle in the presence of Bay K 8644, a calcium channel opener, was also studied.

II. METHODS

A. Determination of Cardiac Output and Blood Flow Measurement with Radio-labeled Microspheres.

1. Surgical Preparation.

Twelve New Zealand White male rabbits were studied. The animals, weighing between 1.8 and 2.2 kg, were anesthetized with intravenous sodium pentobarbital (30 mg/kg). The submandibular region together with the left medial thigh and flank were shaved and sterilized with tincture of iodine and 70% ethanol. A small vertical incision, about 2.5 cm long, was made anteriorly in the right side of the neck and the right common carotid artery was exposed. A polyethylene catheter (i.d. 0.58 mm, o.d. 0.96 mm) was introduced into the right common carotid artery, advanced 6-8 cm into the left ventricle and secured with 3/0 sutures. The catheter exited at the dorsum of the neck through a subcutaneous tunnel. Another catheter was introduced into the abdominal aorta through the left femoral artery. Both catheters were imbedded subcutaneously. Each radioactive microsphere experiment was performed 24 hours after surgery.

2. Treatment of Rabbits.

Two rabbits were used as control animals. They were each given a sham injection of 1 ml of normal saline 12 hours before injection of the microspheres. The remainder of the rabbits were divided into a high dose group receiving a minimum lethal dose (0.44 μg/kg) of ricin and a low dose group receiving a toxic sub-lethal dose (0.22 μg/kg) of ricin. In each group, rabbits were given ricin 12 or 18 hours before microsphere injection.

3. Experimental Procedures.

Before blood flow determinations, the rabbit was fasted 24 hours in order to let the GI tract empty. The animals were kept quiet during the experiment. Approximately

800,000 microspheres (15 μ NEN-Trac microspheres, 40 mCi of Chromium-51 per gram, Du Pont Chemical Co.) in 0.5 ml saline solution from a well-shaken vial were mixed with 1.5 ml rabbit blood, sonicated and warmed to a temperature close to that of the rabbit. Then the mixture was slowly injected into the left ventricle. For ten seconds before and for one minute after the injection, a reference blood sample was withdrawn at 2.16 ml/min using a withdrawal pump (Harvard Apparatus). The pump served as a surrogate organ.

Two minutes after microsphere injection, the rabbit was sacrificed by i.v. injection of excess sodium pentobarbital and tissue samples were obtained. The skin, heart, aorta, lungs, trachea, bronchial tree, fat, liver, gall bladder, spleen, kidneys, adrenals, muscle, testes, brain, esophagus, stomach, and intestines were removed and weighed. Some organs were divided into subsections. For instance with the heart, inner, middle, and outer tissue samples were taken. For small organs, the total counts were determined by placing them into more than one counting vial. For larger organs, several pieces of tissue were counted. Counts were averaged and calculated to obtain the total uptake for the entire organs. Three pieces of skin were taken from the leg, abdomen and chest. The muscle sample was taken from the gluteus maximus muscle. All samples were packed to the same height in counting tubes to minimize differences in counting efficiency.

4. The Radioactive Microsphere Technique and Blood Flow Calculation.

Chromium-51 labeled 15 μm diameter microspheres were prepared for injection. The total amount of radioactivity of the microspheres was determined using a radioisotope dose calibrator CRC-1OR (Capintec). Before injection, the mixture was warmed and well sonicated to keep the microspheres evenly distributed. The injection time was maintained at about 40 seconds. The catheter was flushed with saline to ensure that all microspheres had been injected and clamped to prevent fluid from leaking back. The syringe together with the attached needle was removed and counted in the dose calibrator. The net total radioactivity injected was calculated by subtracting the radioactivity remaining in the

syringe from the original radioactivity. All tissue samples, reference blood samples and both catheters were counted using a gamma counter (Multi-Prias Gamma Counting System, Model A5302, Packard Instrument Co). The relationship between the radioactivity measured in the dose calibrator and the gamma counter (CPM) was calculated by counting several standard samples in both. The cardiac output and tissue blood flow were calculated according to Hale's equation (Hales 1974):

$$\text{Cardiac Output} = F_a \; I_{total} / I_a$$

$$\text{Organ Blood Flow} = F_a \; I_{tissue} / I_a$$

Where F_a = reference sample flow rate into the withdrawal pump.

I_{total} = total dose of radioactivity injected in μCi.

I_a = amount of radioactivity in the reference sample in μCi.

I_{tissue} = amount of radioactivity in each organ in μCi.

Blood flow to tissues or organs was calculated as ml/min per 100 g tissue or percent of total cardiac output. Blood flow to the right and left kidneys were compared in order to determine the adequacy of mixing of microspheres in the left ventricle.

B. Treatment of Rabbits for the Rest of the Experiments.

1. For Experiments with Coronary Arteries.

New Zealand White male rabbits (1.5-2.5kg) were injected with 0.22 μg/kg of ricin or sham injected, into a marginal ear vein and sacrificed with sodium pentobarbital (45 mg/kg) 48 hr later. This dose of ricin was chosen because it is a sub-lethal dose which causes measurable effects on the cardiovascular system (Christiansen *et al.*, 1994a,b). In the following experiments, at least six and no more than nine rabbits were used in control and ricin-injected groups.

2. For Experiments with the Heart and Papillary Muscle.

New Zealand White male rabbits (1.5-2.5 kg), were injected with a minimum lethal dose (0.22 μg/kg) of ricin or sham injected into a marginal ear vein. At forty-eight hours, the rabbits were given ether anesthesia. To prevent blood coagulation, 200 U/kg of sodium heparin in saline were injected intravenously. Rabbits were sacrificed with a blunt blow on the head, then they were exsanguinated and tissues were removed.

C. Determination of the Effects of Ricin on Contractions and Relaxations of Rabbit Coronary Artery Rings.

1. Tissue Preparation:

The heart was removed and placed into cold (10-15°C) Krebs solution of the following composition (mM): 118.5 NaCl, 4.7 KCl, 1.2 $MgCl_2$, 23.8 $NaHCO_3$, 1.2 KH_2PO_4, 11 d-glucose, 2.5 $CaCl_2$ and 0.01 EDTA, aerated with 95% O_2/5% CO_2, at a pH of 7.4. The left ventricular circumflex coronary artery was carefully dissected out and cleaned, while being continuously perfused with cold Krebs solution. The artery was cut into ring segments each 3 mm wide. Endothelium removal was attained by gently rubbing the inner surface with a 0.3 mm diameter stainless steel insect pin (Keef *et al.*, 1991). Rings were mounted onto two triangular tungsten wire supports (152 μm diameter) and suspended in 6 ml water jacketed organ baths containing 4 ml of Krebs solution and maintained at 38°C. A resting tension of 0.6 g (2 mN/mm) was applied to the coronary artery rings. Under this tension the vessels are stretched to the optimal length for tension development (Nielsen-Kudsk *et al.*, 1986). Artery rings were equilibrated for 1.5 hr during which the bathing fluid was changed every 15 min. They were then exposed to 55 mM KCl for 4 min twice at 15 min intervals. Tension was measured using Metrigram isometric force transducers (Model 797159-1, Gould Inc., Cleveland, OH) and recorded by a Gould RS 3800 Recorder.

2. *Measurement of Rabbit Coronary Artery Ring Contraction:*

After equilibration, contractions of coronary artery rings with and without endothelium to 5-HT and histamine were measured. The agents were added to the tissue bath in a cumulative fashion in half-log increments. Each ring segment was allowed to contract maximally to each concentration. The contraction which was no longer increased by the next concentration was regarded as the final maximum contraction. The contraction to each concentration was reported as absolute tension. After each experiment, artery rings were re-equilibrated for at least 30 min with 5-min exposure to 55 mM KCl at 15 min intervals.

3. *Measurement of Rabbit Coronary Artery Ring Relaxation:*

Relaxations of coronary artery rings with and without endothelium to ACh and NE were measured. After the contraction studies, the same rings were pre-contracted with 3.5 x 10^{-4} M 2-(2-aminoethyl)pyridine (AEP) and once a stable contraction was obtained, NE was added in a cumulative fashion in half-log increments. The rings were re-equilibrated and relaxations to ACh were recorded in the same manner. Relaxations are expressed as a percent of the initial AEP contraction.

D. Determination of the Effects of Ricin on MAO and COMT Activities in Rabbit Coronary Artery and Papillary Muscle.

1. *Preparation of Rabbit Coronary Artery.*

After euthanasia the rabbit heart was removed and placed in cold (10-15^{o}C) oxygenated Krebs solution. All branches of the coronary artery (left and right coronary arteries) were isolated as completely as possible while the tissue was continuously perfused with cold Krebs solution. The tissues were stored in a -70^{o}C freezer until enough samples were collected.

2. *Measurement of MAO Activity in Coronary Arteries.*

MAO activity was determined by the method of Wurtman and Axelrod (1963). Fifteen milligrams of tissue were homogenized in 0.4 ml of ice-cold 0.15 M KCl solution with a 2 ml glass homogenizer, then centrifuged at 1,000 g for 20 minutes at 4° C. Forty µl of the supernatant were placed into a 1.5 ml Eppendorf microcentrifuge tube which contained 40 µl of 0.5 M phosphate buffer at pH 7.4, 40 µl of 0.5 mM tryptamine containing 0.005 µCi of [^{3}H]-tryptamine (26.4 Ci/mmol). The vials were agitated for 60 minutes at 37°C, then the reaction was stopped by the addition of 40 µl of 2 N HCl. The tryptamine metabolite (indoleacetic acid) was extracted into 1 ml of toluene by mixing on a vortex mixer for 15 seconds. The layers were separated by centrifuging for 5 minutes at 1000 g. A 0.5 ml aliquot was removed from the organic layer and the radioactivity from the tryptamine metabolite was counted by scintillation spectrometry. Boiled enzyme and zero time blanks were used as controls. A sample of the total labeled tryptamine was placed directly into a counting vial at the same time that it was placed into the incubation medium. This was the `total activity' which was counted along with the tissue samples at the same time. The ratios of these two counts were used to calculate the enzyme activity which was finally expressed as nanomoles of substrate deaminated/min/mg protein. Most measurements were made in triplicate. Some measurements were made in 5 replicates. The protein was assayed using a Bio-Rad Protein Assay Kit.

3. *Determination of Monoamine Oxidase Activity of the Papillary Muscle.*

Determination of monoamine oxidase (monoamine: O_2 oxidoreductase [deaminating] EC 1.4.3.4.) activity in papillary muscles was by the method of Wurtman and Axelrod (1963). Fifty mg of each tissue was homogenized in 3 ml of 0.15 M KCl using a Polytron homogenizer at a setting of 2. The homogenate then was centrifuged at 1,000 g for 20 min in a refrigerated centrifuge (4° C). The supernatant was used for the MAO

assay. The reaction was started by incubating 100 µl of supernatant at 37° C for 20 min with the following solutions: 100 µl of 0.5 M phosphate buffer (pH 7.5), 50 µl of 1.0 mM tryptamine, and 50 µl of 0.05 µCi [^{14}C]-tryptamine bisuccinate (specific activity 55.2 Ci/mmole). Two kinds of blanks were used: a boiled enzyme (90° C, 5 min) and a zero time blank to which 0.2 ml of 2 N HCl was added at zero time, i.e. before incubation. The reaction was stopped and the solution was made acidic with 0.2 ml of 2 N HCl. The metabolite, indoleacetic acid, was extracted with 4 ml of toluene during vortexing for 30 seconds. The organic phase was separated from the aqueous phase by centrifugation at low speed for 5 min. Two ml of the organic phase were collected in a 20 ml counting vial and mixed with 5 ml of scintillation cocktail, ScintiVerse^{TM}, for radioactivity determination. Data were expressed as nanomoles of indoleacetic acid/g wet weight of tissue/min.

4. Measurement of COMT Activity in Coronary Arteries

COMT was determined by the method of Axelrod (1962) as modified by Wrenn *et al.* (1979) and Roth (1980, 1982). Fifteen mg of coronary artery were placed in 0.4 ml of ice-cold 0.05 M phosphate buffer at pH 7.4 and homogenized as described in the MAO assay description. The homogenate was then centrifuged at 10,000 g for 20 minutes at 4° C. Twenty µl of the supernatant were placed into a 1.5 ml Eppendorf tube which contained 5 mM $MgCl_2$, 0.1 mM S-adenosyl-L-methionine, 1 mM pargyline, 0.1 mM dopamine and 0.02 µCi [^{3}H] dopamine (15.5 Ci/mmol) in a final volume of 50 µl 0.05 M phosphate buffer at pH 7.4. The vials were agitated for 60 minutes at 37°C, then the reaction was stopped by the addition of 100 µl of borate buffer (pH 10). The [^{3}H] O-methylated dopamine metabolite was extracted into 1 ml of toluene/isoamyl alcohol (3:2,V:V) by mixing on a vortex mixer for 15 seconds. The layers were separated by centrifugation for 5 minutes at 1000 g. A 500 µl aliquot was removed from the organic layer and the radioactivity from the labeled dopamine metabolite was counted using scintillation

spectrometry. As in MAO assay, the tissue samples and the total radioactivities added in the reaction mixture were counted together. Boiled enzyme and zero time blanks were used as controls. The ratio of DPM extracted to the total DPM was used to calculate the nanomoles of substrate having been O-methylated. The data were expressed as nanomoles of substrate O-methylated/min/mg protein. All measurements were made in triplicate. The protein content was determined as in the MAO assay.

5. *Determination of Catechol-O-Methyltransferase Activity of the Papillary Muscle.*

Catechol-*O*-methyl transferase activity determination was based on the method of Wrenn *et al.* (1979). Thirty to ninety milligrams of papillary muscle were placed in 1 ml of ice-cold 0.05 M phosphate buffer at pH 7.4 and homogenized with a Brinkmann Polytron homogenizer at a setting of 3 for three 15 second bursts. The homogenates were then centrifuged at 43,000 g for 20 minutes at 5° C. Four hundred microliters of the supernatant were placed into a reaction tube which contained 300 µl of 0.05 M phosphate buffer at pH 7.4, 12.5 µl of 0.1 M MgCl, 50 µl of 10mM S-adenosylmethionine, 50 µl of 10 mM pargyline, 50 µl of 4 mM dopamine and 0.2 µCi of [^{3}H]-dopamine. The tubes were agitated for 40 minutes at 38° C, then the reaction was stopped by the addition of 1.5 ml of 0.5 M potassium borate buffer at pH 10.0. The *O*-methylated dopamine metabolite was extracted into 5 ml of toluene/isoamyl alcohol (3:2, V:V) by mixing on a Vortex mixer for 30 seconds. The layers were separated by centrifuging for 5 minutes at 1000 g. A 2 ml aliquot was removed from the organic layer and the radioactivity from the labeled dopamine metabolite was determined using scintillation spectrometry. Boiled enzyme and zero time blanks were used. After conversion of CPM to DPM the greater of the two blank values was subtracted. An equation (fraction of total radioactivity extracted into the organic layer X moles of substrate in the reaction) was used to convert the radioactivity extracted to moles of substrate methylated. The data were expressed as nanomoles of substrate methylated/g wet weight of tissue/minute.

E. Determination of the Effects of Ricin on the cAMP and cGMP Content of Rabbit Coronary Artery and Right Ventricular Papillary Muscle.

1. Basal Concentrations and the Time Course of Stimulated cAMP .

The cAMP contents were determined by radioassay techniques using Amersham cAMP radioimmunoassay kits. The coronary arteries from control and ricin-treated rabbits were cut into 6 parts and incubated without tension for 60 min at 37° C in 4 ml of Krebs solution aerated with 95% O_2 - 5% CO_2, with solution changed every 20 min. The coronary arteries were then stimulated with 10^{-4} M histamine. The stimulations were stopped by removing the tissues and immersing them in an ethanol dry-ice bath as quickly as possible at 15, 30, 60, 120, and 180 seconds. The tissues without histamine stimulations were also immersed in the ethanol dry-ice bath and used as samples for 0 second. After that, the tissues were stored in a -70° C freezer for future assay. Each of the tissues was homogenized with 0.4 ml of 5% TCA at 0° C using a 2 ml glass homogenizer. The homogenate was centrifuged at 3000 x g for 30 min at 4° C to remove cellular debris and precipitated proteins. Because TCA in the supernatant may interfere with the assay, the supernatant was extracted 4 times with 3 volumes of water-saturated ether to remove TCA. The aqueous extract was used for cAMP determination (Vulliemoz *et al.*, 1986). All determinations were made in duplicate. The pellet was used for protein determination using the Bio-Rad protein assay Kit (Bio-Rad Lab, Richmond, CA).

2. Effects of Ricin on Accumulation of cAMP and cGMP in Coronary Artery Following Histamine Stimulation.

The tissue preparations and cAMP or cGMP assays were the same as that in the time course experiment. The coronary arteries were stimulated with two different concentrations of histamine, 10^{-6} M and 10^{-4} M. As stimulated cAMP reaches a maximum at 15 seconds, the reactions were stopped at 15 seconds with ethanol and dry ice.

3. Determination of the Effects of Ricin on Basal Levels of cyclic Nucleotides in Right Ventricular Papillary Muscle.

The right ventricular papillary muscle was homogenized in 5% trichloroacetic acid. The homogenate was centrifuged at 3000 x g for 15 min at 4° C. The supernatant was extracted 4 times with water-saturated ether to remove trichloroacetic acid. The levels of cAMP and cGMP in the aqueous extract were determined by using cAMP and cGMP assay kits (Amersham, Arlington Heights, IL), respectively. The results were expressed as pmol/mg wet weight.

F. Determination of the Effects of Ricin on the Hydrolysis of Inositol Phosphates in Coronary Arteries and Papillary Muscle.

1. Preparation and Incubation of the Rabbit Coronary Artery.

Isolated coronary arteries from control and ricin-treated rabbits were cut into 3 approximately equal portions and incubated without tension for 60 min at 37° C in 100 ml of Krebs solution aerated with 95% O_2 - 5% CO_2. Coronary artery pieces were then transferred into small vials containing 10 μCi/ml of myo[2-^{3}H(N)]-inositol (specific activity: 105 Ci/mmol) in 750 μl Krebs solution for two hours to label endogenous phospholipid stores in smooth muscle. During this two hour period they were maintained at 37° C, aerated with 95% O_2 -5% CO_2, and gently agitated in a shaker-water bath. After a brief rinse, these tissues were placed into three beakers containing 4 ml of fresh 10 mM lithium chloride in Krebs solution for 30 minutes at 30° C with gentle shaking and aerated with 95% O_2 -5% CO_2. One of the beakers contained 10^{-6} and the other 10^{-4} M histamine from the beginning of this incubation to stimulate cyclic nucleotide production. Lithium chloride was used to inhibit inositol phosphate breakdown (Berridge *et al.*, 1982). The

incubation was terminated by immersion in an ethanol/dry ice bath and the tissues were frozen at -70° C for future assay.

2. *Measurement of [^{3}H]-Inositol Phosphates in the Coronary Artery.*

The procedure described by Berridge and co-workers was used (1983) in this study. Tissues were weighed then thawed and homogenized with a 2 ml glass homogenizer in 0.6 ml of ice-cold 3.6% (W/V) perchloric acid and centrifuged at 2,500 RPM at 4° C for 15 minutes. The supernatant of each sample was added with an equal volume of 0.5 M KOH / 9 mM sodium tetraborate / 1.9 mM EDTA / 3.8 mM sodium hydroxide to bring the pH to 8-9 as detected by pH test paper. The supernatant was applied to a 1 ml volume AG 1-X8 anion exchange resin (formate form) columns and eluted sequentially with:

a) 20 ml of distilled water

b) 20 ml of 5 mM disodium tetraborate/60 mM sodium formate

c) 10 ml of 0.2 M ammonium formate/0.1 M formic acid

d) 20 ml of 0.4 M ammonium formate/0.1 M formic acid

f) 20 ml of 1.0 M ammonium formate/0.1 M formic acid

Two ml fractions were collected and counted by standard liquid scintillation counting techniques. The amount of [^{3}H] inositol phosphates accumulated were expressed as counts/mg wet tissue.

3. *Effects of Ricin on Phosphoinositide Hydrolysis in Right Ventricular Papillary Muscle.*

Phosphoinositide Hydrolysis: Right papillary muscles were removed from the heart, weighed, and equilibrated for 30 min at 37° C in 4 ml of Krebs solution aerated with 95% O_2-5% CO_2. After equilibration, the tissue was incubated with 24 μCi of [^{3}H]-myo-inositol in 4 ml of Krebs solution for 3 hrs to label papillary muscle phospholipid stores.

The tissue was then incubated for 30 min in 4 ml of fresh Krebs solution containing 10 ml of lithium chloride. The reaction was terminated by immersing the tissue in ethanol-containing dry ice. The tissue was homogenized in 1.5 ml of ice-cold 3.6% (w/v) perchloric acid and centrifuged at 2500 rpm for 15 min at 5° C. The perchloric acid was removed by adding equal volumes of 0.5 M KOH / 9 mM sodium tetraborate / 1.9 mM EDTA / 3.8 mM sodium hydroxide to bring the pH to 8-9 which was checked by pH test paper. The supernatant was applied to a 1 ml volume column containing AG 1-X8 (anion exchange resin, 100-200 mesh, formate form, Bio-Rad, Richmond, CA) and eluted sequentially with: (1) 20 ml of distilled water, (2) 20 ml of 5 mM disodium tetraborate; 60 mM sodium formate, (3) 10 ml of 0.1 M formic acid; 0.2 M ammonium formate, (4) 20 ml of 0.1 M formic acid; 0.4 M ammonium formate, (5) 10 ml of 0.1 M formic acid; 1.0 M ammonium formate. Two ml fractions were collected and counted in a liquid scintillation counter. The amount of [^{3}H]-inositol phosphates accumulated was expressed as dpm/mg wet weight.

G. Determination of the Effects of Ricin on Contractions of the Electrically-Stimulated Papillary Muscle.

Right ventricular papillary muscles were dissected free and mounted in 40 ml tissue baths containing oxygenated Tyrodes solution (140 mM NaCl, 2.0 mM $CaCl_2$, 1.0 mM $MgCl_2$, 1.0 mM Na_2HPO_4, 5.0 mM KCl, 5.0 mM HEPES, 5 mM NaOH, 10.0 mM glucose, and 0.5 mM aspartic acid) at a pH of 7.35, equilibrated with 100% O_2, and maintained at 37° C. Each papillary muscle was attached to a Grass isometric force-displacement transducer (FT03B), and was coupled to a Grass polygraph (Model 5) for recording. Muscles were stimulated via bipolar punctate platinum electrodes with 2-ms square-wave pulses at a frequency of 1 Hz. A period of at least 1 hour was allowed to elapse to ensure stable performance of the tissues. Force development was continuously recorded on a Grass polygraph with stimulation frequency increasing in increments from an

initial frequency of 0.5 Hz up to 3 Hz. Papillary muscle mass and length were determined and active tension development was expressed as grams/cross-sectional area (mm^2).

H. Determination of the Effects of Ricin on Contractions of the Electrically Stimulated Papillary Muscle in the Presence of Isoproterenol.

Papillary muscles were prepared and the experiments were done as before, but this time in the presence of the *beta*-adrenoceptor agonist isoproterenol. Dose-response relationships for isoproterenol (given in 0.5 log unit increments from 1×10^{-9} to 10^{-7} M) were obtained from cumulative additions of the drug to the tissue baths. The response to each concentration was allowed to plateau over a 15-min interval before further addition of the drug to the bath. The increased active tension development observed with the administration of isoproterenol was expressed as a percentage of the maximum tension generated by paired pacing.

I. Determination of the Effects of Ricin Administration on the Electrophysiological Properties of Rabbit Papillary Muscle.

Rabbit hearts from control and treated rabbits were placed into Krebs solution containing the following mM composition: NaCl, 118.5; $MgCl_2$, 1.2; KCl, 4.7; d-glucose, 11; $NaHCO_3$, 23.8; $CaCl_2$, 2.5; and KH_2PO_4, 1.2. Rabbit right ventricular papillary muscles with some attached ventricular wall were isolated and mounted in a chamber with constant superfusion of Krebs solution, which was maintained at 38°C and aerated with 95% O_2-5% CO_2. The papillary muscles were electrically driven at 60 beats/min via platinum electrodes by rectangular impulses of 4 ms duration and twice threshold intensity delivered from a stimulator.

Excitability was determined by measuring the electrical threshold. The effective refractory period was measured by applying a test stimulus at three times threshold intensity at various times following the driving impulse. Every tenth pacing stimulus was

followed by an extra stimulus placed within the absolute refractory period, and moving out by 10 ms increments until the first extra beat appears.

Action potentials were recorded from the papillary muscle by conventional glass microelectrodes filled with 3 M KCl (impedance 10-15 mΩ) and coupled to a high impedance DC amplifier. The action potential was monitored continuously on a dual beam oscilloscope and recorded. The depolarization phase of the action potential was differentiated with an analogue differentiator and the maximum rate of rise of the action potential, V_{max}, was also recorded.

J. Determining the Effects of Ricin Administration on Cardiac Performance in the Isolated Perfused Rabbit Heart.

New Zealand White rabbits weighing between 2.0 and 3.0 kg were given a MLD of ricin i.v. into a marginal ear vein, or sham injected. At forty-eight hours, the hearts were removed. To prevent blood coagulation, 200 U/kg of sodium heparin in saline was injected intravenously. The rabbits were anesthetized by ether inhalation, euthanized by a blunt blow to the head and decapitated. The thoracic cage was opened, and the heart was quickly excised and perfused retrogradely at 37° C using a constant flow pump (Masterflex, Cole-Parmer Instruments, Chicago, IL) through a plastic cannula inserted into the aorta. The perfusate was a modified Tyrodes solution. Oxygen tension and pH were measured by a blood gas analyzer (Nova Biomedical Statlab 5, Waltham, MA). After initiation of coronary perfusion, a small plastic tube was inserted into the left ventricle through an apical puncture to drain the perfusate. The O_2 tension of the perfusate from the pulmonary artery was also measured by the blood gas analyzer. A latex balloon connected to a short polyethylene tube (10 cm long) was inserted into the left ventricle through the A-V valve. The left and right atria were tied around the tube to prevent the balloon from prolapsing. The balloon was then filled with bubble-free water, and the left ventricular pressure (LVP) generated was measured with a Statham P23 ID transducer (Statham

Instruments, Oxnard, CA) attached to the polyethylene tube. Coronary perfusion pressure (CPP) was measured throughout the experiment. The electrocardiogram (ECG) was obtained using epicardial hook-shaped electrodes attached to the right ventricular outflow and the LV apex proximately. The perfusion flow was fixed. The balloon volume was adjusted as the LV end-diastolic pressure (LVEDP) was set to 5 to 10 mm Hg.

After a stable condition was attained (in about 30 min) with oxygenated modified Tyrodes solution perfusion, baseline measurements of coronary perfusion pressure (CPP), coronary flow, and ECG were made. The balloon volume was then adjusted from 0.3 ml to 1.7 ml with 0.2 ml increments, and the LVP, LVEDP, +dp/dt and -dp/dt were recorded at each step, in triplicate for each rabbit heart. Permanent records were obtained on a Grass Model 7 polygraph.

In seventeen rabbit hearts (nine control and eight from rabbits given ricin 48 hrs earlier), isoproterenol was incrementally added to the perfusate as follows: 10^{-9}, $3.2x10^{-9}$, and 10^{-8} M. Hemodynamic measurements were repeated at each isoproterenol concentration. All parameters were recorded after a stable condition was attained in 10 min at each dose-step in each group.

The experiment was continued after a 30 minute washout period. The perfusate was switched from the control modified Tyrodes to one containing 10^{-7} M propranolol to block any possible *beta*-adrenoceptor stimulation by phenylephrine. Stepwise phenylephrine perfusion was then started as follows: 10^{-9}, 10^{-8}, 10^{-7}, and 10^{-6}-M with a 10 minute stabilization interval between concentrations. The concentration of propranolol in the perfusate was maintained at 10^{-7} M throughout the phenylephrine infusion. At the end of the experiment, the heart was detached from the perfusion apparatus. The left and right ventricles were lightly blotted and weighed.

K. Determination of the Effects of Ricin Administration on the Affinity and Density of ß-Adrenergic Receptors in the Rabbit Myocardium.

The rabbit myocardium was placed in an ice-cold buffer (5 mM Tris-HCl and 1 mM $MgCl_2$, pH 7.4), minced with scissors and homogenized 3 times with a Brinkman Polytron for 20 sec at a setting of 8. The homogenate was filtered through 4 layers of gauze. The filtrate was centrifuged at 500 g for 10 min at 4° C. The supernatant was then centrifuged at 40,000 g for 30 min at 4° C. The resulting pellet was resuspended in buffer (50 mM Tris-HCl, 10 mM $MgCl_2$ and 1 mM EDTA, pH 7.5) and used in the binding assays.

The radioligand binding in the membrane preparations was determined by incubating 100 µl of the suspended pellet with various concentrations of I-[4, 6, propyl-^{3}H]-dihydroalprenolol, a beta-adrenergic antagonist, in a final volume of 150 µl for 60 min at 38° C in a shaking water bath (150 cycles/min). The reaction was terminated by adding 4 ml of ice-cold incubation buffer, and the reaction mixture was filtered rapidly through GF/C glass fiber filters (Whatman, Clinton NJ) on a manifold under vacuum. The filters were washed twice with 4 ml of ice-cold incubation buffer at room temperature and counted in a liquid scintillation counter. Non-specific binding of ^{3}H-dihydroalprenolol was defined as the radioactivity bound to membranes which was not displaced by 10 µM propranolol. Specific binding of ^{3}H-dihydroalprenolol was defined as total radioactivity minus nonspecific binding. All assays were done in duplicate. Protein content of the membrane preparation was determined using the Bio-Rad kit (Bio-Rad Lab, Richmond, CA).

L. Determination of the Effects of Ricin Administration on the Electrically Stimulated Papillary Muscle in the Presence of the Calcium Channel Opener, Bay K 8644.

Papillary muscles were prepared and the experiments were done as before except in the presence of an L-type calcium channel opener, Bay K 8644. Dose-response

relationships for Bay K 8644 (given in 0.5 log unit increments from 1 x 10^{-9} to 10^{-6} M) were obtained from cumulative additions of the drug to the tissue baths. The response to each concentration was allowed to plateau over a 15-min interval before further addition of the drug to the bath. The increased active tension development observed with the administration of Bay K 8644 was expressed as a percentage of the maximum tension generated by paired pacing.

M. Determination of Intracellular Calcium Concentrations (Fura-2).

The rabbit heart was perfused retrogradely in the Langendorff mode for 10 min with a Ca^{2+}-containing modified Tyrodes buffer at 37° C gassed with 100% O_2 to maintain a pH of 7.30. The heart was then perfused for 5 min with an identical buffer from which $CaCl_2$ was omitted. The effluent from the first 10 min was discarded. Collagenase (Cooper Biomedical class II) and bovine serum albumin (BSA) (Miles Laboratories, Pentex fraction V) were added to the Ca^{2+}-free buffer (1 mg/ml each) and the hearts were perfused in a recirculating mode with 50-60 ml of this medium for 10 min until they became flaccid. The heart was removed from the apparatus, and the atria and large vessels were cut away and discarded. The left ventricle muscle was minced with fine scissors and incubated for 5 min in perfusion buffer containing 20 mg/ml BSA. The remainder of the isolation procedures were patterned after those of Powell and Twist (1976).

Intracellular calcium levels in myocytes after ricin administration were determined by the method previously described by Grammas and Fugate (1992). The instrumentation used for the measurement of $[Ca^{2+}]_i$ consisted of a Nikon Diaphot (Tokyo, Japan) inverted microscope optically interfaced to an SLM DMX-1000 (Urbana, IL) fluorometer. Excitation light at either 340 or 380 nm was chopped at 300 Hz while emission was isolated by a long-pass (KV470) filter. The objective was a Nikon Fluor 40X oil with 1.30 numerical aperture. A cooled Hamamatsu R928P (Ridgewater, NJ) was used as the

detector. The signal was recorded on the SLM DMX-1000 fluorometer as the intensity ratio. A video camera (Hamamatsu C2400 SIT) was used to locate the cells.

Subsequent to isolation, cells were diluted 10 times with a N-2-hydroxyethylpiperazine-N'-2-ethanesulfonic acid (HEPES) buffer contain (in mM): 118 NaCl, 4.8 KCl, 25 HEPES, 1.2 KH_2PO_4, 1.2 $MgSO_4$, 1 $CaCl_2$, 2 sucrose, and 5 pyruvate. Myocytes from control rabbits and those receiving ricin were loaded with the acetoxymethyl ester (AM) of fura-2, the membrane-permeable form of the fluor. Optimal conditions for loading myocytes were 30-min incubation at room temperature at a final concentration of 1 μM fura-2 AM [dissolved in dimethyl sulfoxide (DMSO)] in Dulbecco's minimum essential medium (DMEM) supplemented with pluoronic acid. The final concentration never exceeded 0.1% of DMSO in the cellular suspension. These conditions provided a diffusely-labeled cell, with no discernable compartmentation of the dye. In myocytes these conditions led to a calculated $[Ca^{2+}]_i$ of 100 ± 14 nM. The equation $[Ca^{2+}]_i = K_d[(R - R_{min})/(R_{max} - R)]$ ß was used to calculated the $[Ca^{2+}]_i$. Here, R is the ratio of emission intensities when exciting at 340 and 380 nm, R_{min} is the ratio in the absence of Ca^{2+} (10 mM EGTA in Ca^{2+}-free buffer), and R_{max} is the ratio in the presence of saturating Ca^{2+}. The K_d used was 224 nM in accordance with the appropriate literature value for our conditions (Grammas, 1992) and ß was the ratio of intensities for the Ca^{2+}-free and saturated forms when excited at 380 nm. Experiments were performed as indicated to establish basal levels.

N. Determination of Calcium Uptake by Rabbit Papillary Muscle.

Rabbit hearts from control and treated rabbits were placed into oxygenated Tyrodes solution (pH 7.35) containing the following mM composition: NaCl, 140; $MgCl_2$, 1.0; KCl, 5; d-glucose, 10; NaOH, 5; $CaCl_2$, 2; HEPES, 5; aspartic acid, 0.5 and Na_2HPO_4, 1.0. Each rabbit right ventricular papillary muscle with some attached ventricular wall was attached to a Grass isometric force-displacement transducer (FT03B) and stimulated via

bipolar punctate platinum electrodes with 2 ms square-wave pulses of two times threshold voltage at a frequency of 1 Hz. Length was adjusted to provide twitch tension equal to 70% of the maximum. After an hour of equilibration, the paced muscle was placed in 4 ml of Krebs solution containing $^{45}Ca^{2+}$ (10.5 μCi/ml) for 2.5 or 5 min. Then the tissues were dipped into 100 ml of Krebs solution for 30 sec, blotted and weighed. The muscle was then dissolved overnight in 0.5 ml of Soluene-350 (Packard). Ten ml of scintillation cocktail (ScintiVerse^{TM}) was added and the vials were counted in a liquid scintillation counter. Uptake of $^{45}Ca^{2+}$ was calculated using the following equations: $^{45}Ca^{2+}$ (mmol/kg wet weight) = dpm in muscle x mmol Ca^{2+} in medium/dpm in medium x weight (kg).

O. Preparation of Cardiac Microsomes and Determination of Microsomal Calcium Uptake.

The left ventricle was homogenized in a medium composed of 0.25 *M* sucrose, 5 m*M* sodium azide, and 2 m*M* ascorbic acid in 5 m*M* Tris buffer (pH 6.8 at 4° C). Microsomes were isolated as described by Shlafer and co-workers (1978). The final pellet was resuspended in 50 m*M* KCl in 20 m*M* Tris-maleate buffer solution (pH 6.8 at 4° C). Microsomal protein concentrations were determined in triplicate with bovine serum albumin as the standard.

Calcium accumulation (as $^{45}CaCl_2$) was studied using Millipore filtration of a medium containing 0.1 *M* KCl, 10 m*M* $MgCl_2$, 100 μM $CaCl_2$ (0.1 μCi ^{45}Ca/l), 5 m*M* Tris-ATP, and 30-50 μg/ml microsomal protein in 20 m*M* Tris-maleate (pH 6.8) at 25° C. Radioactive Ca^{2+} accumulation was calculated by counting the dried filter. Counts due to simple absorption of the isotope and Ca^{2+} accumulation in the absence of added ATP (parallel sample) were subtracted. All determinations were based upon the results of duplicate samples measured at each time.

P. Mitochondria Preparation and Determination of Mitochondrial Calcium Uptake.

The left ventricle was homogenized in 12 volumes of KCl-ethylenediaminetetraacetate (KEA) medium per gram of tissue for three or four seconds with a Polytron tissue processor at a rheostat setting of two. The KEA medium (pH 7.2-7.4) consists of 0.18 M KCl, 10 mM ethylenediaminetetraacetate (EDTA), and 0.5 percent bovine serum albumin (Sigma, Fraction V). The homogenate was centrifuged at 1,200 x g for 10 minutes. The supernatant was strained through several layers of cheesecloth and centrifuged at 10,000 x g for 15 minutes. The resulting mitochondrial pellet was resuspended in KEA medium (approximately half the volume used in the initial homogenization) and centrifuged at 10,000 x g for 8 minutes. This washing procedure was repeated once or twice to remove cellular contaminants adhering to the mitochondria. The mitochondria were finally suspended in KEA medium (approximately half a ml of medium per gram of original tissue) to yield a suspension containing 20 to 30 mg of mitochondrial protein per ml. The protein concentration was determined by the Biuret method (Jacobs *et al.*, 1956).

The effect of ricin administration on calcium uptake into mitochondria was determined by incubating 100 µl of the mitochondrial fraction at 37° C with 900 µl of incubation medium (pH 7.0) containing the following: 30 mM tris (hydroxymethyl) aminomethane; 80 mM of the salt of adenosine triphosphate; and 4 x 10^{-4} mCi $^{45}CaCl_2$ in 30 µM Ca^{2+}. Aliquots of 100 µl of the incubation mixture were pipetted at 2, 4, 6, and 8 min into a 0.45 µl Millipore filter held by a 10-port manifold under vacuum and washed with 2 ml of isotonic sucrose solution. The Millipore filter, which retained the microsomes, was counted in a liquid scintillation counter. Prior to use, each Millipore filter was prewashed with 2 ml of 0.25 M KCl and 10 ml of distilled water to reduce non-specific retention of ^{45}Ca on the filter. Results were expressed as µmoles Ca^{2+}/g protein.

Protein concentration were determined using the Bio-Rad kit (Bio-Rad Lab, Richmond, CA).

Q. Determination of Calcium Efflux from Rabbit Papillary Muscles.

Rabbit hearts from control and treated rabbits were placed into oxygenated Tyrodes solution containing the following mM composition: NaCl, 140; $MgCl_2$, 1.0; KCl, 5; d-glucose, 10; NaOH, 5; $CaCl_2$, 2; HEPES, 5; aspartic acid, 0.5 and Na_2HPO_4, 1.0 and titrated to pH 7.35. Each rabbit right ventricular papillary muscle with some attached ventricular wall was attached to a Grass isometric force-displacement transducer (FT03B) and stimulated via bipolar punctate platinum electrodes with 2 ms square-wave pulses of two times threshold voltage at a frequency of 1 Hz. Length was adjusted to provide twitch tension equal to 70% of the maximum. After an hour of equilibration, the muscle was equilibrated in aerated calcium efflux physiological solution (pH 7.2) containing $^{45}Ca^{2+}$ (1.0 μCi/ml) for 3 hours at 37° C. Each strip was then rinsed with 150 ml Krebs solution for 5 sec and transferred at 5 min intervals for the first 60 minutes and at 10 minute intervals for another 60 minutes through a series of vials each containing 3 ml of Krebs solution. At the end of the 120 min period, the strips were blotted and weighed. The muscle was dissolved overnight in 0.5 ml of Soluene-350. Radioactivities in the series of vials and in the muscles were determined in a liquid scintillation counter after adding 7 ml of scintillation cocktail. Calcium efflux was expressed as percent of $^{45}Ca^{2+}$ remaining in the tissues.

R. Determination of Norepinephrine-Induced Calcium Efflux from Rabbit Papillary Muscles.

Rabbit hearts from control and treated rabbits were placed into oxygenated Tyrode solution containing the following mM composition: NaCl, 140; $MgCl_2$, 1.0; KCl, 5; d-glucose, 10; NaOH, 5; $CaCl_2$, 2; HEPES, 5; aspartic acid, 0.5 and Na_2HPO_4, 1.0 and

titrated to pH 7.35. Each rabbit right ventricular papillary muscle with some attached ventricular wall was attached to a Grass isometric force-displacement transducer (FT03B) and stimulated via bipolar punctate platinum electrodes with 2 ms square-wave pulses of two times threshold voltage at a frequency of 1 Hz. Length was adjusted to provide twitch tension equal to 70% of the maximum. After an hour of equilibration, the muscle was equilibrated in aerated calcium efflux physiological solution (pH 7.2) containing $^{45}Ca^{2+}$ (1.0 μCi/ml) for 3 hours at 37° C. Each strip was then rinsed with 150 ml Krebs solution for 5 sec and transferred at 5 min intervals through a series of vials each containing 3 ml of Krebs. Some vials into which they were placed at 20 and 25 min contained 100 μM NE in Krebs solution. At the end of the 30 min period, the strips were blotted and weighed. The muscle was dissolved overnight in 0.5 ml of Soluene-350. Radioactivity in the series of vials and the muscle was determined in a liquid scintillation counter after adding 7 ml of scintillation cocktail. The calcium fractional efflux was determined (3 ml effluent released divided by the radioactivity remaining in the tissues). Finally, the calcium fractional efflux ratio was calculated by dividing the fractional efflux from the NE treated group by that from groups without NE treatment for either control rabbits and those receiving ricin.

S. Statistical Methods.

1. For Studies with Coronary Arteries.

Data from all experiments were expressed as mean ± SEM. In cases in which the same experiment was performed on replicates or on more than one artery ring from the same rabbit, the mean values were used. The EC_{50} (The concentration of agonists that produce 50% of the maximum effect) values were calculated from curve fitting for the dose response curve of each experiment using the Boomer Program (Bourne, 1989). Data with more than one factor were analyzed using factorial analysis of variance (ANOVA) procedures. For most data with a single factor the two tailed unpaired Student *t* test

assuming equal variances was used to compare the two means. Because the cAMP data had big differences among variations the two tailed unpaired Student *t* test assuming unequal variances was used to analyze the effects of ricin on cAMP levels and a trend analysis (sign test) was applied to detect the effects of histamine stimulation on cAMP levels. $P \leq 0.05$ was considered significant.

2. *For Studies with the Heart and Isolated Papillary Muscle.*

Tissue contractions to isoproterenol and phenylephrine administration and to increased stimulation frequency were statistically examined using Analysis of Variance techniques appropriate for a two factor design with repeated measures on the drug concentration or stimulating frequency factor. The calcium efflux and calcium influx data were tested for statistical significance using Analysis of Variance and Duncan's New Multiple Range Test. The results of all other experiments where two independent groups existed were tested using the Student t test. In this study, p values of 0.05 or less were considered significant.

T. Chemicals and Solutions

Chemicals obtained from Sigma Chemical Co. (St. Louis, MO):

Ricin (RCA60), 3.4 mg protein/ml with a purity of 98%.

Dopamine hydrochloride

Tryptamine hydrochloride

Pargyline hydrochloride

S-adenosyl-L-methionine p-toluenesulfonate

Borax (sodium tetraborate)

Formic acid, 99%

Sodium formate

Lithium chloride

EDTA disodium

Propranolol

Isoproterenolol

Phenylephrine

Lanthanum Cl

Tris-hydroxymethylaminomethane

Ammonium formate

Tris salt of adenosine triphosphate

Chemicals obtained from Research Biochemicals International (Natick, MA):

Histamine dihydrochloride

Acetylcholine chloride

Serotonin creatinine sulfate complex

Norepinephrine bitartrate

Chemicals obtained from Du Pont Chemical Co. (Boston, MA):

NEN-Trac chromium-51, 15 μ microspheres, 40 mCi/g

[Ethyl-^{3}H]-tryptamine HCL, 26.4 Ci/mmol

Myo[2-^{3}H(N)]-inositol, 105 Ci/mmol

Inositol-1,4,5-triphosphate, D-[inositol-1-^{3}H(N)], 21 Ci/mmol

Inositol-1,4-biphosphate, D-[inositol-2-^{3}H(N)], 9.9 Ci/mmol

Inositol-1-phosphate, D-[inositol-2-^{3}H(N)], 13 Ci/mmol

Chemicals obtained from Amersham (Arlington Heights, IL)

[2,5,6-^{3}H]-Dopamine, 15.5 Ci/mmol and 11.9 Ci/mmol

cAMP and cGMP assay kits

^{45}Ca, 20 mCi/ml

I-[4, 6, propyl-^{3}H]-dihydroalprenolol

[^{3}H]-Myo Inositol

Chemicals from Aldrich Chemical. Co. (Milwaukee, WI):

Trichloroacetic Acid, 98%

3-Methyl-1-butanol (isoamyl alcohol), 59%

2-(2-aminoethyl)pyridine, 95%

Chemicals obtained from other companies:

Heparin, 1000 units/ml - Elkins-Sinn, Inc. (Cherry Hill, NJ)

Gentamicin, 40mg/ml - Elkins-Sinn, Inc. (Cherry Hill, NJ)

Ether Anhydrous - J.T. Baker Chemical Co. (Phillipsburg, NJ)

Perchloric acid - J.T. Baker Chemical Co. (Phillipsburg, NJ)

AG 1-X8 Resin, 100-200 Mesh (formate form) - Bio-Rad Laboratories (Hercules, CA)

Bio-Rad Protein Assay - Bio-Rad Laboratories (Hercules, CA)

Pentobarbital sodium, 64.8 mg/ml - Fort Dodge Lab Inc. (Ft. Dodge, KS)

Lidocaine Hydrochloride, 2% - Steris Laboratories, Inc. (Phoenix, AZ)

Scintillation Toluene - Beckman Instruments Inc. (Fullerton, CA)

Bay K 8644 (ICN Biomedicals, Irvine, CA)

Bovine serum albumin (Miles Laboratories, Pentex fraction V)

Soluene-350 (Packard, Downers Groves, IL)

Collagenase (Cooper Biomedical class II)

Krebs solution contained the following (mM):

118.5 NaCl, 4.7 KCl, 1.2 $MgCl_2$, 23.8 $NaHCO_3$, 1.2 KH_2PO_4,

11 d-glucose, 2.5 $CaCl_2$ and 0.01 EDTA,

Physiological solutions were made fresh daily using millipore-filtered distilled water. Stock solutions were prepared in distilled water and frozen at -20° C, with the exception of norepinephrine which was prepared in 0.1 N HCL and made fresh daily within 30 minutes of use. Other solutions were made fresh daily from concentrated stock solutions in distilled water, except ricin which was made up once for the entire experiment. Ricin was purchased in a concentrated solution of 3.4 mg of protein/ml. It was diluted in sterile water to yield a concentration of 8.5 µg/ml.

III. RESULTS

A. Effects of Ricin Administration on Rabbit Hemodynamics Using Radio-labeled Microspheres

Cardiac outputs were increased in the four ricin-administered groups ($p < 0.0022$) (Figure 1). The toxic sub-lethal dose of ricin increased cardiac output by 28% at 12 hours after injection and by 29% at 18 hours. The minimal lethal dose increased cardiac output by 33% at 12 hours but then cardiac output decreased slightly to 27% above the control value at 18 hours post-ricin.

Ricin increased blood flow to most tissues of rabbits in four ricin-treated groups (Tables 1, 2). The brain is somewhat of an exception to that. Twelve hours after injection of a toxic sub-lethal dose of ricin, blood flow to all areas of the brain had markedly increased, but six hours later, blood flow to the various areas had substantially returned to normal (Table 1). The minimal lethal dose, however, decreased the blood flow to the brain at 12 hours, and markedly decreased its blood flow at 18 hours, to 36% of the initial blood flow (Table 2).

Another exception is the lungs. Because the microspheres were injected into the left ventricle, the lungs would receive microspheres from bronchial arteries, those that passed through capillaries and were not trapped by them or those that passed directly through A-V shunts. In either case, a toxic sub-lethal dose of ricin slightly increased blood flow to the lungs at 12 hours, and greatly increased it at 18 hours (Table 1). On the other hand, a minimum lethal dose of ricin did not alter blood flow to the lungs at 12 hours, but did so at 18 hours to a great degree, reducing it to 39% of control (Table 2). The effects of a toxic sub-lethal dose and a minimal lethal dose of ricin on the percent of total cardiac output received by organs are shown in table 3 and table 4.

Blood flow to the left and right kidneys were very similar (Figure 2) and thus we can assume adequate mixing of microspheres and blood.

Figure 1. The cardiac output of control and ricin treated rabbits. TSD = Toxic Sub-lethal Dose (0.22 ug/kg), MLD = Minimal Lethal Dose (0.44 ug/kg), -12 and -18 = Hours post-ricin i.v. injection. n = 3 for TSD-18 hour values. In others, n = 2.

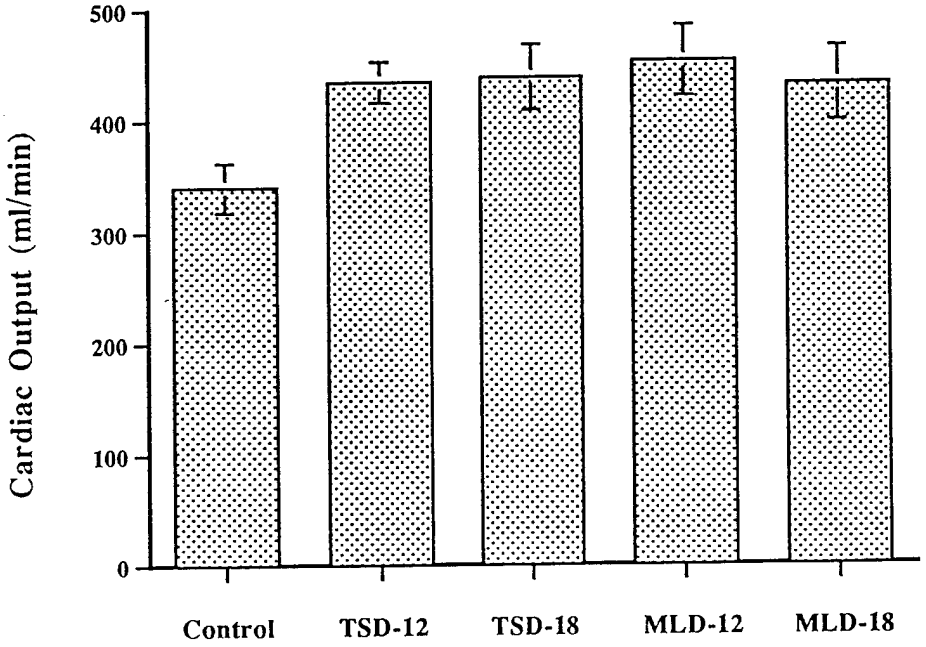

Table 1. The effects of toxic sub-lethal dose of ricin on blood flow ml/min per 100g tissue[a].

ORGANS OR TISSUES	CONTROL	TOXIC SUBLETHAL DOSE	
		12hr	18hr
SKIN	7 ± 0.5	6 ± 6.3	13 ± 2.7
HEART	297 ± 44.1	674 ± 22.2	743 ± 82.5
Inner Layer	462 ± 66.9	1050 ± 187.6	1123 ± 109.9
Middle Layer	421 ± 137.0	819 ± 67.7	1028 ± 107.0
Outer Layer	426 ± 114.5	866 ± 107.8	1036 ± 101.4
AORTA	19 ± 1.8	22 ± 4.8	38 ± 7.3
LUNGS	70 ± 41.2	88 ± 84.1	204 ± 73.3
TRACHEA	20 ± 0.1	17 ± 7.1	32 ± 9.6
BRONCHII	23 ± 10.9	26 ± 1.1	62 ± 7.2
FAT	36 ± 12.6	28 ± 15.9	80 ± 20.6
LIVER	7 ± 1.9	19 ± 1.2	11 ± 4.3
GALL BLADDER	113 ± 19.5	128 ± 16.6	197 ± 62.5
SPLEEN	469 ± 115.8	217 ± 206.6	466 ± 168.2
KIDNEY	434 ± 32.9	641 ± 244.5	460 ± 52.9
Medullary	74 ± 6.8	99 ± 10.7	78 ± 21.8
Cortex	882 ± 55.9	1065 ± 261.5	925 ± 114.1
ADRENALS	139 ± 49.8	435 ± 283.8	231 ± 12.2
MUSCLE[b]	11 ± 3.7	6 ± 3.8	11 ± 1.0
TESTES	205 ± 48.6	715 ± 636.8	331 ± 51.3
BRAIN	73 ± 12.7	180 ± 124.0	76 ± 7.9
Cerebrum	75 ± 13.8	168 ± 113.0	76 ± 8.5

Table 1 (cont'd). The effects of toxic sub-lethal dose of ricin on blood flow ml/min per 100g tissue[a].

ORGANS OR TISSUES	CONTROL	TOXIC SUBLETHAL DOSE	
		12hr	18hr
Pituitary	493 ± 53.8	543 ± 121.6	290 ± 101.4
Thalamus	54 ± 12.2	160 ± 113.3	66 ± 7.0
Midbrain	85 ± 5.4	206 ± 146.3	78 ± 12.2
Cerebellum	87 ± 12.2	256 ± 190.3	94 ± 12.2
Pons	50 ± 9.9	146 ± 94.5	68 ± 3.9
Medulla	52 ± 7.6	142 ± 91.1	50 ± 6.5
GI TRACT[c]	60 ± 5.3	58 ± 26.3	83 ± 5.5
Esophagus	28 ± 7.2	24 ± 8.8	30 ± 3.8
STOMACH	63 ± 17.1	51 ± 38.3	143 ± 20.2
Cardiac	22 ± 1.4	67 ± 53.9	32 ± 8.7
Pylorus	60 ± 21.2	21 ± 13.7	150 ± 19.4
Lessor Curv.	44 ± 20.1	82 ± 68.9	104 ± 21.1
Great Curv.	139 ± 40.2	132 ± 60.5	253 ± 83.9
SM. INTESTINE	78 ± 0.3	105 ± 54.6	124 ± 29.8
Duodenum	103 ± 0.4	117 ± 71	163 ± 12.5
Upper Jejunum	45 ± 2.7	92 ± 3.3	136 ± 72.6
Lower Jejunum	75 ± 6.0	85 ± 42.2	112 ± 32.3
ILEUM	88 ± 19.6	134 ± 100.5	96 ± 24.8
CECUM	76 ± 6.3	61 ± 29.5	78 ± 10.4
L. INTESTINE	55 ± 4.4	49 ± 0.5	41 ± 4.2

a. Measured by injection of radiolabeled microspheres into the left ventricle. n = 2 except for the TSD, 18 hour group, where n = 3.
b. Calculated from 100 g of Gluteus maximus muscle.
c. The GI tract did not include the appendix, cecum and rectum.

Table 2. The effects of minimal lethal dose of ricin on blood flow ml/min per 100g tissue[a].

ORGANS OR TISSUES	CONTROL	MINIMAL LETHAL DOSE	
		12hr	18hr
SKIN	7 ± 0.5	19 ± 3.6	7 ± 0.1
HEART	297 ± 44.1	831 ± 36.4	906 ± 44.5
Inner Layer	462 ± 66.9	757 ± 48.1	1128 ± 108.8
Middle Layer	421 ± 137.0	947 ± 17.4	1363 ± 137.9
Outer Layer	426 ± 114.5	1014 ± 73.8	1434 ± 204.8
AORTA	19 ± 1.8	33 ± 10.8	29 ± 3.9
LUNGS	70 ± 41.2	72 ± 1.4	33 ± 24.9
TRACHEA	20 ± 0.1	32 ± 9.7	17 ± 0.1
BRONCHII	23 ± 10.9	57 ± 39.6	30 ± 8.1
FAT	36 ± 12.6	37 ± 3.6	20 ± 2.4
LIVER	7 ± 1.9	11 ± 1.1	12 ± 4.1
GALL BLADDER	113 ± 19.5	277 ± 1.0	236 ± 63.6
SPLEEN	469 ± 115.8	684 ± 51.0	611 ± 209.3
KIDNEY	434 ± 32.9	594 ± 27.1	673 ± 120.6
Medullary	74 ± 6.8	56 ± 9.5	71 ± 33.1
Cortex	882 ± 55.9	1052 ± 136.8	1247 ± 179.6
ADRENALS	139 ± 49.8	244 ± 78.7	219 ± 54.0
MUSCLE[b]	11 ± 3.7	14 ± 6.0	18 ± 6.1
TESTES	205 ± 48.6	801 ± 363.4	355 ± 16.9
BRAIN	73 ± 12.7	48 ± 5.3	36 ± 4.7
Cerebrum	75 ± 13.8	44 ± 2.3	34 ± 4.6

Table 2 (cont'd). The effects of minimal lethal dose of ricin on blood flow ml/min per 100g tissue[a].

ORGANS OR TISSUES	CONTROL	MINIMAL LETHAL DOSE	
		12hr	18hr
Pituitary	493 ± 53.8	476 ± 60.4	727 ± 31.7
Thalamus	54 ± 12.2	63 ± 9.7	35 ± 1.2
Midbrain	85 ± 5.4	30 ± 1.5	40 ± 8.7
Cerebellum	87 ± 12.2	66 ± 13.3	41 ± 3.6
Pons	50 ± 9.9	60 ± 21.7	46 ± 4.1
Medulla	52 ± 7.6	42 ± 5.6	29 ± 6.3
GI TRACT[c]	60 ± 5.3	77 ± 14.3	77 ± 6.2
Esophagus	28 ± 7.2	45 ± 3.5	25 ± 4.3
STOMACH	63 ± 17.1	103 ± 31.7	97 ± 22.6
Cardiac	22 ± 1.4	31 ± 38.8	27 ± 4.8
Pylorus	60 ± 21.2	129 ± 79.8	109 ± 22.0
Lessor Curv.	44 ± 20.1	86 ± 1.0	98 ± 61.2
Great Curv.	139 ± 40.2	177 ± 80.4	170 ± 40.7
SM. INTESTINE	78 ± 0.3	131 ± 12.8	127 ± 42.5
Duodenum	103 ± 0.4	222 ± 100.2	158 ± 37.4
Upper Jejunum	45 ± 2.7	102 ± 47.8	146 ± 33.5
Lower Jejunum	75 ± 6.0	132 ± 34.2	102 ± 32.6
ILEUM	88 ± 19.6	104 ± 35.3	129 ± 61.1
CECUM	76 ± 6.3	67 ± 13.6	95 ± 14.7
L. INTESTINE	55 ± 4.4	37 ± 16.7	40 ± 0.9

a. Measured by injection of radiolabeled microspheres into the left ventricle. n = 2 except for the TSD, 18 hour group, where n = 3.
b. Calculated from 100 g of gluteus maximus muscle.
c. The GI tract did not include the appendix, cecum and rectum.

Table 3. The effects of toxic sublethal dose of ricin on the percent of total cardiac output received by organs[a].

ORGANS	CONTROL	TOXIC SUBLETHAL DOSE	
		12 hours	18 hours
	% Output	% Output	% Output
Heart	3.69 ± 0.182	6.53 ± 0.098	6.95 ± 0.156
Aorta	0.01 ± 0.001	0.02 ± 0.008	0.03 ± 0.007
Lungs (total)	1.26 ± 0.725	1.36 ± 1.304	2.81 ± 1.108
L. Lung	0.57 ± 0.284	0.55 ± 0.527	1.22 ± 0.476
R. Lung	0.69 ± 0.441	0.81 ± 0.777	1.59 ± 0.633
Trachea	0.03 ± 0.003	0.02 ± 0.006	0.05 ± 0.014
Bronchii	0.01 ± 0.007	0.01 ± 0.002	0.03 ± 0.004
Liver	1.37 ± 0.470	2.91 ± 0.075	1.49 ± 0.497
Gall bladder	0.04 ± 0.003	0.05 ± 0.035	0.04 ± 0.006
Spleen	0.88 ± 0.108	0.50 ± 0.485	0.74 ± 0.269
Kidney	14.99 ± 0.908	19.10 ± 7.023	9.72 ± 0.791
Adrenals	0.06 ± 0.012	0.16 ± 0.127	0.07 ± 0.006
Muscle[b]	3.03 ± 0.008	1.56 ± 1.000	3.13 ± 0.701
Testes	0.02 ± 0.001	0.01 ± 0.006	0.02 ± 0.002
Brain	0.79 ± 0.23	3.27 ± 2.254	1.38 ± 0.164
GI Tract[c]	13.28 ± 2.561	11.01 ± 5.218	16.80 ± 3.655
Esophagus	0.09 ± 0.028	0.07 ± 0.018	0.08 ± 0.006
Stomach	3.41 ± 0.891	2.23 ± 1.647	5.73 ± 1.102
Sm. intestine	7.66 ± 1.578	7.42 ± 3.597	9.75 ± 3.274
L. intestine	1.69 ± 0.006	1.08 ± 0.11	0.97 ± 0.023

a. Measured by injection of radiolabeled microspheres into the left ventricle. n = 2 except for the TSD, 18 hour group, where n = 3.

b. Calculated from 100 g of gluteus maximus muscle.

c. The GI tract did not include the appendix, cecum and rectum.

Table 4. The effects of minimal lethal dose of ricin on the percent of total cardiac output received by organs[a].

ORGANS	CONTROL	MINIMAL LETHAL DOSE	
		12hr	18hr
	% Output	% Output	% Output
Heart	3.69 ± 0.182	7.75 ± 0.134	8.44 ± 0.312
Aorta	0.01 ± 0.001	0.02 ± 0.009	0.02 ± 0.004
Lungs (total)	1.26 ± 0.725	0.93 ± 0.075	0.49 ± 0.371
L. Lung	0.57 ± 0.284	0.36 ± 0.029	0.21 ± 0.161
R. Lung	0.69 ± 0.441	0.57 ± 0.046	0.28 ± 0.21
Trachea	0.03 ± 0.003	0.04 ± 0.009	0.02 ± 0.002
Bronchii	0.01 ± 0.007	0.03 ± 0.018	0.01 ± 0.001
Liver	1.37 ± 0.470	1.74 ± 0.273	2.04 ± 0.926
Gall bladder	0.04 ± 0.003	0.03 ± 0.002	0.04 ± 0.001
Spleen	0.88 ± 0.108	0.81 ± 0.011	1.05 ± 0.373
Kidney	14.99 ± 0.908	13.72 ± 1.343	18.70 ± 1.844
Adrenals	0.06 ± 0.012	0.07 ± 0.019	0.08 ± 0.012
Muscle[b]	3.03 ± 0.008	4.74 ± 1.701	5.09 ± 0.301
Testes	0.02 ± 0.001	0.02 ± 0.007	0.02 ± 0.002
Brain	0.79 ± 0.23	0.99 ± 0.050	0.64 ± 0.060
GI Tract[c]	13.28 ± 2.561	14.76 ± 1.747	15.16 ± 2.151
Esophagus	0.09 ± 0.028	0.13 ± 0.018	0.07 ± 0.022
Stomach	3.41 ± 0.891	4.07 ± 1.001	4.31 ± 1.030
Sm. intestine	7.66 ± 1.578	9.29 ± 0.344	9.38 ± 3.098
L. intestine	1.69 ± 0.006	0.95 ± 0.375	1.00 ± 0.090

a. Measured by injection of radiolabeled microspheres into the left ventricle. n = 2 except for the TSD, 18 hour group, where n = 3.
b. Calculated from 100 g of gluteus maximus muscle.
c. The GI tract did not include the appendix, cecum and rectum.

Figure 2. Comparison of blood flow to the rabbit right and left kidneys as determined by radioactive microspheres in all of the rabbits studied.

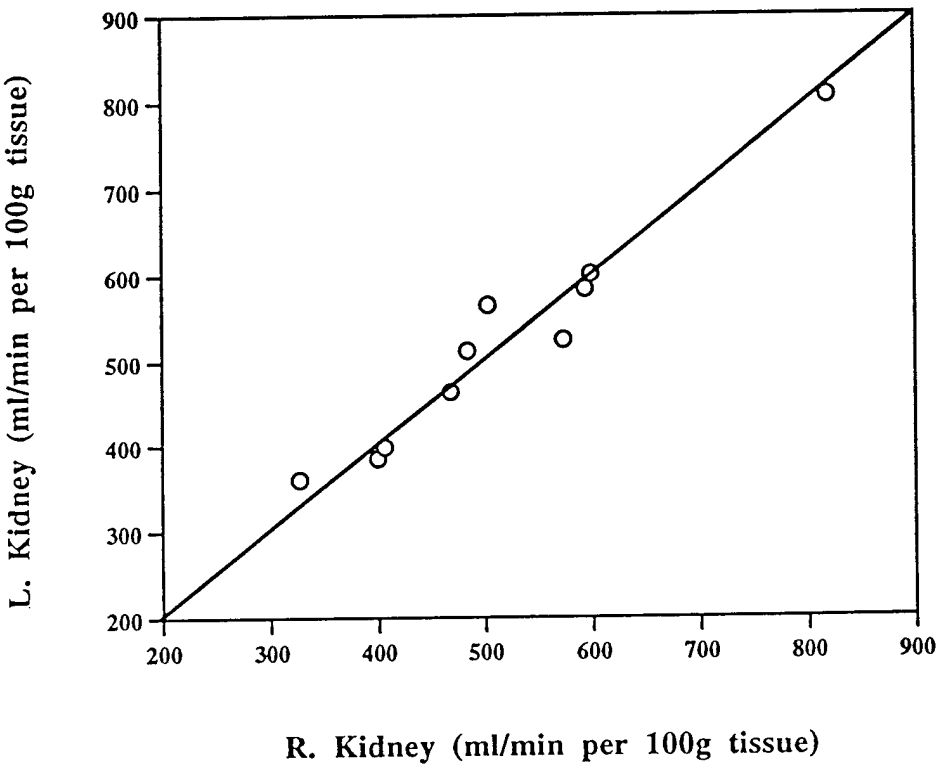

B. Effects of Ricin on Contractions and Relaxations of Rabbit Coronary Artery Rings

1. Contractions of Rabbit Coronary Artery Rings to 5-HT, Histamine, and AEP:

Contractions of the rabbit left circumflex coronary artery to cumulatively increasing concentrations of 5-HT and histamine are shown: 5-HT with endothelium (Figure 3), 5-HT without endothelium (Figure 4), histamine with endothelium (Figure 5), and histamine without endothelium (Figure 6). The maximal contractions in response to histamine were 3.4-11.7 times those in response to 5-HT. Ricin administration significantly increased the EC_{50}s of both agents in coronary arteries (Table 5). Ricin administration significantly increased the maximal contractile tension of coronary arteries to both agents and the tension achieved to the single dose of 350 μM AEP (Table 6). In the rabbits receiving ricin, the contractile tension of rings to lower concentrations (0.3-10 μM) of histamine were reduced (Table 7) and to higher concentrations (30-300 μM) of histamine were enhanced, with (Figure 5) and without (Figure 6) endothelium. Endothelium removal markedly increased contractions of coronary artery rings to these agents from either control rabbits or those receiving ricin (Table 6).

2. Relaxations of Rabbit Coronary Artery Rings to ACh and NE:

Relaxations to cumulatively increasing concentrations of ACh and NE in the AEP contracted rings are shown: NE with endothelium (Figure 7), NE without endothelium (Figure 8), and ACh with endothelium (Figure 9). The concentration-response curve to NE in coronary artery rings from rabbits given ricin was shifted to the left of control (Figure 7). Ricin administration significantly decreased the EC_{50}s of the coronary artery to NE (Table 8). Acetylcholine caused endothelium-dependent relaxation in coronary artery rings; those without endothelium did not relax to ACh (data not shown). Ricin administration did not alter the EC_{50} of the coronary artery to ACh (Table 8). The maximal

Figure 3. Contractions of rabbit coronary artery rings with endothelium intact 48 hr after i.v. injection of 0.22 μg/kg of ricin. Each point is the mean ± SEM of rings from 7-8 rabbits.

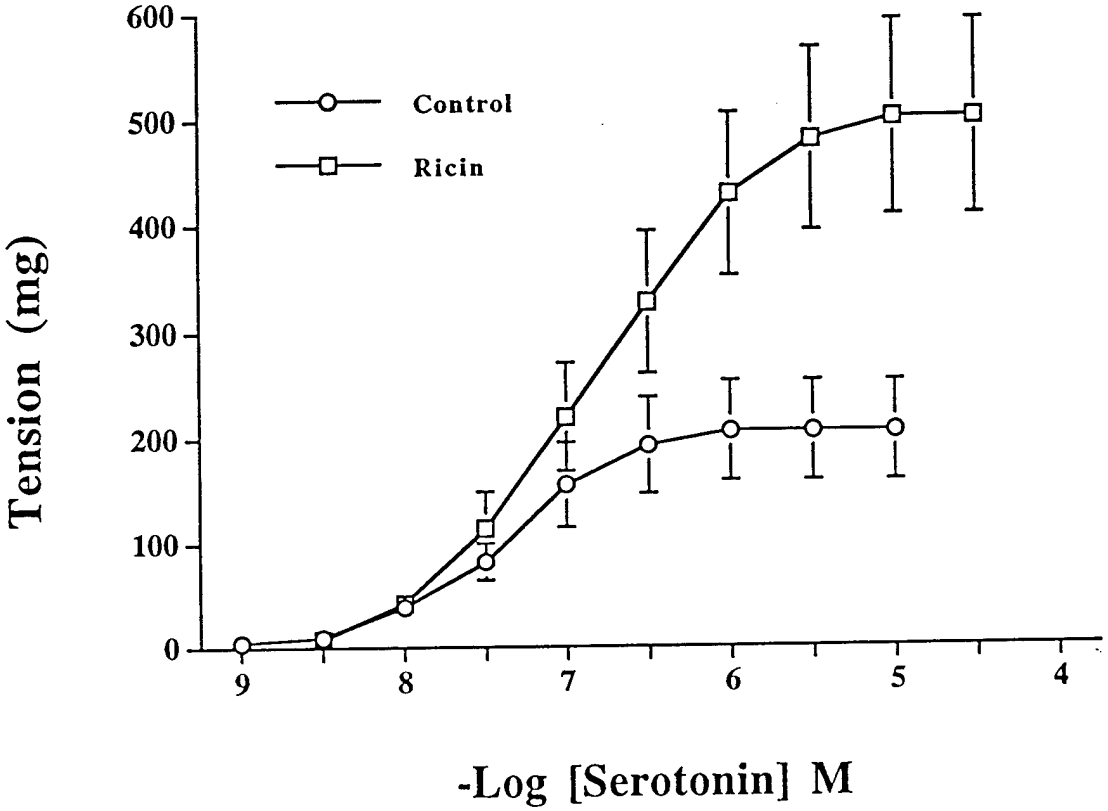

Figure 4. Contractions of rabbit coronary artery rings with endothelium removed 48 hr after i.v. injection of 0.22 μg/kg of ricin. Each point is the mean ± SEM of rings from 7 rabbits.

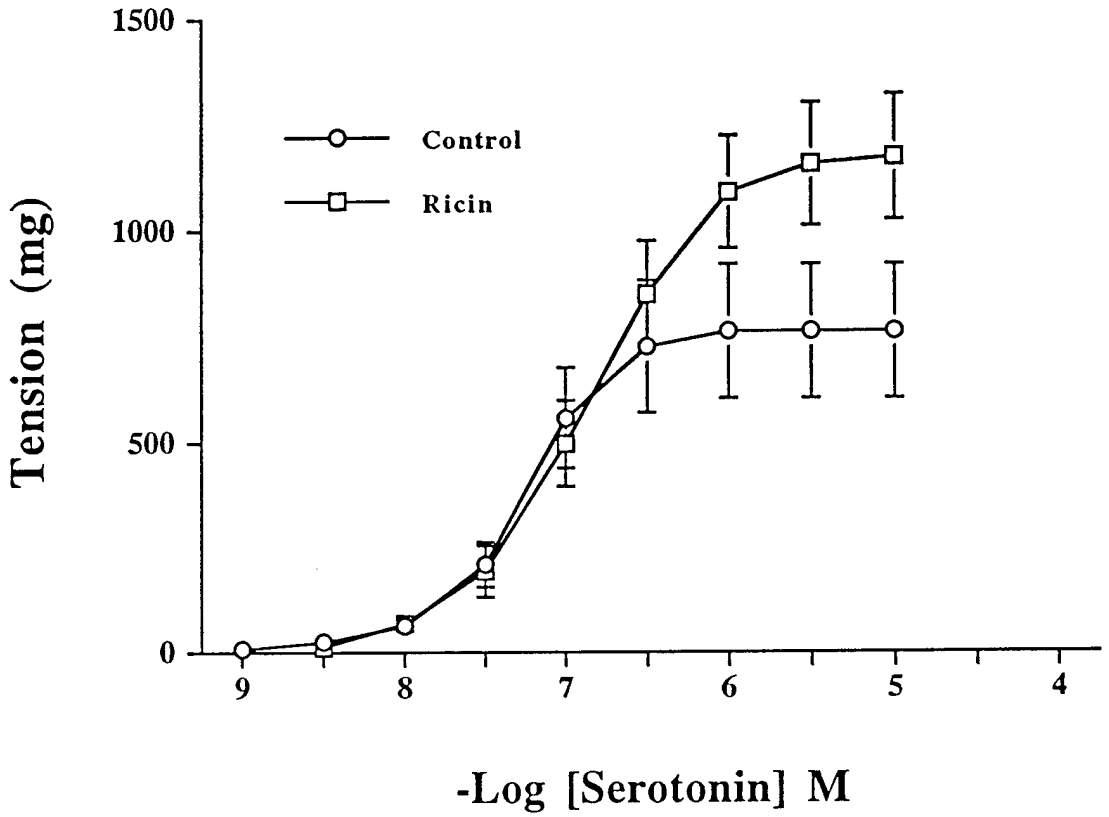

Figure 5. Contractions of rabbit coronary artery rings with endothelium intact 48 hr after i.v. injection of 0.22 μg/kg of ricin. Each point is the mean ± SEM of rings from 8 rabbits.

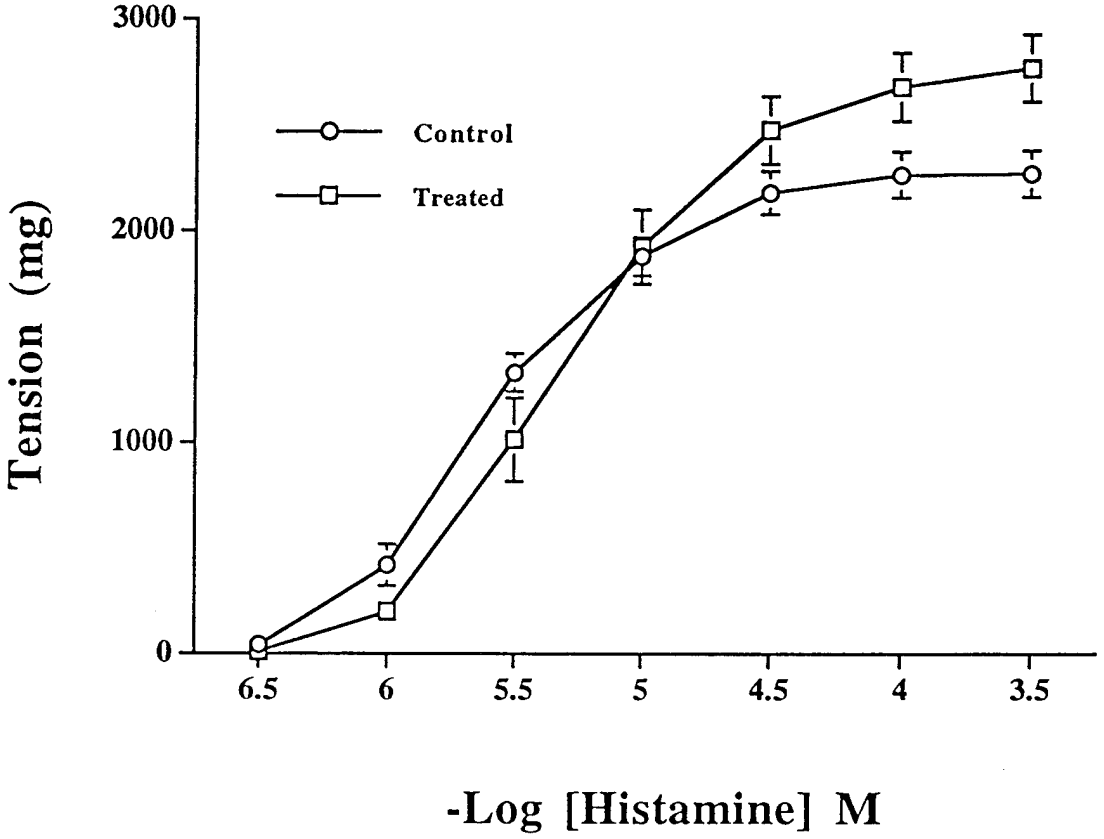

Figure 6. Contractions of rabbit coronary artery rings with endothelium removed 48 hr after i.v. injection of 0.22 μg/kg of ricin. Each point is the mean ± SEM from 8 rabbits.

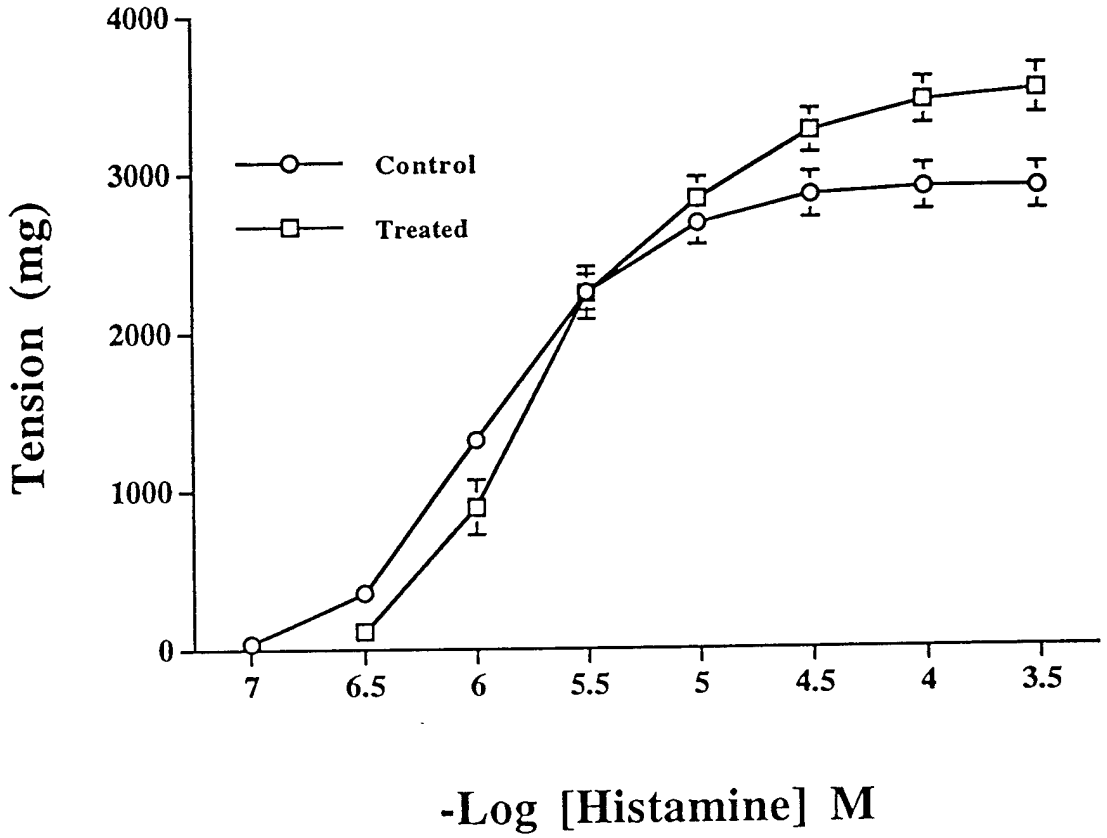

Table 5. The EC_{50} for contraction by agonists of coronary artery rings from rabbits receiving ricin and control rabbits.

	EC_{50} ($x10^{-8}M$)			
	Control		Ricin (0.22 μg/kg)	
	endothelium present	endothelium removed	endothelium present	endothelium removed
Agent	Mean±SEM (n)[a]	Mean±SEM (n)	Mean±SEM (n)	Mean±SEM (n)
5-HT[b]	4.70±0.49 (7)	7.01±1.05 (8)	10.8±1.64 (7)	15.4±2.50 (8)
Histamine[c]	240±27.4 (8)	106±9.42 (8)	460±67.7 (8)	230±14.9 (8)

[a] Number in parenthesis indicates number of rabbits in each group.

[b] Significant main effects were detected between the control and ricin groups ($p<0.0058$) and between the endothelium present and endothelium removed groups ($p<0.0014$). There was no significant interaction found between the factors ($p>0.21$).

[c] Significant main effects were detected between the control and ricin groups ($p<0.0008$) and between the endothelium present and endothelium removed groups ($p<0.0004$). There was not significant interaction found between the factors ($p>0.25$).

Table 6. The maximal tension of coronary artery rings from control and ricin treated rabbits to agonists.

	Tension (g)			
	Control		Ricin (0.22 μg/kg)	
	endothelium present	endothelium removed	endothelium present	endothelium removed
Agent	Mean±SEM (n)[a]	Mean±SEM (n)	Mean±SEM (n)	Mean±SEM (n)
5-HT[b]	0.19±0.04 (8)	0.73±0.14 (8)	0.50±0.09 (8)	1.05±0.19 (8)
Histamine[c]	2.22±0.11 (9)	2.85±0.14 (8)	2.80±0.14 (9)	3.52±0.16 (8)
350μM AEP[d]	1.76±0.12 (8)	2.20±0.12 (9)	2.18±0.11 (9)	2.66±0.12 (9)

[a] Number in parenthesis indicates number of rabbits in each group.

[b] Significant main effects were detected between the control and ricin groups ($p<0.006$) and between the endothelium present and endothelium removed groups ($p<0.0001$). There was no significant interaction found between the factors ($p>0.52$).

[c] Significant main effects were detected between the control and ricin groups ($p<0.0032$) and between the endothelium present and endothelium removed groups ($p<0.0001$). There was no significant interaction found between the factors ($p>0.84$).

[d] Significant main effects were detected between the control and ricin groups ($p<0.0038$) and between the endothelium present and endothelium removed groups($p<0.0008$). There was no significant interaction found between the factors ($p>0.85$).

Table 7. The tensions of coronary artery rings from control and ricin treated rabbits to lower concentrations of histamine (These data were from Fig. 5).

	Tension(100mg)			
	Control		Ricin (0.22 μg/kg)	
	endothelium present	endothelium removed	endothelium present	endothelium removed
Histamine	Mean±SEM (n)[a]	Mean±SEM (n)	Mean±SEM (n)	Mean±SEM (n)
$10^{-6.5}$ M[b]	0.43±0.19[c] (8)	3.52±0.59[c,d] (8)	0.12±0.06 (8)	1.03±0.41[d] (8)
$10^{-6.0}$ M[e]	4.19±1.04 (9)	12.93±1.85 (8)	2.02±0.73 (9)	8.06±1.86 (8)
$10^{-5.5}$ M[f]	13.32±0.98 (8)	22.20±1.41 (9)	11.39±1.57 (9)	20.88±2.23 (9)

[a] Number in parenthesis indicates number of rabbits in each group.

[b] Significant main effects were detected between the control and ricin groups ($p<0.006$) and between the endothelium present and endothelium removed groups ($p<0.0001$). There was also a significant interaction found between the factors ($p<0.05$).

[c,d] Significant differences were detected between each two means by simple effect ANOVA tests ([c,d] both $p<0.0032$).

[e] Significant main effects were detected between the control and ricin groups ($p<0.05$) and between the endothelium present and endothelium removed groups ($p<0.0001$). There was no significant interaction found between the factors ($p>0.36$).

[f] No Significant main effect was detected between the control and ricin groups ($p>0.42$). But the endothelium present and endothelium removed groups do have a significant main effect ($p<0.0001$). There was no significant interaction found between the factors ($p>0.77$).

Figure 7. Relaxations to NE of rabbit coronary artery rings with endothelium intact, contracted with AEP, 48 hrs after i.v. injection of 0.22 μg/kg of ricin. Each point is the mean ± SEM of rings from 7-8 rabbits.

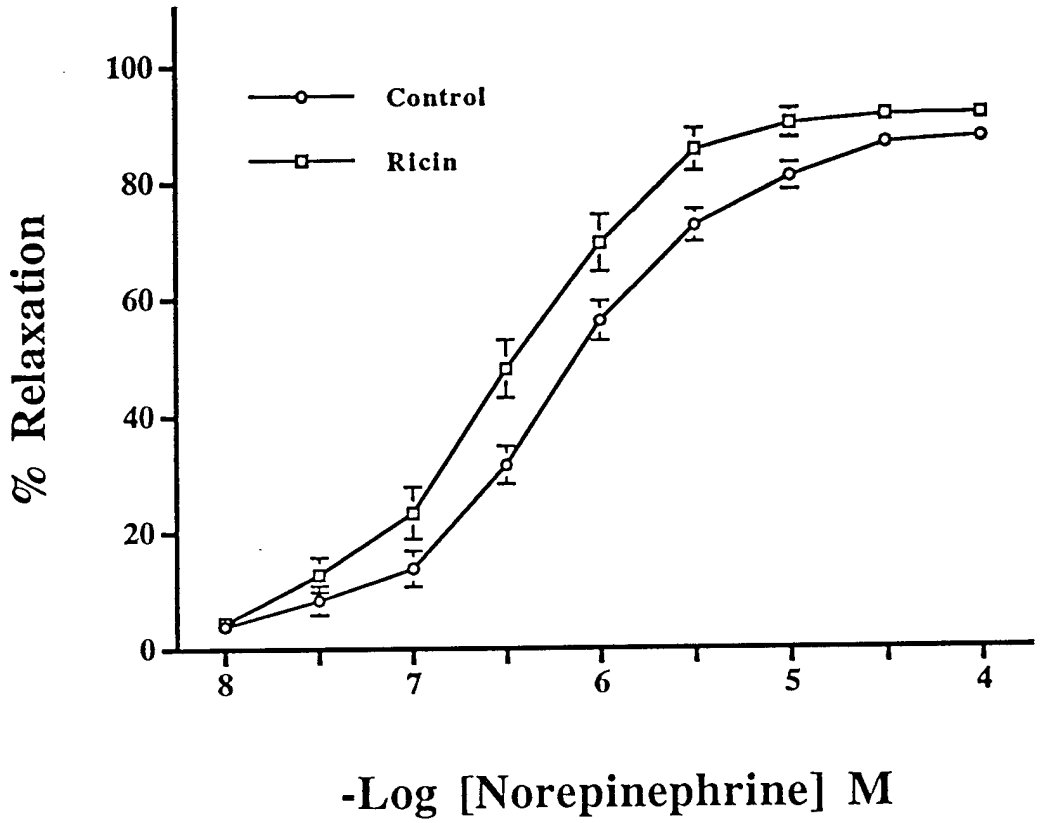

Figure 8. Relaxations to NE of rabbit coronary artery rings with endothelium removed, contracted with AEP, 48 hrs after i.v. injection of 0.22 μg/kg of ricin. Each point is the mean ± SEM of rings from 7 rabbits.

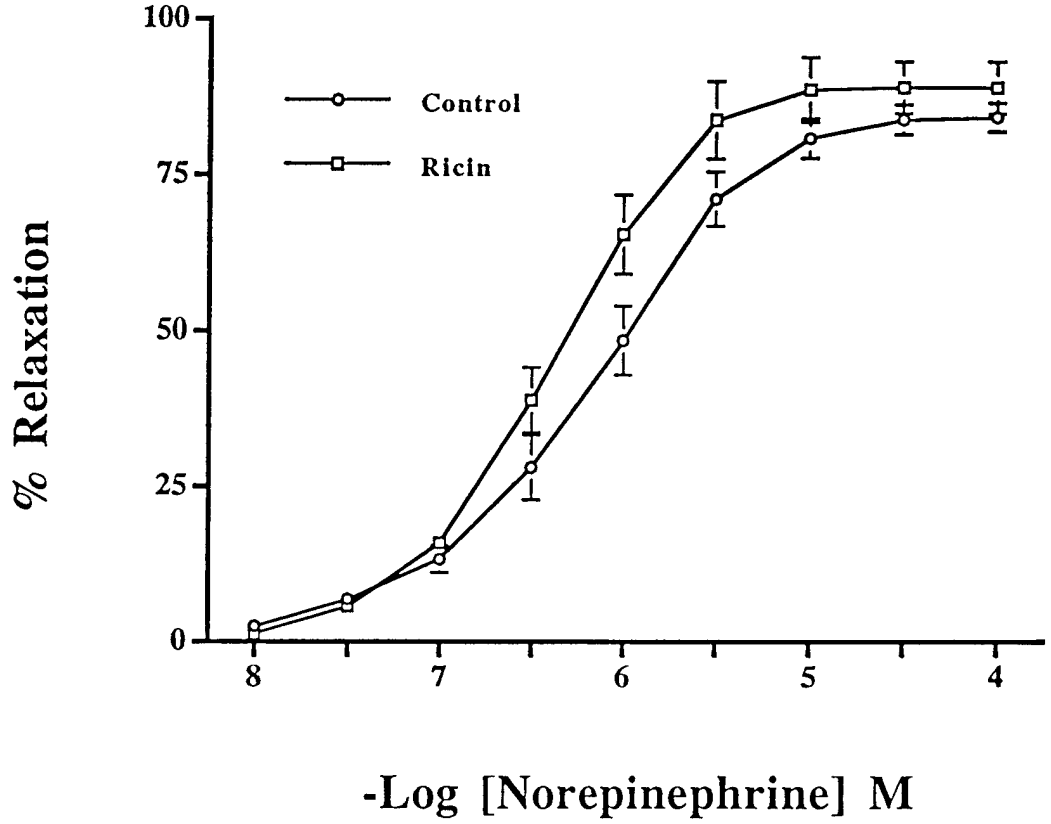

Figure 9. Relaxations to ACh of rabbit coronary artery rings contracted with AEP, 48 hrs after i.v. injection of 0.22 μg/kg of ricin. Each point is the mean ± SEM from 7-8 rabbits.

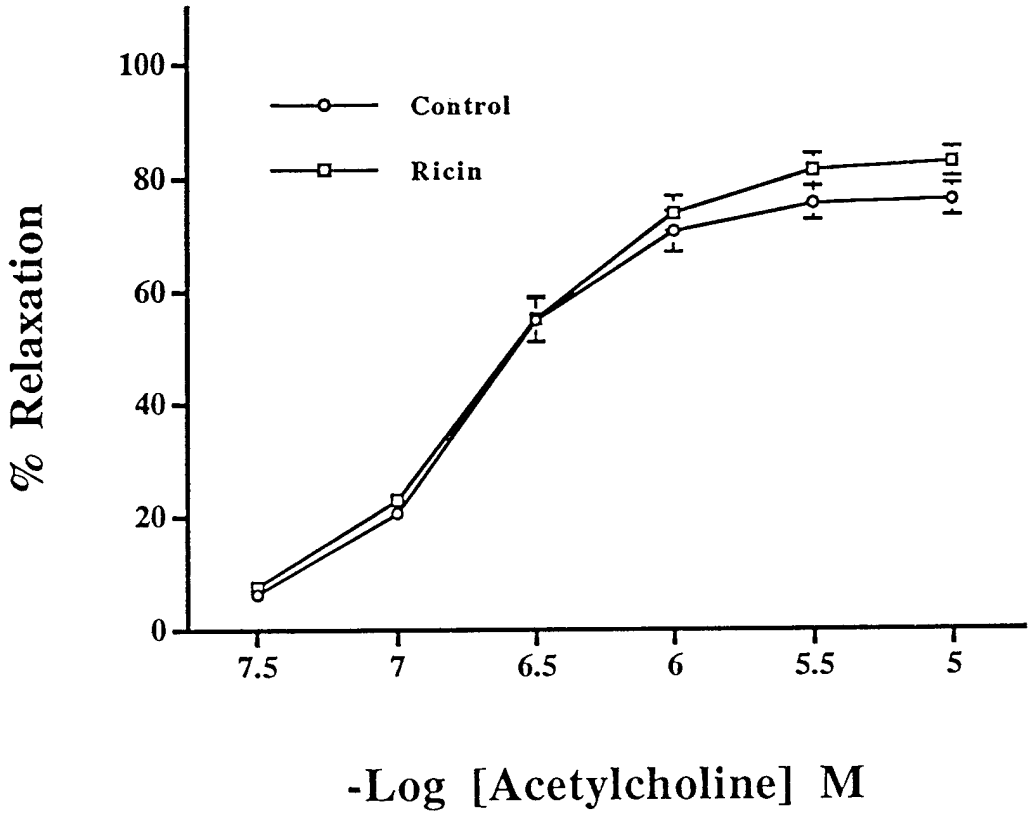

Table 8. The EC_{50} for relaxation by agonists of AEP-contracted coronary artery rings from rabbits receiving ricin and control rabbit.

	EC_{50} ($x10^{-8}M$)			
	Control		Ricin (0.22μg/kg)	
	endothelium present	endothelium removed	endothelium present	endothelium removed
Agent	Mean$\pm$SEM (n)[a]	Mean$\pm$SEM (n)	Mean$\pm$SEM (n)	Mean$\pm$SEM (n)
NE[b]	77.2$\pm$9.51 (7)	65.4$\pm$10.8 (7)	24.2$\pm$4.79 (7)	40.4$\pm$3.44 (7)
ACh	21.3$\pm$0.97 (6)	———	21.0$\pm$2.90 (8)	———

[a] Number in parenthesis indicates number of rabbits in each group.

[b] Significant main effect was detected between the control and ricin groups ($p<0.0015$). There was no main effect between the endothelium present and endothelium removed groups ($p>0.46$). No significant interaction was found between the factors ($p>0.62$).

relaxations of rabbit coronary arteries to both ACh and NE were not significantly different (Table 9).

C. Effects of Ricin Administration on the MAO and COMT Activity

1. Rabbit Coronary Artery

The MAO activity of control rabbit coronary arteries was 190.73 ± 23.15 nmoles/min/g protein and that of rabbits injected with ricin was 192.39 ± 22.45 nmoles/min/g protein (Table 10, Figure 10). The COMT activities of control and ricin injected groups were 9.88 ± 0.42 and 7.51 ± 0.52 respectively (Table 10, Figure 11). The COMT activity of coronary arteries from the rabbits in ricin group is significantly different from that of control ($p < 0.005$).

2. Rabbit Papillary Muscle.

Papillary muscle from rabbits receiving ricin and sham injected rabbits both had detectable monoamine oxidase (MAO) activities (Figure 12). Ricin increased the MAO activity of papillary muscle, mean ± SEM (1.44 ± 0.09 nmol/g/min, n=6), compared to that of control rabbits (1.16 ± 0.04 nmol/g wet weight/min, p = 0.04, n=6). However, ricin decreased the catechol-*O*-methyltransferase (COMT) activity of papillary muscle (mean ± SEM, pmol/g wet weight/min), compared to that of control rabbits (control: 107.3 ± 4.27; ricin: 72.02 ± 5.06, n=6, p = 0.021).

D. Effects of Ricin Administration on cAMP and cGMP Levels

1. The Effects of Ricin on the Time Course of Histamine Stimulated cAMP Levels in Rabbit Coronary Arteries.

Table 9. The maximal relaxation of the rabbit coronary artery to NE and ACh. The coronary artery was precontracted with 3.5 x 10-4 M AEP.

	% of Initial Contraction			
	Control		Ricin (0.22 μg/kg)	
	endothelium present	endothelium removed	endothelium present	endothelium removed
Agent	Mean±SEM (n)[a]	Mean±SEM (n)	Mean±SEM (n)	Mean±SEM (n)
NE	87.4±1.2 (7)	84.2±2.3 (7)	89.3±2.5 (8)	89.0±4.2 (7)
ACh	76.0±2.9 (7)	———	82.7±2.6 (8)	———

[a] Number in parenthesis indicates number of rabbits in each group.

Table 10. The activities of MAO and COMT in coronary arteries from control rabbits and rabbits receiving ricin.

Enzymes	Enzyme Activities (nmoles/min/g protein)	
	Control Mean ± SEM (n)[a]	Ricin Mean ± SEM (n)
MAO	190.73 ± 23.15 (6)	192.39 ± 22.45 (6)
COMT	9.88 ± 0.42 (6)	7.51 ± 0.52b (6)

a The number in parenthesis indicates the number of rabbits

b Significant different from corresponding control (unpaired *t* test, $p < 0.005$)

Figure 10. The effects of ricin administration to rabbits on MAO activity in their coronary arteries 48 hr after i.v. injection of 0.22 μg/kg of ricin. Each bar is the mean ± SEM from artery samples from 6 rabbits.

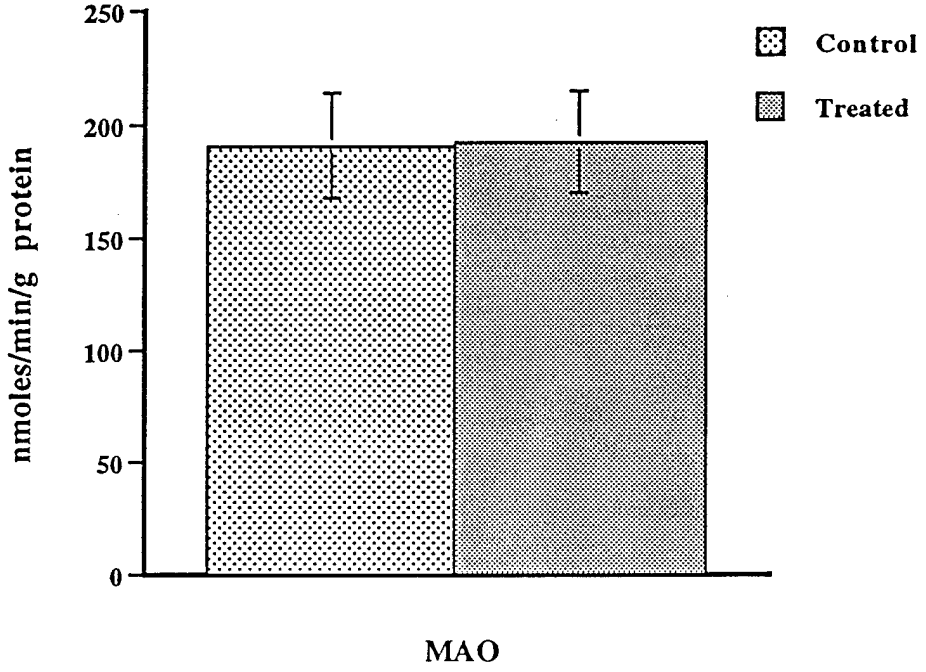

Figure 11. The effects of ricin administration to rabbits on COMT activity in their coronary arteries 48 hr after i.v. injection of 0.22 μg/kg of ricin. Each bar is the mean ± SEM from artery samples from 6 rabbits.

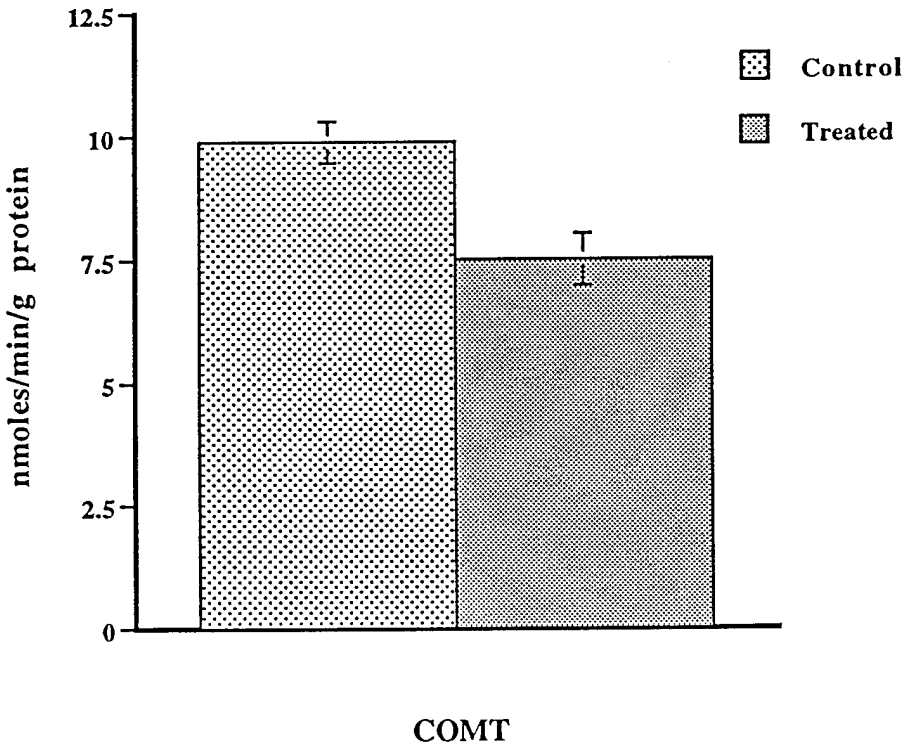

Figure 12. Effects of ricin on MAO and COMT in the myocardium from the rabbit heart. Each bar is the mean ± SEM from six rabbits. *Different from control at p = 0.04 for MAO and p = 0.02 for COMT.

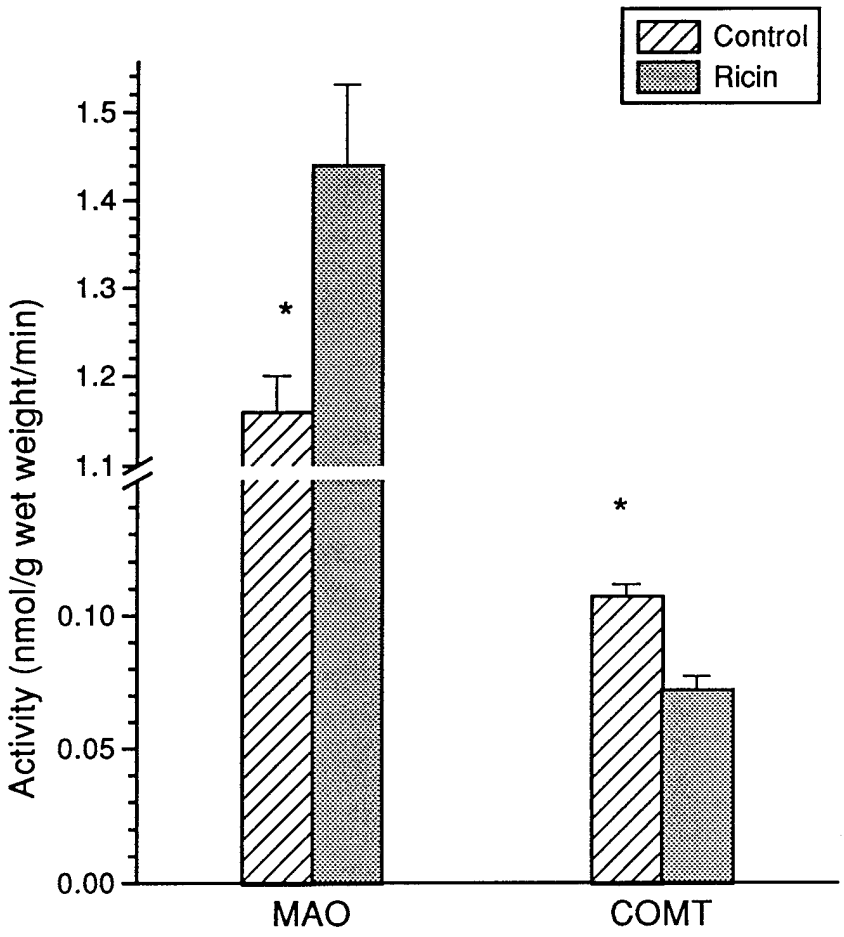

In control rabbits, histamine stimulation increased the amount of cAMP in coronary artery. The cAMP content reached a maximum at 15 seconds during the stimulation and quickly fell below the basal level at 30 seconds and then returned to close to basal levels (Table 11). The cAMP concentrations in coronary arteries from ricin intoxicated rabbits started to fall at the first time point after simulation, 15 seconds, instead of reaching a peak in the control. Whether the peak occurred earlier, or did not occur, was not investigated. The remainder of the curve is similar to that of control rabbits (Table 11).

2. *Effects of Ricin on Histamine-Stimulated cAMP Levels in Coronary Arteries.*

Histamine stimulation increased the cAMP content of coronary arteries from control rabbits (Figure 13, Table 12). The 10^{-6} M histamine stimulation increased the cAMP content of coronary arteries from rabbits receiving ricin. However, 10^{-4} M histamine stimulation did not increase but rather decreased the cAMP content in the ricin group (Figure 12, Table 12). Because of large differences present among experimental groups, instead of ANOVA analysis, an unpaired *t* test assuming unequal variances was used to analyze the difference between control and ricin groups, and a sign test was used to detect the effect of histamine on cAMP levels in rabbit coronary arteries (Tables 13, 14).

3. *Effects of Ricin on Responses of Histamine-Stimulated cGMP Levels in Coronary Arteries.*

The cGMP content in coronary arteries was significantly decreased by ricin administration ($p < 0.027$). In control rabbits histamine stimulation decreased cGMP content and with the simulation of 10^{-4} M histamine this depression was greater. The lower basal cGMP content in the ricin-treated rabbits was slightly depressed by histamine (Figure 14, Table 15).

Table 11. The cAMP content of coronary arteries from control rabbits and from rabbits receiving ricin following exposure to 0.1 mM histamine.

Time (seconds)	cAMP Content (pmoles/mg protein)	
	Control Mean ± SEM (n)[a]	Ricin Mean ± SEM (n)
0[b]	14.23 ± 0.54 (4)	17.93 ± 1.18 (3)
15	18.43 ± 1.82[c](6)	15.26 ± 1.33 (5)
30	13.28 ± 1.77 (5)	12.50 ± 2.19 (5)
60	15.03 ± 1.38 (5)	14.09 ± 3.44 (4)
120	14.49 ± 2.78 (5)	15.49 ± 3.53 (5)
240	14.08 ± 4.00 (4)	15.66 ± 3.32 (4)

[a] The number in parenthesis indicates the number of rabbits.

[b] The basal cAMP contents were used as its contents at 0 second.

[c] Significantly different from the control at 0 second (paired *t* test, $p < 0.040$).

Figure 13. The effects of ricin administration to rabbits on basal and histamine stimulated cAMP levels in their coronary arteries 48 hr after i.v. injection of 0.22 μg/kg of ricin. Each point was the mean ± SEM from 6 rabbits. * indicates significantly different from corresponding control.

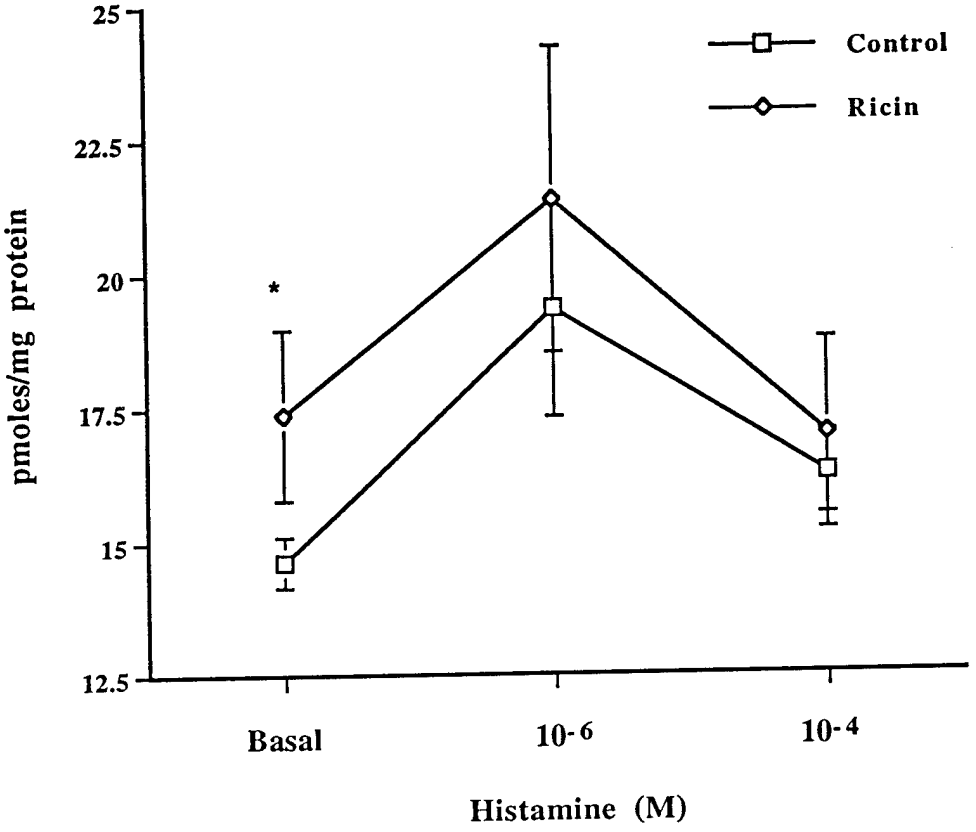

Table 12. Basal and 15 second histamine-stimulated cAMP content of coronary arteries from control rabbits and rabbits receiving ricin.

Histamine (M)	cAMP Content[a] (pmoles/mg protein)	
	Control Mean ± SEM (n)[b]	Ricin Mean ± SEM (n)
Basal	14.63 ± 0.48 (6)	17.78 ± 1.18[c] (6)
10^{-6}	19.34 ± 2.02 (6)	21.37 ± 3.05 (6)
10^{-4}	16.26 ± 1.49 (6)	16.87 ± 1.74 (6)

[a] Since big difference among the variations of the experimental groups, ANOVA is not an appropriate statistical procedure for this data set. The unpaired *t* test for two-samples assuming unequal variances was used to test the difference between corresponding ricin and control groups. The effects of histamine stimulation were examined by the sign test in the next pages.

[b] The number in parenthesis indicates the number of rabbits.

[c] Significant difference from corresponding control was detected by unpaired *t* test assuming unequal variances ($p < 0.048$).

Table 13. Sign Test for the effects of histamine stimulation on cAMP levels of rabbit coronary arteries in the control groups.

	Control Group					
Subject	1	2	3	4	5	6
Basal	16.21	13.14	14.16	14.65	13.84	.78
10^{-6}M	18.54	14.22	21.51	28.06	17.82	5.87
Gain	+	+	+	+	+	+

The null hypothesis is H_o: $p(+) = p(-) = 0.50$. If it is true, the probability of obtaining increases (+) in histamine stimulated cAMP levels in all six rabbits is:

$$p(6) = 6!(0.5^6 \text{ X } 0.5^0)/(6! \text{ X } 0!) = 0.0156$$

Thus, the null hypothesis is rejected and the 10^{-6} M histamine stimulation increased the cAMP levels in control rabbit coronary arteries.

Subject	1	2	3	4	5	6
Basal	15.21	13.14	14.16	14.65	13.84	15.78
10^{-4}M	17.74	20.59	16.07	9.721	15.58	17.89
Gain	+	+	+	-	+	- +

The null hypothesis is H_o: $p(+) = p(-) = 0.50$. If it is true, the probability of obtaining increases (+) in histamine stimulated cAMP levels in all six rabbits is:

$$p(6) + p(5) = 6!(0.5^6 \text{ X } 0.5^0)/(6! \text{ X } 0!) + 6!(0.5^5 \text{ X } 0.5^1)/(5! \text{ X } 1!) = 0.109$$

According to the p value, we failed to reject the null hypothesis, H_o. The 10^{-4} M histamine may not raise the cAMP levels in coronary arteries from control rabbits.

Table 14. Sign Test for the effects of histamine stimulation on cAMP levels of rabbit coronary arteries in the ricin groups.

	Ricin Group					
Subject	1	2	3	4	5	6
Basal	19.97	13.30	21.27	18.68	17.67	5.82
10^{-6}M	21.75	14.21	21.37	30.33	23.73	6.81
Gain	+	+	+	+	+	+

The null hypothesis is H_o: $p(+) = p(-) = 0.50$. If it is true, the probability of obtaining increases (+) in histamine stimulated cAMP levels in all six rabbits is:

$$p(6) = 6!(0.5^6 \text{ X } 0.5^0)/(6! \text{ X } 0!) = 0.0156$$

Thus, the null hypothesis is rejected and the 10^{-6} M histamine stimulation increased the cAMP levels in coronary arteries from rabbits given ricin.

Subject	1	2	3	4	5	6
Basal	19.97	13.30	21.27	18.68	17.67	5.82
10^{-4}M	19.76	20.32	9.952	19.99	17.81	3.39
Gain	-	+	-	+	+	-

The null hypothesis is H_o: $p(+) = p(-) = 0.50$. If it is true, the probability of obtaining increases (+) in histamine stimulated cAMP levels in all six rabbits is:

$$p(6) + p(5) + p(3) = 6!(0.5^6 \text{ X } 0.5^0)/(6! \text{ X } 0!) + 6!(0.5^5 \text{ X } 0.5^1)/(5! \text{ X } 1!) + 6!(0.5^4 \text{ X } 0.5^2)/(4! \text{ X } 2!)$$

$$= 0.343$$

We failed to reject the null hypothesis, H_o. The 10^{-4} M histamine may not raise the cAMP levels in coronary arteries from rabbits given ricin.

Figure 14. The effects of ricin administration to rabbits on basal and histamine stimulated cGMP levels in their coronary afters 48 hrs after i.v. injection of 0.22 μg/kg of ricin. Each point was the mean ± SEM from 6 rabbits.

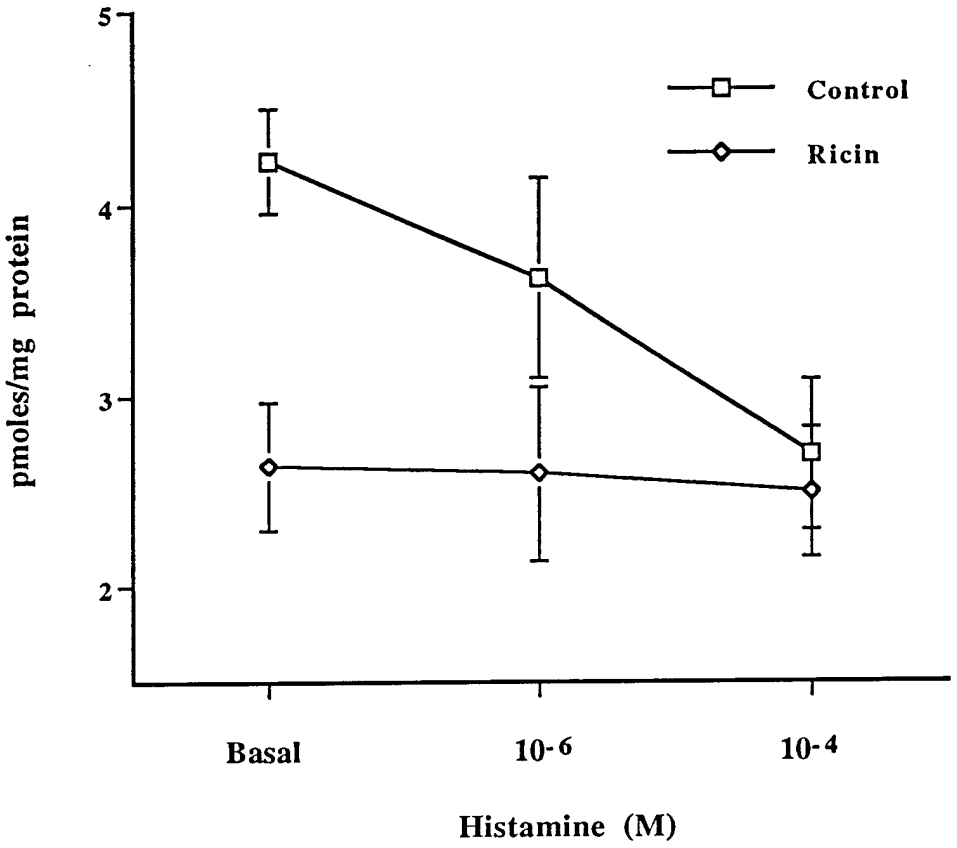

Table 15. Basal and 15 second histamine-stimulated cGMP content of coronary arteries from control rabbits and rabbits receiving ricin.

Histamine (M)	cGMP Content[a] (pmoles/mg protein)	
	Control[b] Mean ± SEM (n)[d]	Ricin[c] Mean ± SEM (n)
Basal	4.23 ± 0.27 (6)	2.62 ± 0.34 (6)
10^{-6}	3.62 ± 0.52 (6)	2.59 ± 0.46 (6)
10^{-4}	2.69 ± 0.40 (6)	2.48 ± 0.47 (6)

[a] ANOVA for two factors with repeat on histamine stimulation was used to analyze these data. A significant main effect was detected between the ricin group and the control group ($p < 0.027$). No significant main effect was detected among histamine groups. There was no significant interaction found between the two factors ($p > 0.17$).

[b] With ANOVA regression analysis, a significant linear relationship was detected between histamine dose and cGMP content in control group ($p < 0.013$).

[c] With ANOVA regression analysis, no significant linear relationship was detected between histamine dose and cGMP content in ricin group ($p > 0.83$).

[d] The number in parenthesis indicates the number of rabbits.

4. Effects of Ricin Administration on Basal Levels of cAMP and cGMP in Right Papillary Muscle

Ricin administration depressed the basal formation of cyclic AMP (mean ± SEM, pmol/mg wet tissue weight) (control: 3.12 ± 0.06; ricin: 2.87 ± 0.04, n=12, p = 0.0001) (Figure 15). The basal formation of cyclic GMP (mean ± SEM, pmol/mg wet tissue weight) (control: 0.21 ± 0.03; ricin: 0.18 ± 0.02, n=12, p = 0.003) (Figure 15) in the right ventricular papillary muscle from rabbits receiving ricin was also significantly depressed.

E. Effects of Ricin on Phosphatidylinositol Hydrolysis

1. Rabbit Coronary Arteries.

The elution curve obtained for inositol phosphate standards by anion-exchange columns is shown in Figure 16. The volumes of eluting solutions with different strengths were identical to those used in a previous report (Lang and Lewis, 1988).

Ricin administration depressed both basal and histamine-stimulated accumulation of IP_1 in rabbit coronary arteries ($p \leq 0.006$). Histamine stimulation increased IP_1 accumulation ($P \leq 0.0001$) both in the control and ricin group (Figure 17). With 10^{-4} M histamine stimulation IP_1 levels were increased by 2.98 times in control rabbits and by 2.89 times in rabbits receiving ricin (Table 16). Histamine stimulation also increased IP_2 levels ($p < 0.0001$) both in control rabbits and rabbits given ricin (Table 17, Figure 18). The basal IP_3 level was increased by ricin administration ($p \leq 0.0004$) but the 10^{-4} M histamine stimulated IP_3 level was decreased ($p < 0.0049$) (Table 18, Figure 19). Histamine stimulation also increased IP_3 levels in control rabbits but did not do so in rabbits receiving ricin (Figure 19, Table 18).

The basal and histamine-stimulated relative levels of IP_3, IP_2 and IP_1 from control rabbits and rabbits given ricin are shown in Figures 20, 21 and 22, respectively. The comparisons of the relative ratios of IP_2/IP_3 and IP_1/IP_2 of basal and histamine stimulated

Figure 15. Effects of ricin on intracellular cyclic AMP and cyclic GMP in rabbit papillary muscle or myocardium (whichever). Each bar is the mean ± SEM from twelve rabbits. *Different at p = 0.0001 for cAMP and p = 0.003 for cGMP from control.

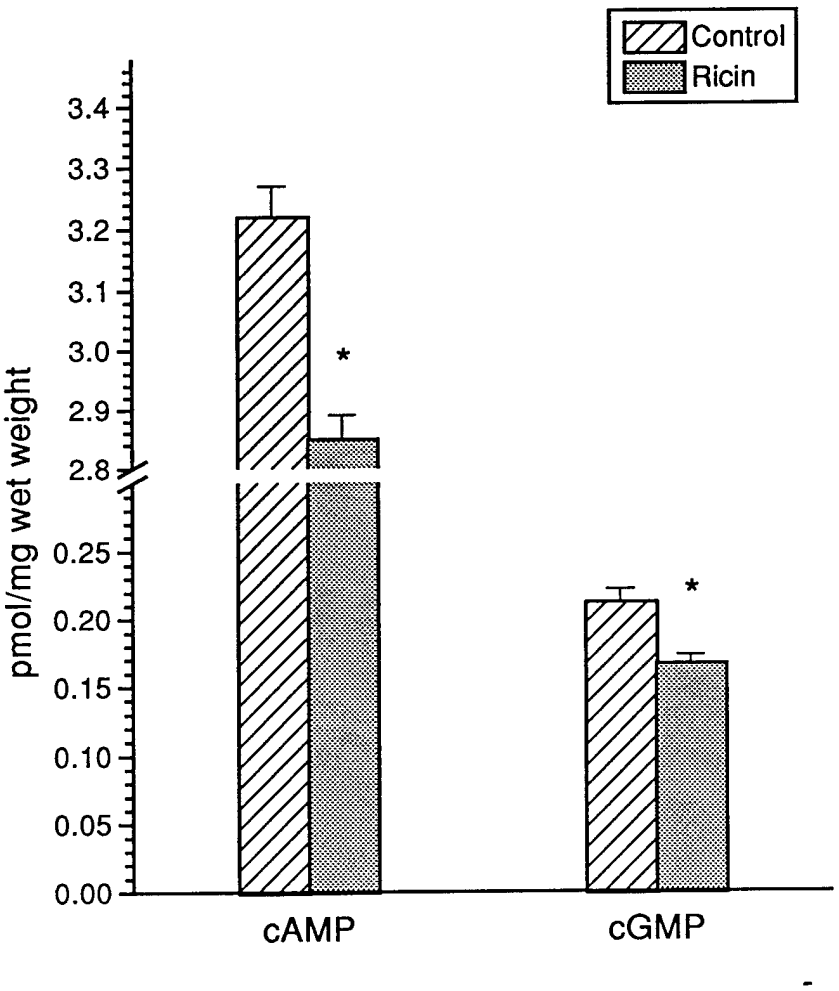

Figure 16. Elution profile of standard phosphoinositols, [^{3}H] IP_1, [^{3}H] IP_2 and [^{3}H] IP_3 on AG 1x8 resin anio -exchange column. The column was eluted with (1) distilled water; (2) 5 nM-disodium tetraborate / 60 mM-sodium formate; (3) 0.1 M-formic acid / 0.2 M-ammonium formate; (4) 0.1 M-formic acid / 0.4 M ammonium formate; (5) 0.1 M-formic acid / 1.0 M-ammonium formate. Each fraction was 2 ml.

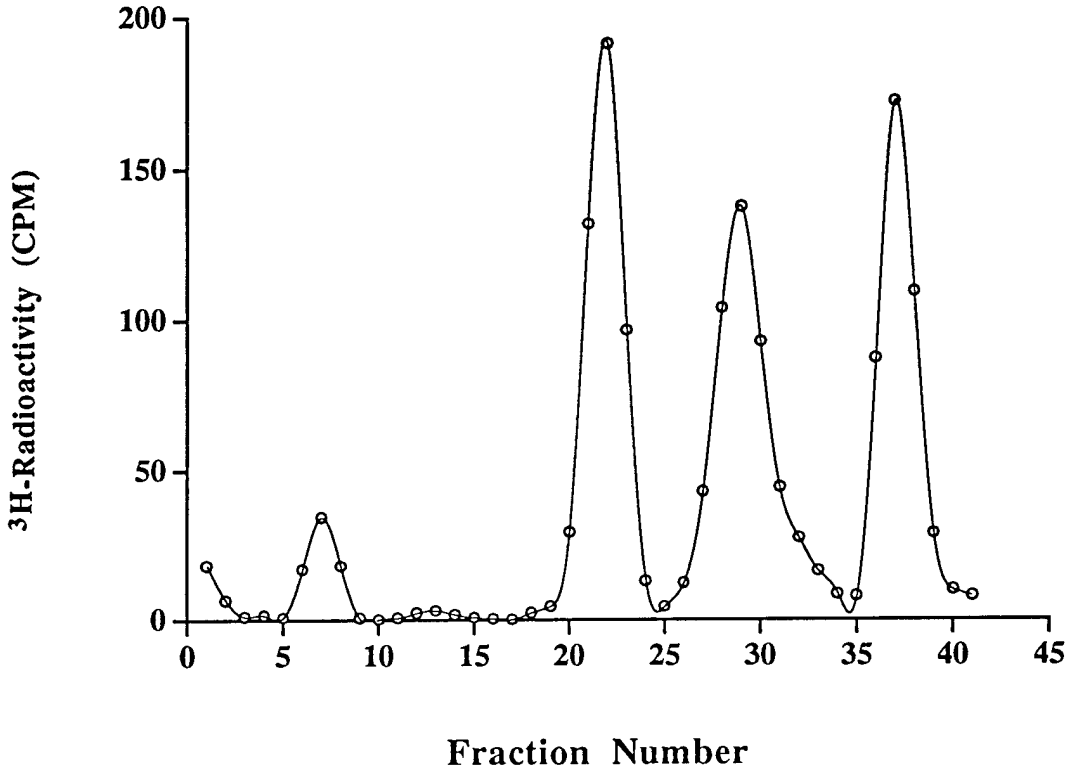

Figure 17. The effects of ricin administration to rabbits on basal and histamine stimulated IP1 levels in their coronary arteries 48 hr. after i.v. injection of 0.22 μg/kg of ricin. Each point was the mean ± SEM from 6-9 rabbits. *indicates significantly different from control.

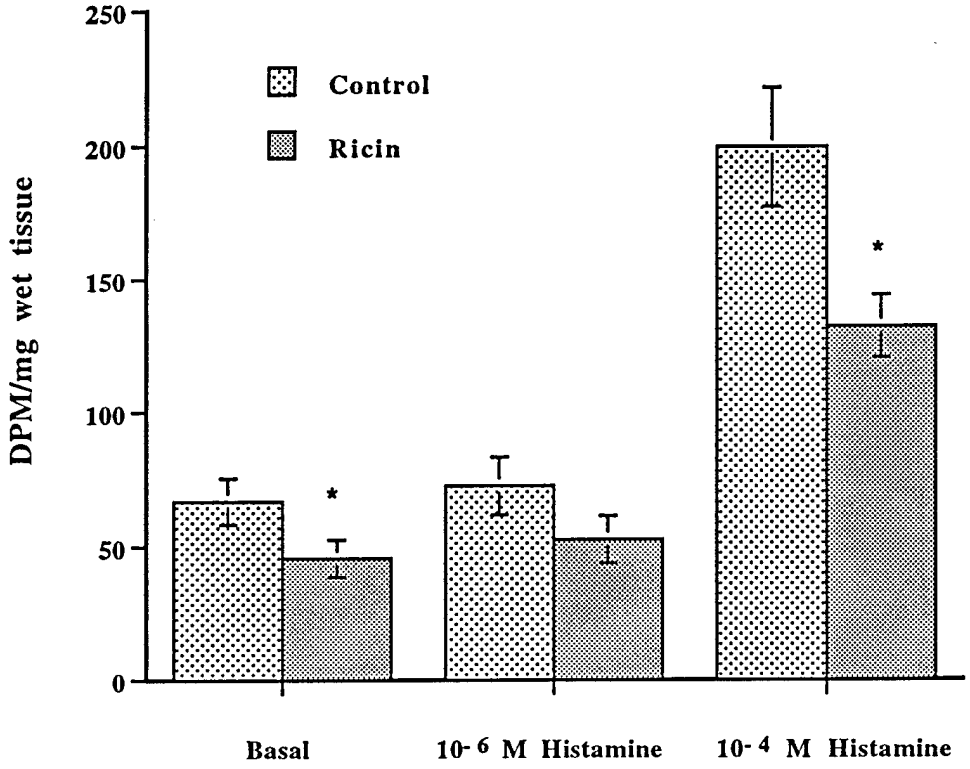

Table 16. Basal and histamine-stimulated IP_1 content of coronary arteries from control rabbits and rabbits receiving ricin.

Histamine (M)	IP_1 Content[a] (dpm/mg wet weight)	
	Control Mean ± SEM (n)[b]	Ricin Mean ± SEM (n)
Basal	66.89 ± 8.60 (7)	45.68 ± 6.89 (7)
10^{-6}	72.57 ± 10.60 (7)	52.64 ± 8.82 (7)
10^{-4}	199.34 ± 22.10 (7)	132.18 ± 11.82 (7)

[a] ANOVA for two factors with repeat on histamine stimulation was used to analyze these data. Significant main effects were detected between control and ricin groups ($p < 0.006$) and among histamine groups ($p < 0.0001$). There was no significant interaction found between the two factors ($p > 0.106$).

[b] The number in parenthesis indicates the number of rabbits.

Table 17. Basal and histamine-stimulated IP_2 content of coronary arteries from control rabbits and rabbits receiving ricin.

Histamine (M)	IP_2 Content[a] (dpm/mg wet weight)	
	Control Mean ± SEM (n)[b]	Ricin Mean ± SEM (n)
Basal	23.92 ± 2.79 (7)	33.59 ± 2.66 (7)
10^{-6}	31.89 ± 4.34 (7)	34.12 ± 1.97 (7)
10^{-4}	51.97 ± 5.85 (7)	45.56 ± 5.44 (7)

[a] ANOVA for two factors with repeat on histamine stimulation was used to analyze these data. A significant main effect was detected among histamine groups ($p < 0.0001$). No significant main effect was detected between control and ricin groups ($p > 0.65$). There was no significant interaction found between the two factors ($p > 0.11$).

[b] The number in parenthesis indicates the number of rabbits.

Figure 18. The effects of ricin administration to rabbits on basal and histamine stimulated IP2 levels in their coronary arteries 48 hr after i.v. injection of 0.22 μg/kg of ricin. Each point was the mean ± SEM from 6-9 rabbits.

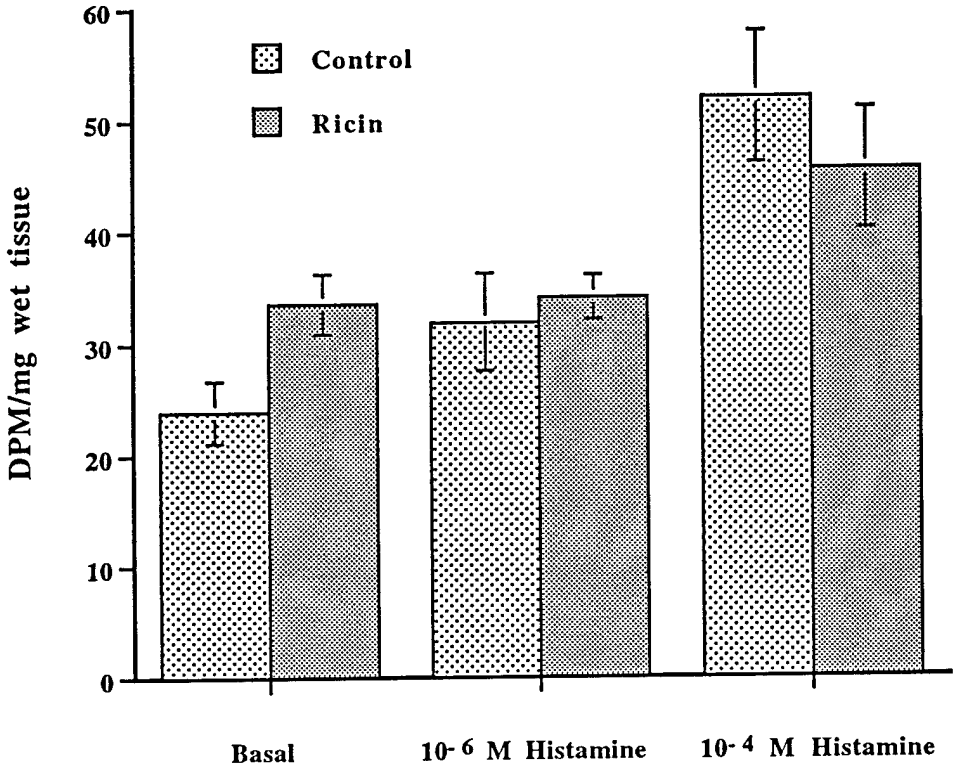

Figure 19. The effects of ricin administration to rabbits on basal and histamine stimulated IP3 levels in their coronary arteries 48 hr after i.v. injection of 0.22 μg/kg of ricin. Each point was the mean ± SEM from 6-9 rabbits. * indicates significantly different from control.

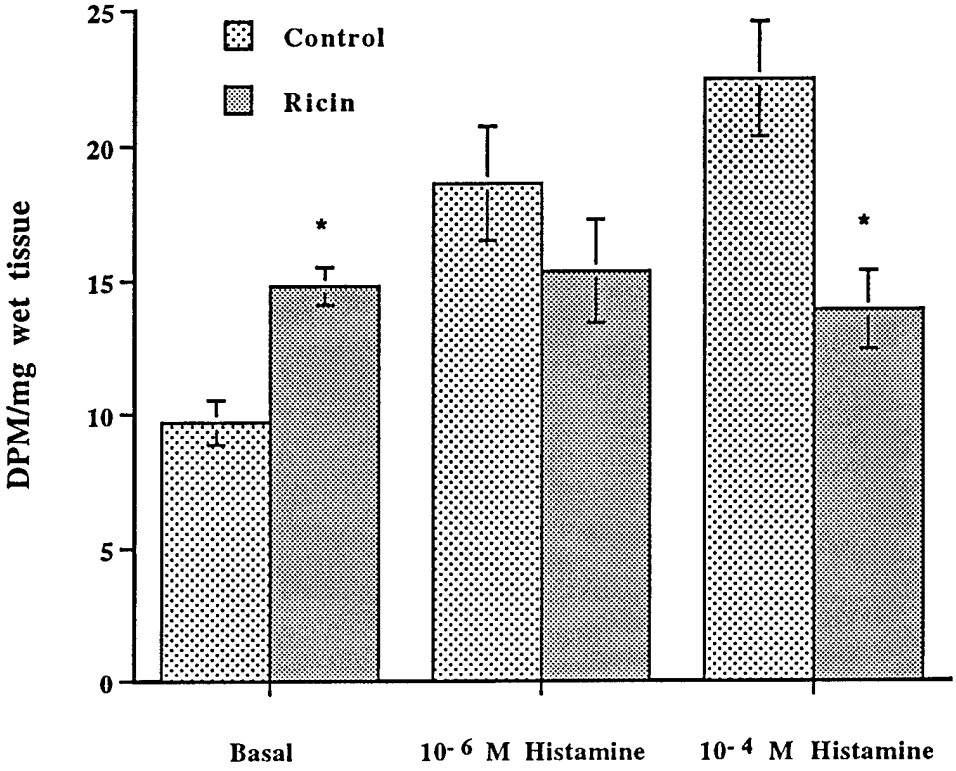

Table 18. Basal and histamine-stimulated IP_3 content of coronary arteries from control rabbits and rabbits receiving ricin.

Histamine (M)	IP_3 Content[a] (dpm/mg wet weight)	
	Control Mean ± SEM (n)[b]	Ricin Mean ± SEM (n)
Basal	9.68 ± 0.83 (7)	14.80 ± 0.71[e] (7)
10^{-6}	18.63 ± 2.11 (7)	15.36 ± 1.94 (7)
10^{-4}	22.47 ± 2.12 (7)	13.90 ± 1.48[f] (7)

[a] ANOVA for two factors with repeat on histamine stimulation was used to analyze these data. There was a significant interaction found between the two factors ($p < 0.0017$).

[b] With ANOVA simple effect analysis, a significant simple effect of histamine was detected in control group ($p < 0.0014$).

[c] With ANOVA simple effect analysis, no significant simple effect of histamine was detected in ricin group ($p > 0.79$).

[d] The number in parenthesis indicates the number of rabbits.

[e] With ANOVA simple effect analysis, a significant difference was detected between the ricin group and the corresponding control group ($p < 0.0004$).

[f] With ANOVA simple effect analysis, a significant difference was detected between the ricin group and the corresponding control group ($p < 0.0049$).

Figure 20. The effects of ricin administration to rabbits on the basal inositol triphosphate hydrolysis in their coronary arteries 48 hr after i.v. injection of 0.22 μg/kg of ricin. Each point was the mean ± SEM from 6-9 rabbits. *indicates significantly different from control.

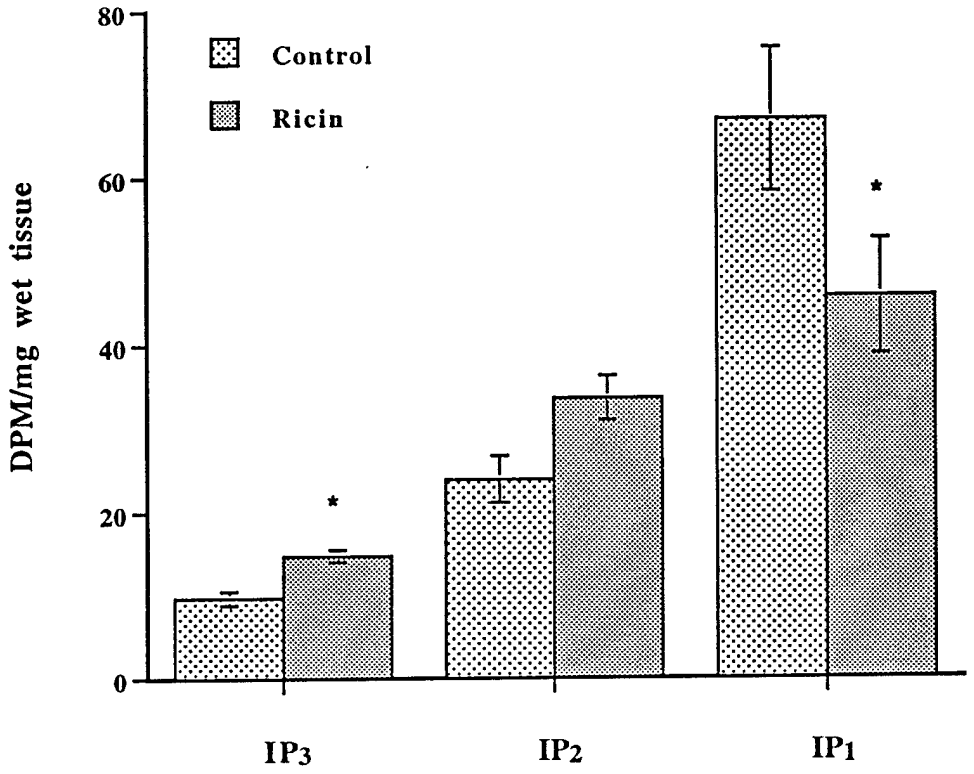

Figure 21. The effects of ricin administration to rabbits on the 10^{-6} M histamine stimulated inositol triphosphate hydrolysis in their coronary arteries 48 hr after i.v. injection of 0.22 μg/kg of ricin. Each point was the mean ± SEM from 6-9 rabbits. * indicates significnatly different from control.

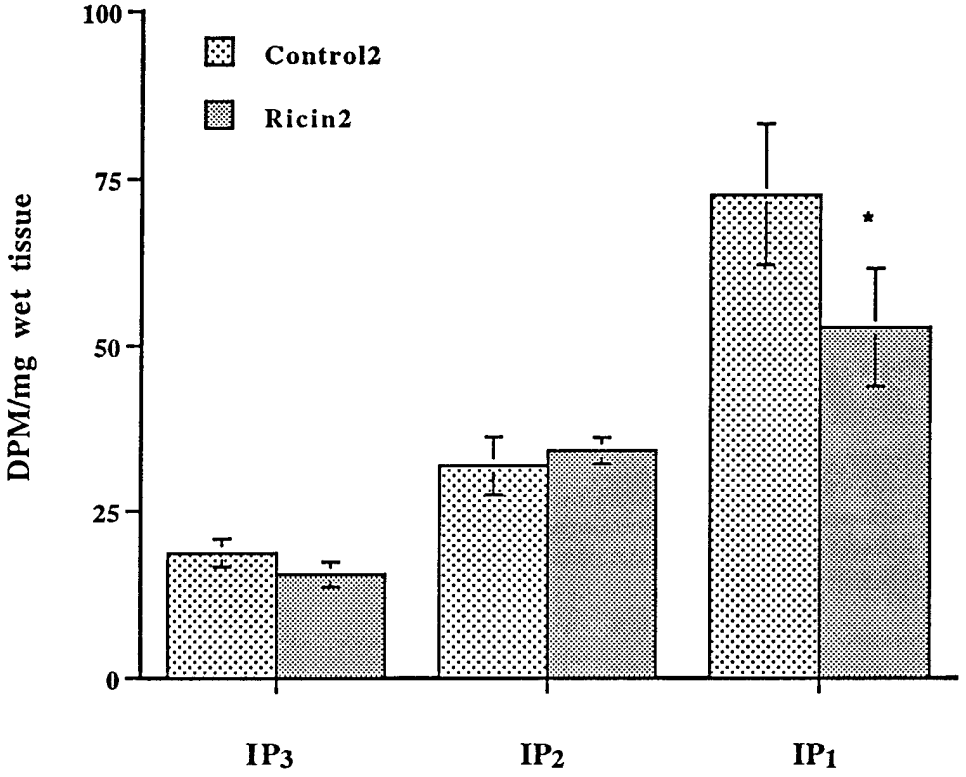

Figure 22. The effects of ricin administration to rabbits on the 10^{-4} M histamine stimulated inositol triphosphate hydrolysis in their coronary arteries 48 hr after i.v. injection of 0.22 μg/kg of ricin. Each point was the mean ± SEM from 6-9 rabbits. * indicates significantly different from control.

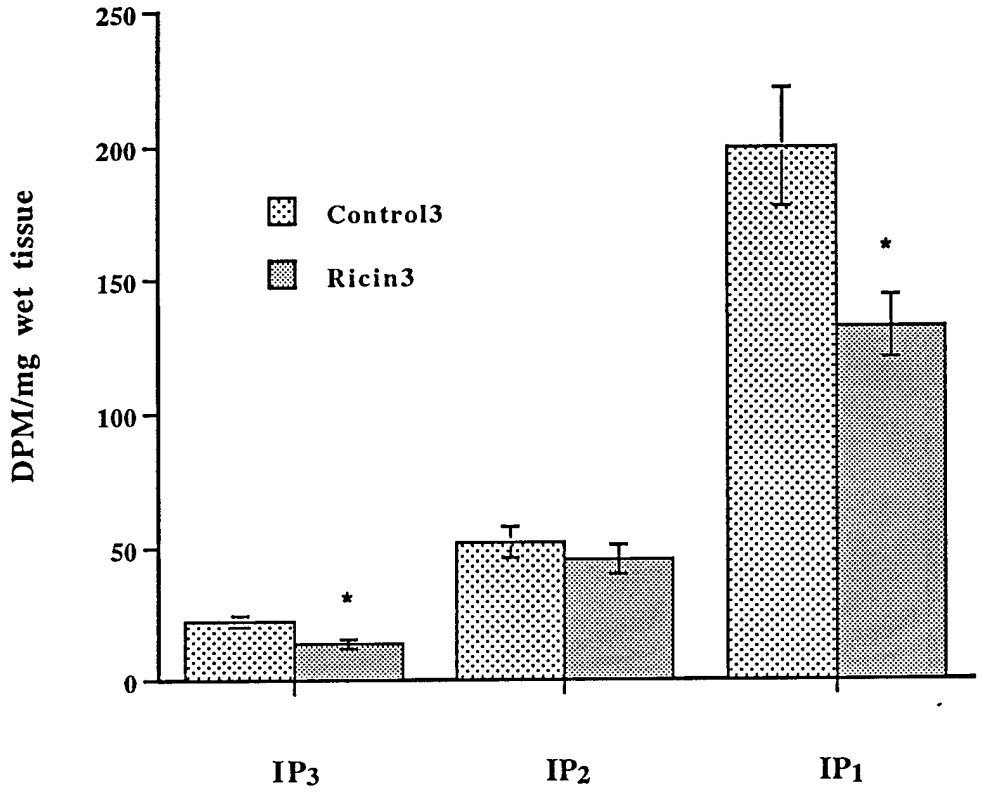

inositol phosphates from control and ricin group are shown in Table 19, 20 and 21, respectively. The basal ratio of IP_1/IP_2 in the ricin group was significantly lower than that of the corresponding control group ($p < 0.029$) (Table 19).

2. *Right Papillary Ventricular Muscle.*

No alterations in the basal levels of inositol 1-phosphate (IP_1), inositol 1,4-biphosphate (IP_2), and inositol 1,4,5-triphosphate (IP_3) were observed. The basal levels of IP_1, IP_2, and IP_3 were not different in right ventricular papillary muscle from control rabbits and rabbits receiving ricin (p = 0.13, 0.85, and 0.78, respectively) (Figure 23).

F. Effects of Ricin on Contractions of Paced Papillary Muscle.

Responses of papillary muscles from rabbits given ricin were compared with those of sham injected control rabbits. Two mechanical parameters, time to peak tension and duration of papillary muscle contractions, did not differ between the two groups (Figure 24) with p values of 0.47 and 0.74, respectively. Frequency responses of papillary muscles paced at from 0.5 to 3.0 Hz showed a frequency-depedent in force development for both control and rabbits receiving ricin. Frequency responses of control papillary muscles were not significantly different from that of papillary muscle from ricin-treated rabbits (P = 0.34) (Figure 25). Figure 26 shows the effects of ricin on contractions of rabbit papillary muscle stimulated at 1 Hz and by paired pacing. The tension generated by papillary muscles paced at 1 Hz was not different between the two groups (p = 0.21). The maximal contraction of papillary muscle generated by paired pacing was no different in either case between rabbits receiving ricin and control rabbits (p = 0.21).

G. Effects of Ricin Administration on Contractions of Papillary Muscle in the Presence of Isoproterenol.

Table 19. Comparison of the ratios of basal inositol phosphates of coronary arteries from control rabbits and rabbits receiving ricin.

Ratio	Control Mean ± SEM (n)[a]	Ricin Mean ± SEM (n)
IP_2/IP_3	2.63 ± 0.30 (8)	2.38 ± 0.17 (8)
IP_1/IP_2	2.56 ± 0.32 (7)	1.33 ± 0.19[b](6)

[a] The number in parenthesis indicates the number of rabbits.

[b] Significantly different from the corresponding control (unpaired *t* test, $p < 0.029$)

Table 20. Comparison of the ratios of 10^{-6} M histamine-stimulated inositol phosphates of coronary arteries from control rabbits and rabbits receiving ricin.

Ratio	Control Mean ± SEM (n)[a]	Ricin Mean ± SEM (n)
IP_2/IP_3	1.82 ± 0.24 (8)	2.30 ± 0.27 (8)
IP_1/IP_2	2.14 ± 0.40 (8)	1.52 ± 0.24 (8)

[a] The number in parenthesis indicates the number of rabbits.

Table 21. Comparison of the ratios of 10^{-4} M histamine-stimulated inositol phosphates of coronary arteries from control rabbits and rabbits receiving ricin.

Ratio	Control Mean ± SEM (n)[a]	Ricin Mean ± SEM (n)
IP_2/IP_3	3.03 ± 0.48 (8)	3.45 ± 0.34 (7)
IP_1/IP_2	2.79 ± 0.36 (8)	3.05 ± 0.33 (8)

[a] The number in parenthesis indicates the number of rabbits.

Figure 23. Effects of ricin administration on phosphoinositide hydrolysis in myocardium. Each bar is the mean ± SEM from six rabbits. IP1: inositol 1-phosphate, IP2: inositol 1,4-biphosphate, IP3: inositol 1,4,5-triphosphated.

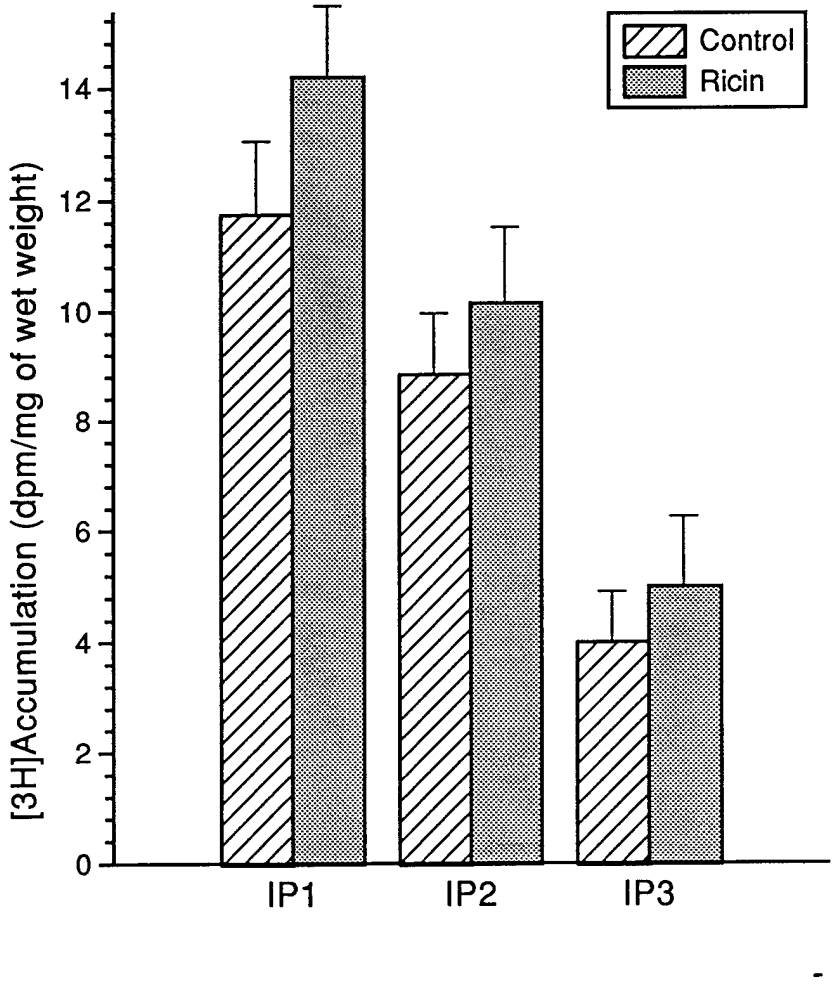

Figure 24. Effects of ricin on the rabbit papillary muscle contraction duration, and time to peak tension. Each bar is the mean ± SEM from six rabbits.

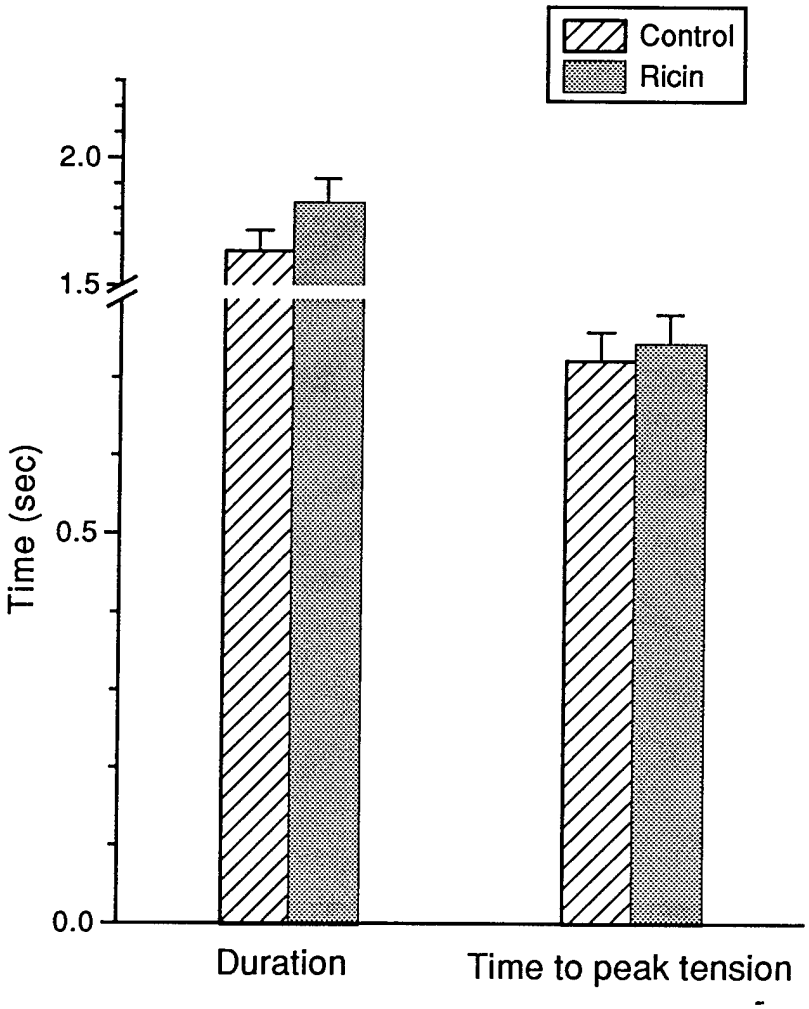

Figure 25. Effects of ricin on contractions of rabbit papillary muscle to electrical stimulation. Each point represents the mean ± SEM from 6 rabbits.

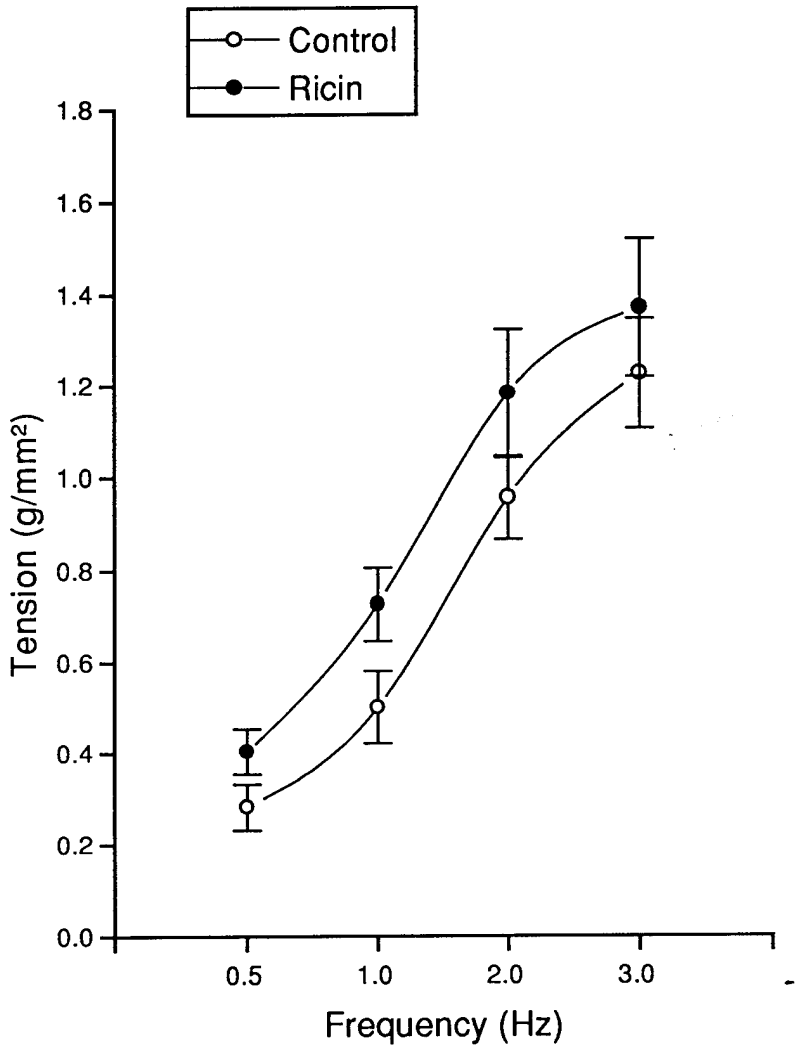

Figure 26. Effects of ricin on contractions of rabbit papillary muscle stimulated by 1 Hz and by paired pacing. Each bar is the mean ± SEM from six rabbits.

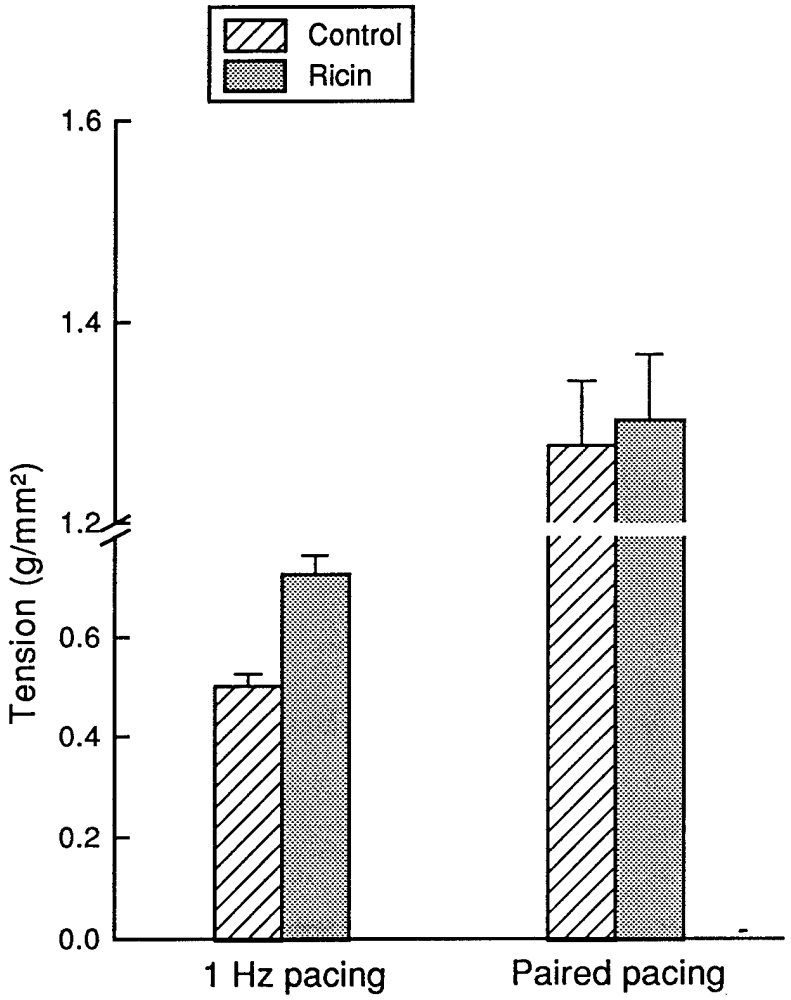

Papillary muscle paced at 1 Hz was exposed to cumulatively increasing concentrations of isoproterenol (Figure 27). Increasing force generation of papillary muscles with increasing concentrations of isoproterenol in the tissue bath was observed in both control rabbits and those receiving ricin. No differences in contractions between papillary muscles from control rabbits and those receiving ricin were significant ($P = 0.75$).

H. Effects of Ricin Administration on the Electrophysiological Properties of Rabbit Papillary Muscle.

Electrophysiological parameters of rabbit papillary muscle were determined (Table 22). These included measuring the resting membrane potential, the action potential amplitude, the overshoot potential, the maximal dv/dt of Phase 0, the action potential duration, and the effective refractory period. In comparing papillary muscle data from rabbits receiving ricin and control rabbits, a slight prologation of the action potential duration was observed ($p = 0.06$) and the effective refractory period was significantly increased ($P = 0.04$).

I. Effects of Ricin Administration on Cardiac Performance in the Isolated Perfused Rabbit Heart.

Administration of an intravenous bolus of a minimum lethal dose of ricin 48 hours earlier did not alter oxygen consumption, heart rate, and electrocardiographic parameters (Table 23). No arrhythmias or conduction abnormalities were observed during the baseline recording period. However, ricin administration significantly reduced left ventricular compliance (Figure 28) and diminished the left ventricular developed pressure per balloon volume (Figure 29). The maximal left ventricular developed pressure and the maximal positive dp/dt in the ricin treated group was decreased ($p = 0.007$, and $p = 0.006$, respectively) (Table 24). The maximal relaxation of the isolated heart as assessed by -dp/dt was slightly decreased by ricin administration ($p = 0.056$). The ANOVA analysis showed

Figure 27. Effects of ricin on contractions of rabbit papillary muscle to electrical stimulation in the presence of isoproterenol. Each point represents the mean ± SEM from 6 rabbits.

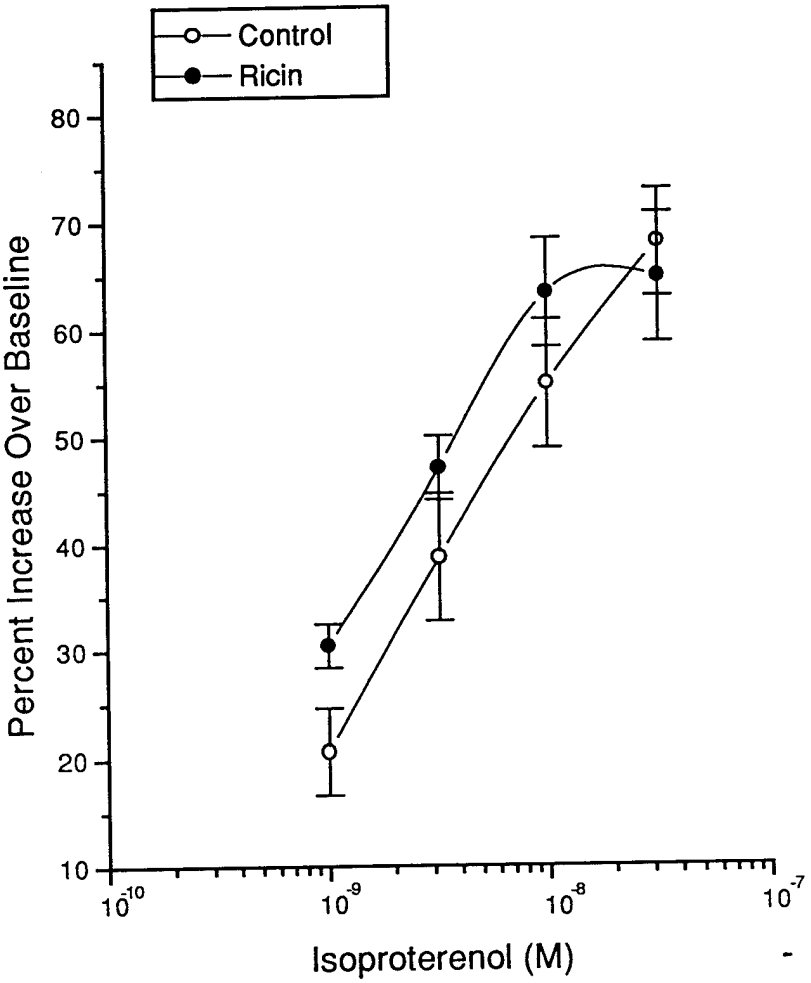

Table 22. Electrophysiological parameters of rabbit papillary muscle from control rabbits and those given ricin.

Parameters	Control (n=6) mean ± SEM	Ricin (n=6) mean ± SEM	p values
Resting Membrane Potential (mV)	-77 ± 1	-81 ± 2	0.54
Action Potential Amplitude (mV)	87 ± 4	93 ± 4	0.38
Overshoot Potential (mV)	20 ± 2	22 ± 3	0.63
Maximal dv/dt of Phase 0 (V/sec)	68 ± 4	71 ± 4	0.65
Action Potential duration (ms)	128 ± 8	150 ± 7	0.06
Effective Refractory Period (ms)	125 ± 12	162 ± 12	0.04

n = six different rabbits.

Table 23. Effects of ricin on coronary resistance oxygen consumption and electrocardiographic parameters of the isolated heart.

Measurements	Control (n=10) (mean ± SEM)	Ricin (n=9) (mean ± SEM)	p value
Heart Rate (bpm)	166.44 ± 24.62	147.89 ± 19.86	0.10
PR Interval (ms)	80.44 ± 16.71	73.23 ± 12.14	0.38
QRS Duration (ms)	47.20 ± 6.84	60.46 ± 7.21	0.83
QT Interval (ms)	180.72 ± 32.62	191.64 ± 19.00	0.43
Oxygen Consumption (ml/mi/gm)	0.057 ± 0.006	0.054 ± 0.001	0.65
Coronary Resistance (mmHg/min/ml)	2.57 ± 0.49	2.88 ± 0.53	0.21

n = number of rabbits.

Figure 28. Effects of ricin on the left ventricular compliance of the rabbit heart. Each point is the mean ± SEM from 9 to 10 rabbits. *Different from control at p = 0.007.

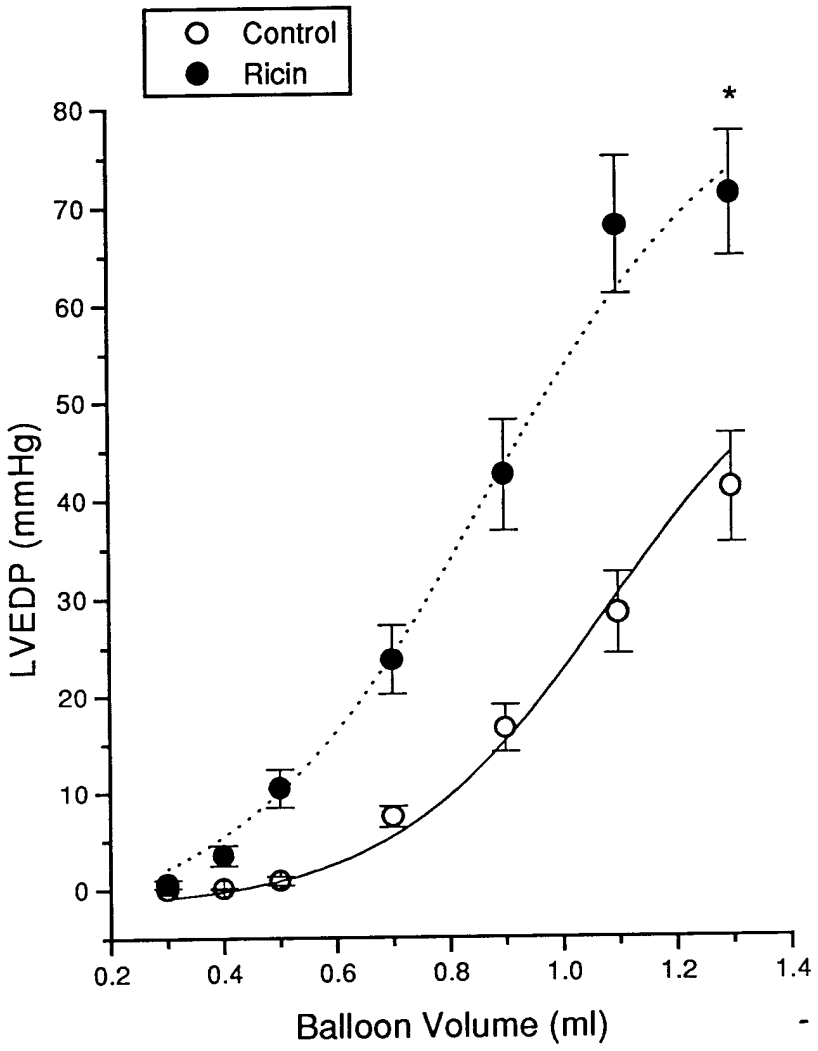

Figure 29. Effects of ricin on the left ventricular developed pressure per balloon volume. Each point represents the mean ± SEM from 9 to 10 rabbits. *Different from control at p = 0.045.

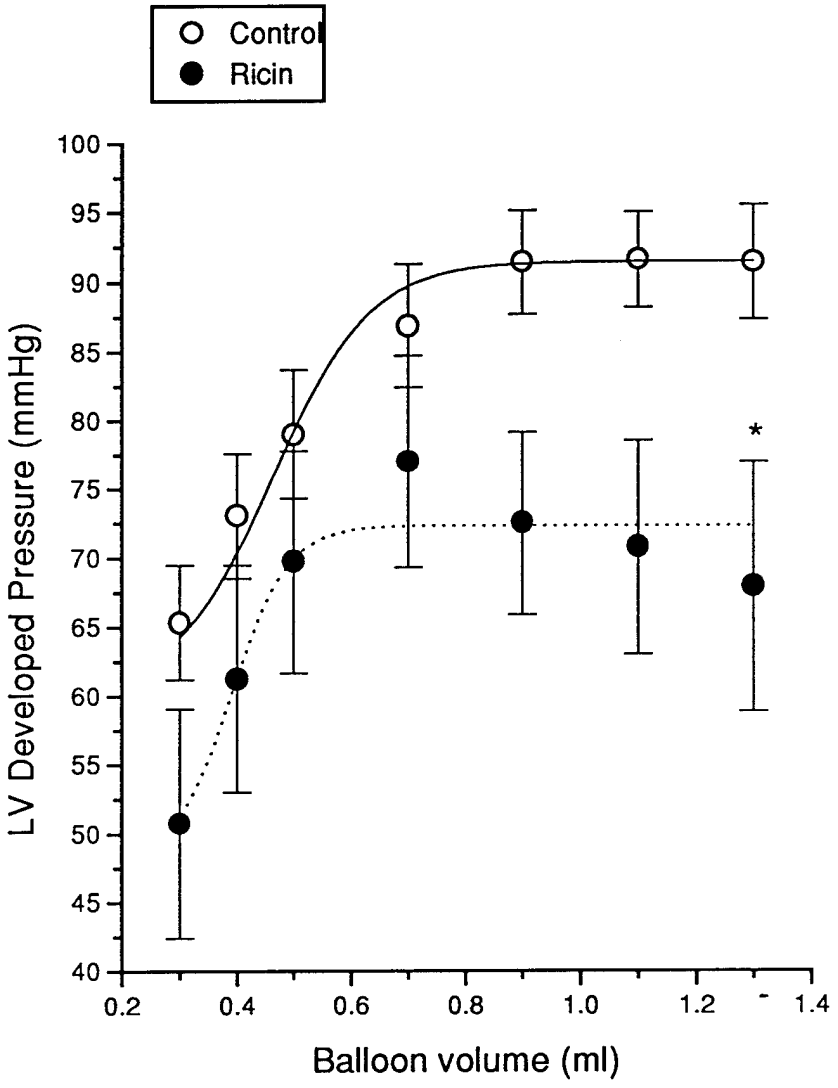

Table 24. Effects of ricin on maximal LVDP, contractility and relaxation of the isolated rabbit heart.

	Responses		
Measurements	Control (n=10) (mean ± SEM)	Ricin (n=9) (mean ± SEM)	p value
LVDP (mmHg)	95.25 ± 4.3	80.80 ± 7.1	0.007
Positive dp/dt (mmHg/sec)	521.95 ± 37.28	455.38 ± 55.92	0.006
Negative dp/dt (mmHg/sec)	354.18 ± 23.96	372.83 ± 77.23	0.056

LVDP = left ventricular developed pressure, n = number of rabbits.

ricin administration had different effects at different levels of volume-induced increase in left ventricular end diastolic pressure (Figure 28) and contractililty as assessed by positive dp/t (Figure 30). The results from trend analysis indicated that the relaxation of the isolated heart as assessed by the negative dp/dt (Figure 31) were altered by ricin administration ($p = 0.04$).

To assess the effects of ricin on *beta*-adrenoceptor-mediated inotropic effects in the isolated rabbit heart, isoproterenol was incrementally added to the perfusate to generate dose response curves. Left ventricular developed pressure, +dp/dt and -dp/dt were recorded and there was no difference in those measurements between the control group and the one receiving ricin (Table 25) (for -dp/dt, data are not shown). Figures 32 and 33 show the effects of ricin on the isoproterenol-induced increase in left ventricular developed pressure and contractility as reflected by the positive dp/dt.

The effects of ricin on *alpha* adrenoceptor-mediated inotropic responses were also evaluated. Propranolol was used to block possible *beta*-adrenoceptor stimulation by phenylephrine. Concentration-dependent changes in the above hemodynamic parameters by phenylephrine were not affected by ricin administration (Figures 34, 35, and Table 25). Thus, administration of a minimum lethal dose of ricin did not alter the EC_{50}s of either isoproterenol and phenylephrine in the isolated heart.

J. Determination of the Effects of Ricin Administration on the Affinity and Density of Beta-Adrenergic Receptors in the Rabbit Myocardium.

Radioligand binding in the membrane preparations from rabbits given ricin and control rabbits were compared (Figure 36). Ricin did not significantly alter the number of [^{3}H]-dihydroalprenolol binding sites (ricin: mean ± SEM, B_{max} = 386.6 ± 123.0 fmol/mg, n = 6; control: B_{max} = 328.3 ± 144.9 fmol/mg, n=6) (Figure 37). Ricin did not alter the K_d for [^{3}H]-dihydroalprenolol binding, mean ± SEM, (ricin: 9.1 ± 2.0 nM, n = 6; control: 9.1 ± 5.7 nM, n = 6), indicating that ricin did not alter the affinity of the *beta*-adre-

Figure 30. Effects of ricin on the contractility of rabbit heart as reflected by the +dp/dt at balloon volume. Each point is the mean ± SEM from 9 to 10 rabbits.

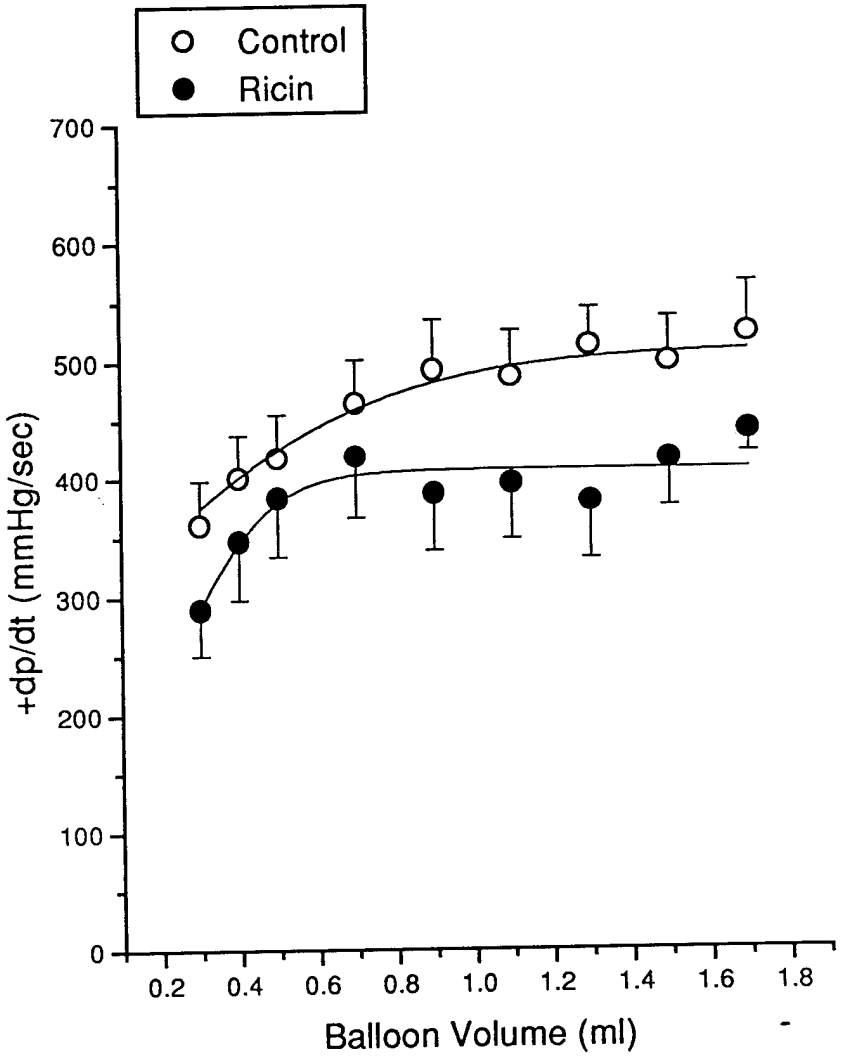

Figure 31. Effects of ricin on the relaxation of the rabbit heart as reflected by -dp/dt per balloon volume. Each point is the mean ± SEM from 9 to 10 rabbits.

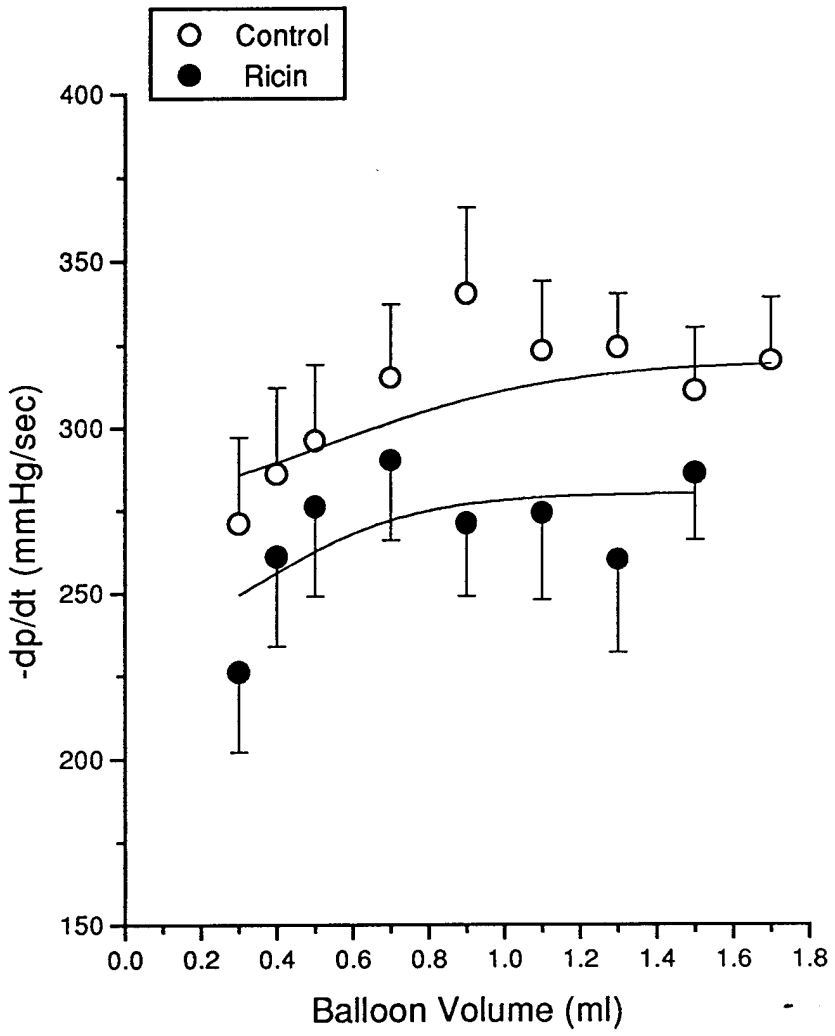

Table 25. The EC_{50} for left ventricular developed pressure and contraction of rabbit isolated heart by *alpha-* and *beta*-adrenergic receptor agonists.

	EC_{50} (x 10^{-9} M)		
Parameters	Control (n=9) (mean ± SEM)	Ricin (n=8) (mean ± SEM)	p values
LVDP by Isoproterenol	6.26 ± 2.69	1.34 ± 0.84	0.08
LVDP by Phenylephrine	22.02 ± 3.84	15.72 ± 1.74	0.25
Contraction by Isoproterenol	2.25 ± 0.54	4.74 ± 1.69	0.36
Contraction by Phenylephrine	44.64 ± 4.71	40.84 ± 4.63	0.37

LVDP = left ventricular developed pressure, n = number of rabbits.

Figure 32. Effects of ricin on the isoproterenol-induced increase in left ventricular developed pressure in rabbit heart. Each point is the mean ± SEM from 9 to 10 rabbits.

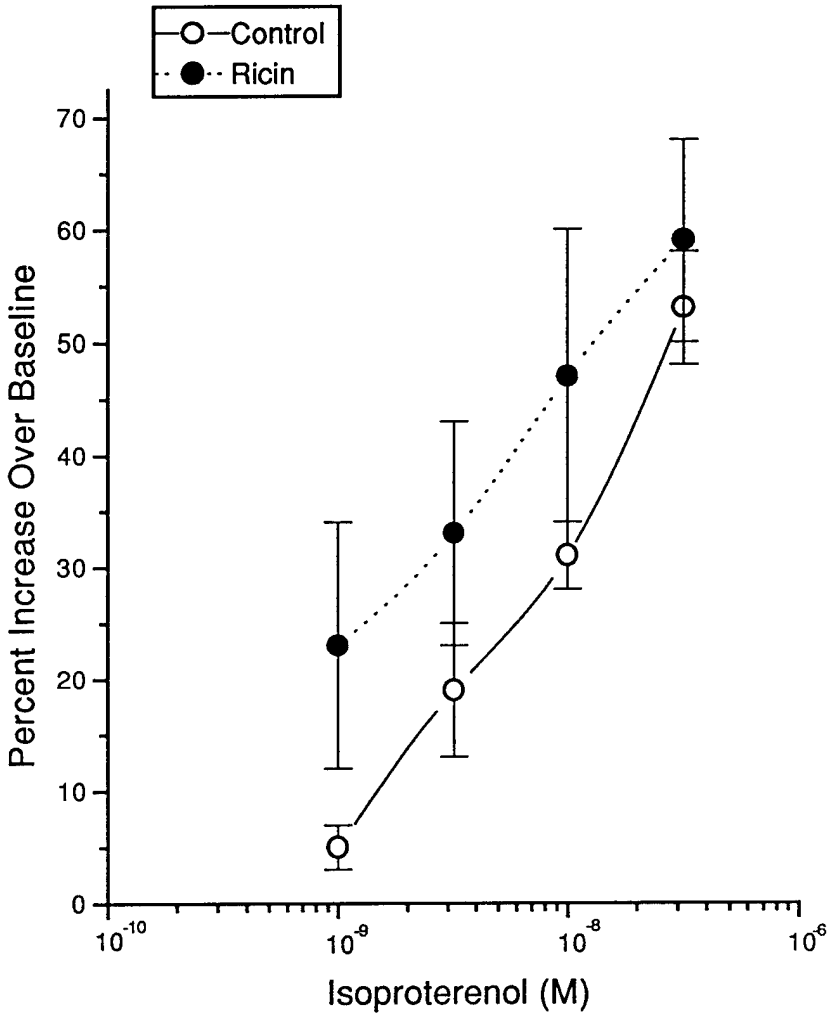

Figure 33. Effects of ricin on the contractility of the rabbit heart as reflected by +dp/dt as influenced by isoproterenol. Each point is the mean ± SEM from 9 to 10 rabbits.

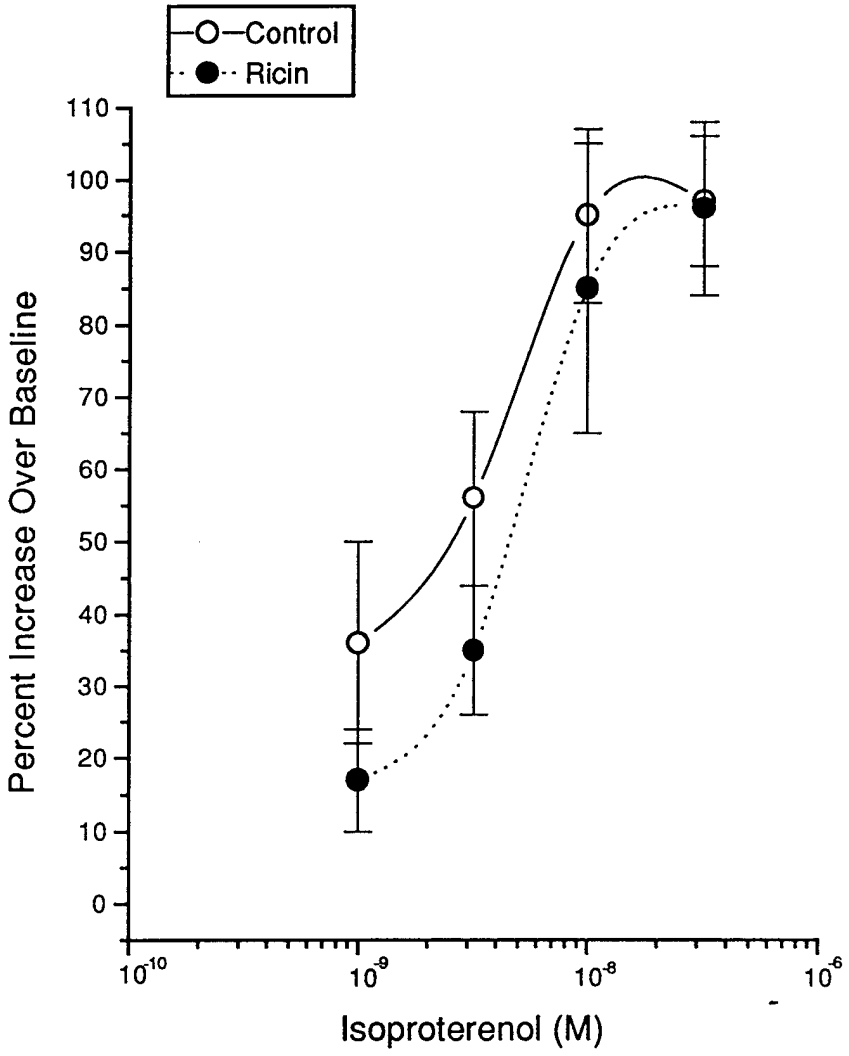

Figure 34. Effects of ricin on the phenylephrine-induced increase in left ventricular developed pressure in rabbit heart. Each point is the mean ± SEM from 9 to 10 rabbits.

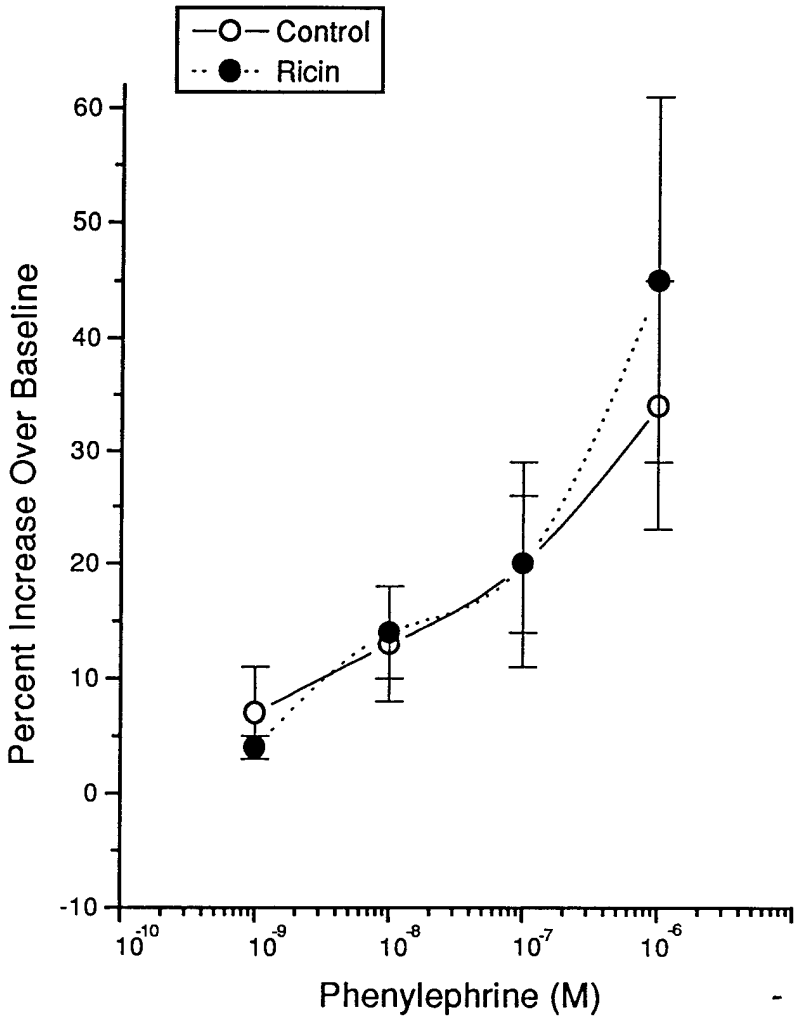

Figure 35. Effects of ricin on the contractility of the rabbit heart as reflected by +dp/dt as influenced by phenylephrine. Each point is the mean ± SEM from 8 to 10 rabbits.

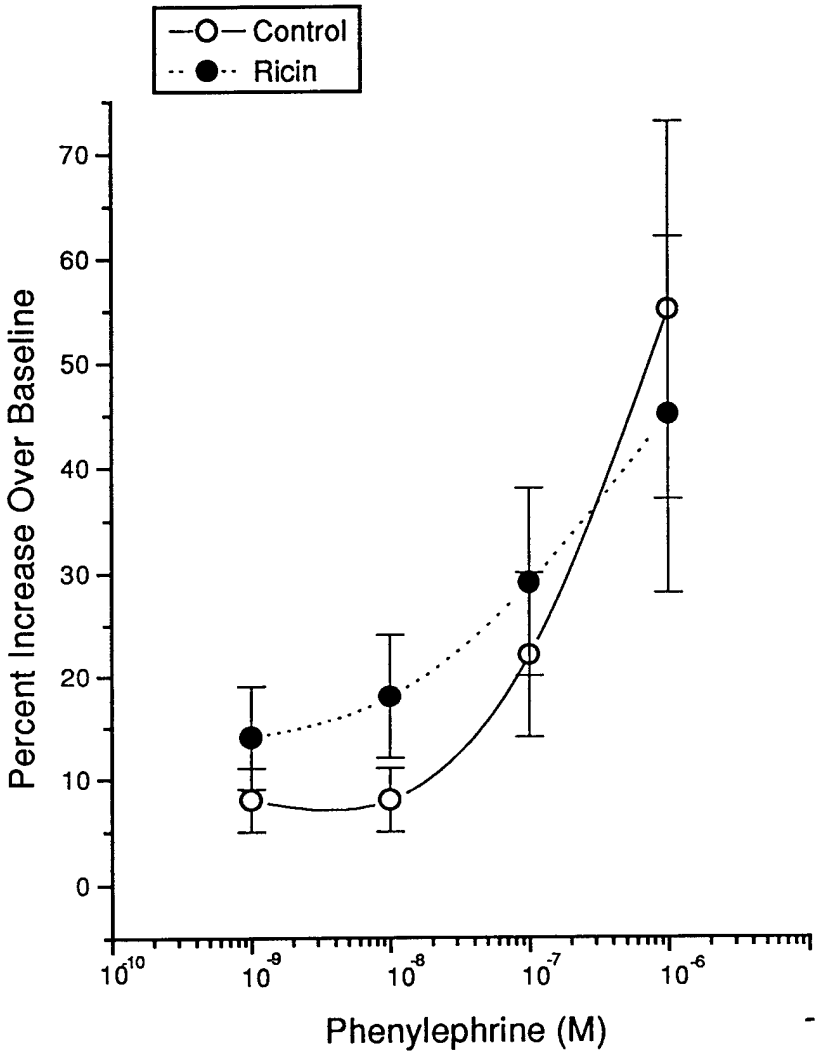

Figure 36. Effects of ricin administration on binding of a *beta*-adrenergic receptor agonist in the rabbit myocardium. Each point is the mean ± SEM from 6 rabbits.

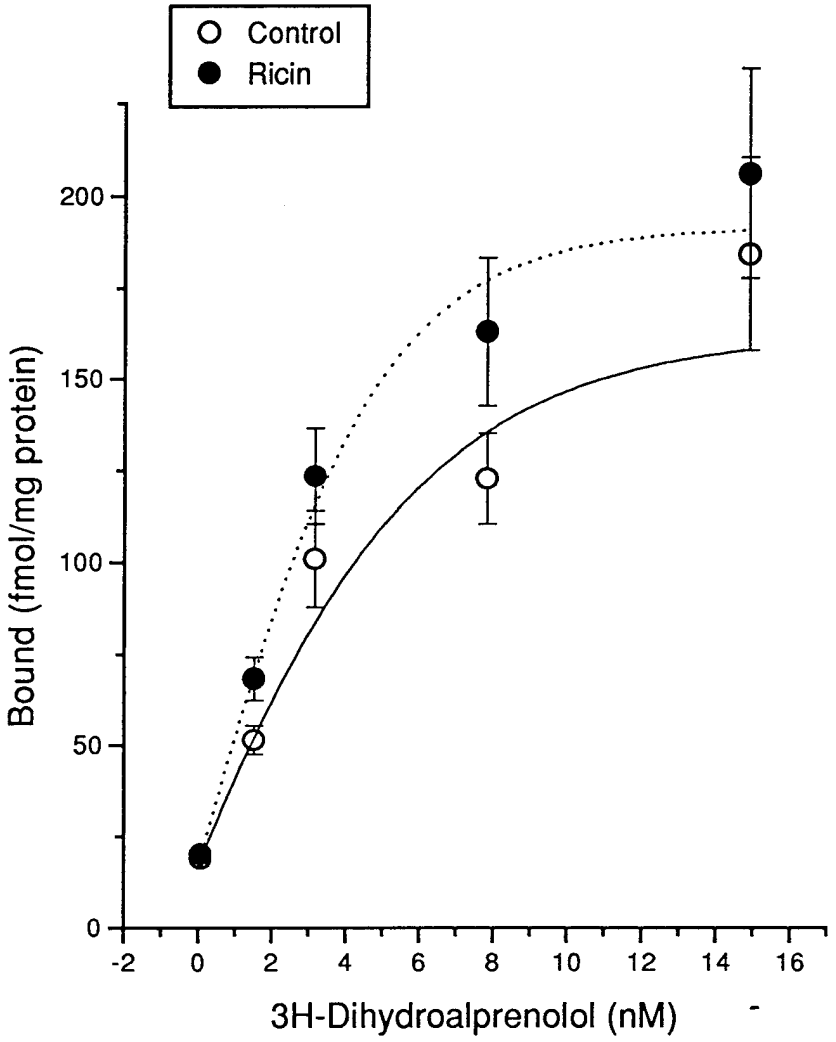

Figure 37. Sctachard plot of binding of a beta-adrenergic receptor agonist in the rabbit myocardium. Each point is the mean ± SEM from 6 rabbits.

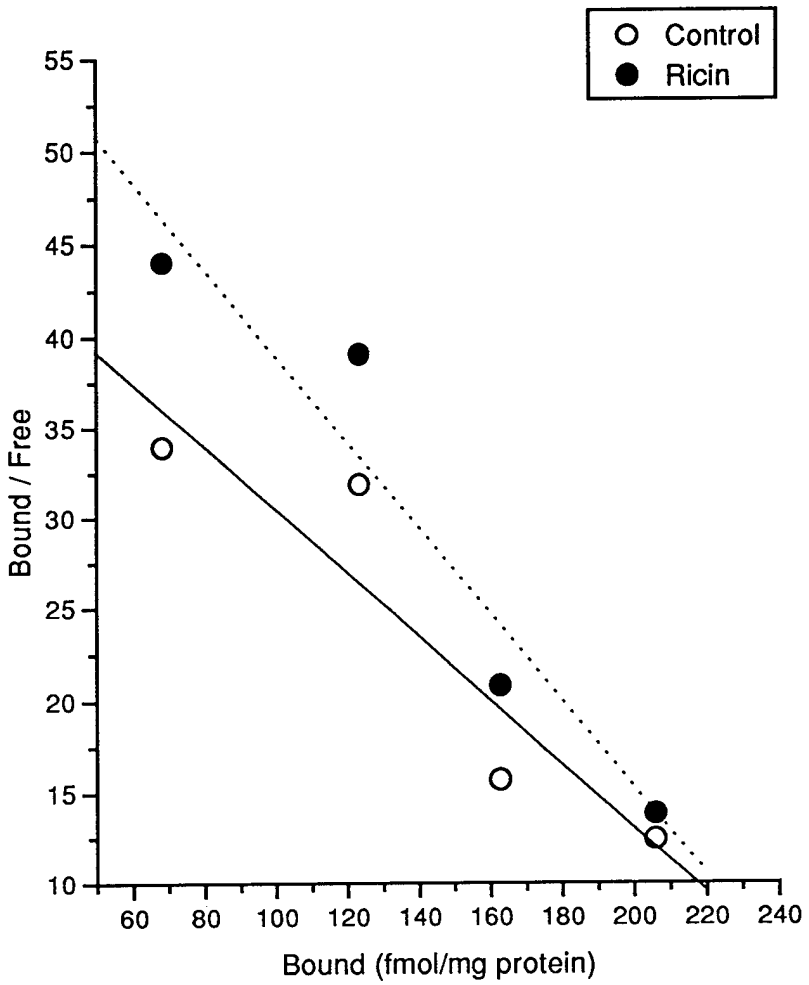

nergic receptor binding sites for dihydroalprenolol. This indicates that ricin administration did not affect the *beta*-adrenergic receptor system.

K. Effects of Ricin on Papillary Muscle Contraction to Administration of the Calcium Channel Agonist, Bay K 8644.

Papillary muscle paced at 1 Hz was exposed to cumulatively-increasing concentrations of the calcium channel agonist, Bay K 8644 (Figure 38). In the control group, Bay K 8644 caused an increase in the force of contraction that was half-maximal at $5.7 \times 10^{-8} \pm 2.9 \times 10^{-9}$ M compared to that induced in papillary muscle from rabbits given ricin ($3.3 \times 10^{-8} \pm 4.8 \times 10^{-9}$ M, $p = 0.046$). The increased electrically stimulated contraction amplitude in the presence of Bay K 8644 was significant at a concentration of 10^{-8} M ($p = 0.03$).

L. Effects of Ricin on the Intracellular Calcium Concentration in Myocardium.

An increase in basal intracellular calcium levels ($[Ca^{2+}]_i$) was observed. Ricin administration nearly doubled the intracellular free $[Ca^{2+}]$ concentration as measured by fura-2 fluorescence microscopy in isolated myocytes ($p = 0.002$) (Figure 39).

M. Effects of Ricin Administration on Calcium Efflux and Influx in Isolated Rabbit Papillary Muscle from the Rabbit Heart.

The basal ^{45}Ca efflux (expressed as percent of initial radioactivity remaining in the tissue) from papillary muscles from control and ricin-treated rabbits are shown in figure 40. Ricin did not alter basal calcium efflux in isolated papillary muscle. However, ricin inhibited the NE-induced calcium efflux (expressed as fractional efflux ratios) (Figure 41) in papillary muscles from rabbits receiving the minimum lethal dose of ricin at 25 - 30 minutes ($p = 0.002$ and 0.003, respectively).

Figure 38. Effects of ricin on contractions of rabbit papillary muscle to electrical stimulation in the presence of Bay K 8644. Each point represents the mean ± SEM from 6 rabbits. *Different from control at p = 0.03.

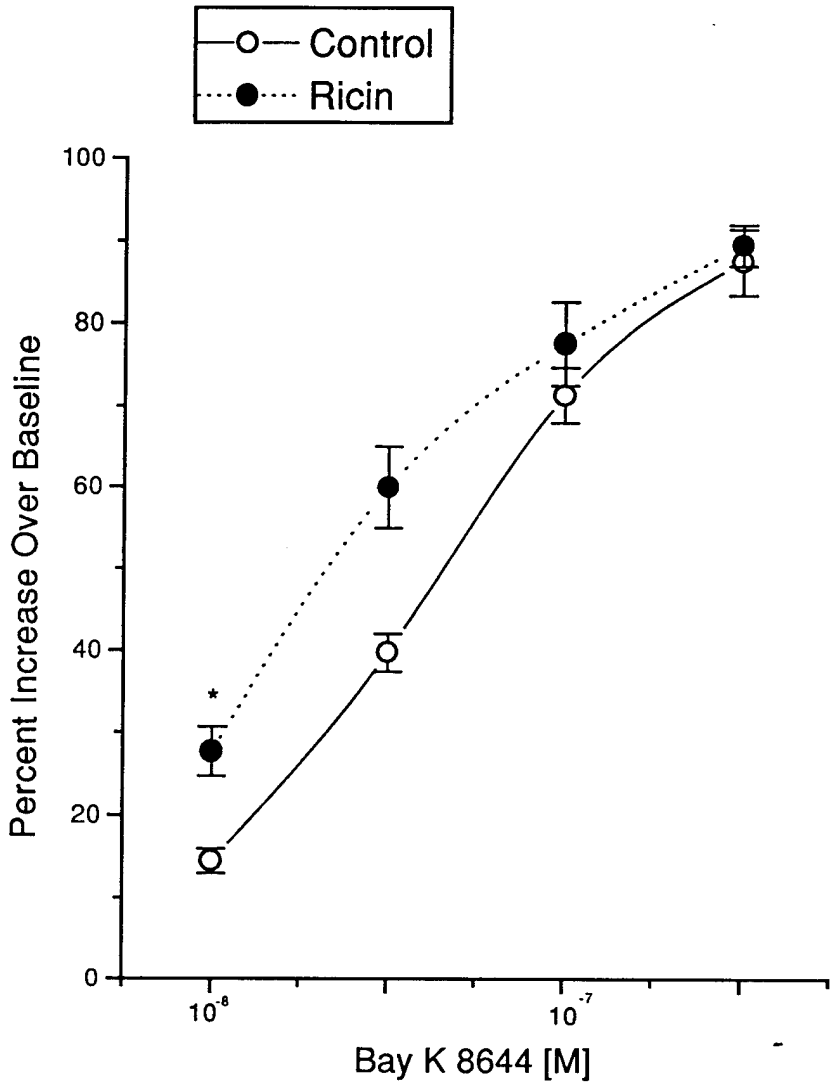

Figure 39. Effects of ricin on the intracellular calcium levels in isolated myocytes from rabbit and those receiving ricin. Each band is the mean ± SEM from 5-6 rabbits. *Different from control at p = 0.002.

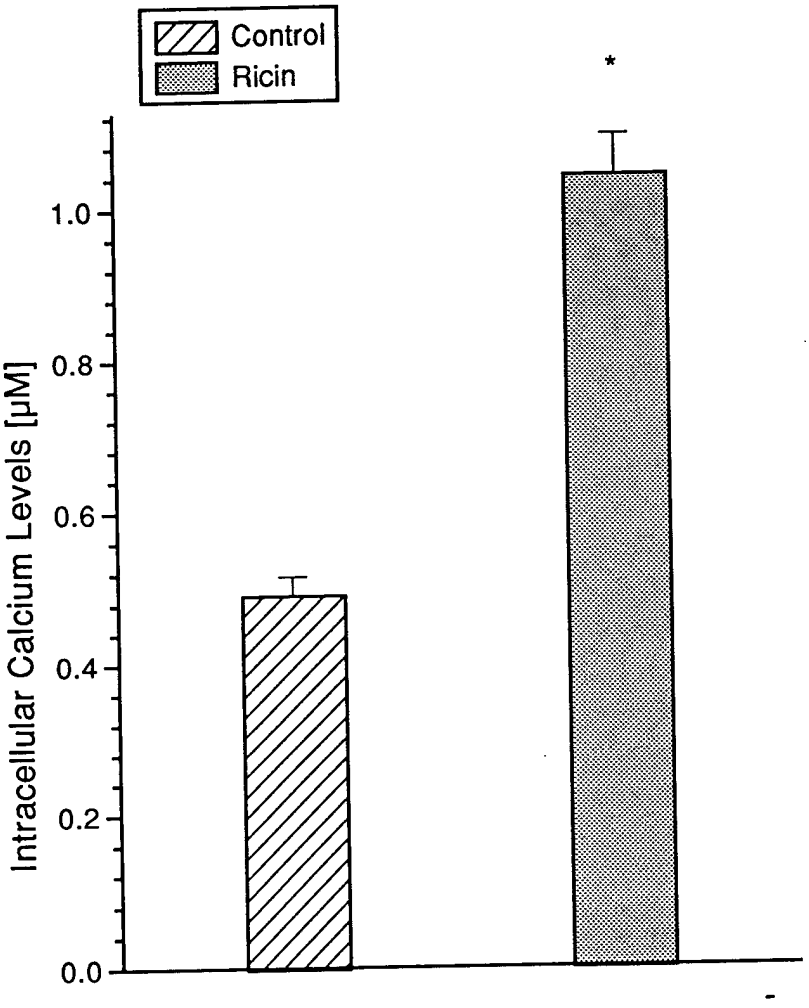

Figure 40. Effects of ricin on calcium efflux from the rabbit papillary muscles (desaturation curve). Each point is the mean ± SEM from six rabbits.

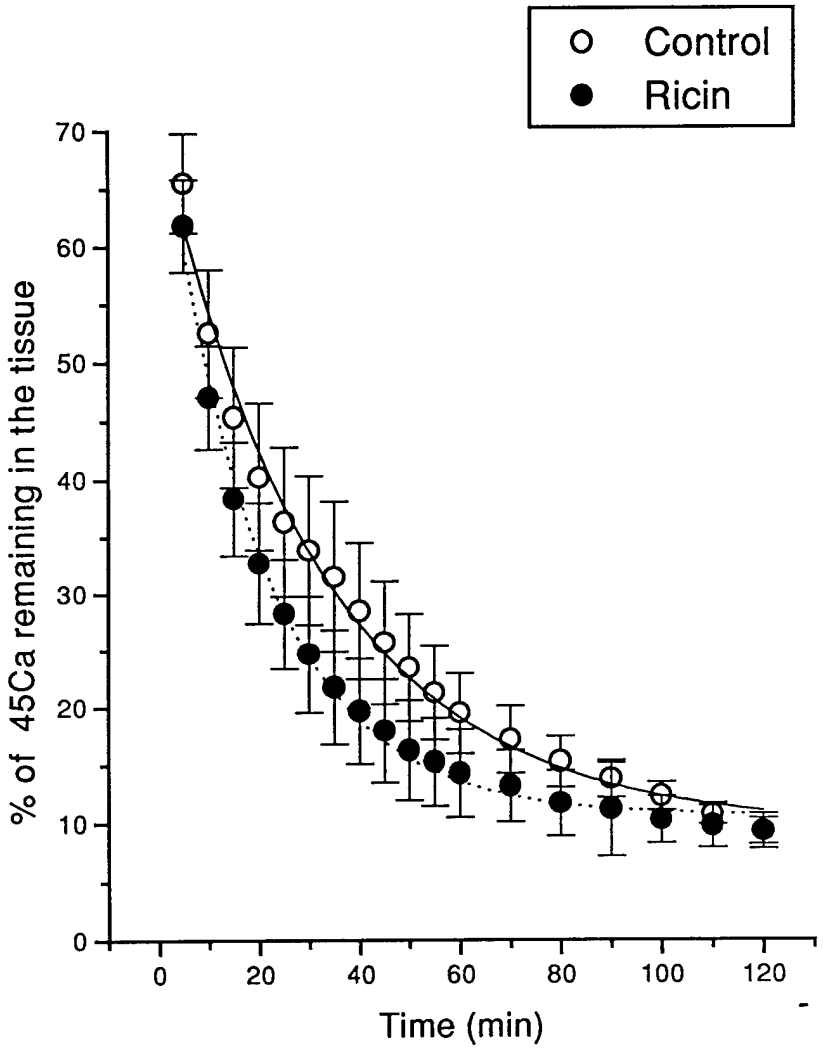

Figure 41. Effects of ricin on stimulated calcium release (fractional efflux ratios) from the rabbit papillary muscle. Norepinephrine (100 μM) added at 20 & 25 min and remained in contact with the muscle for 5 min. Each point is the mean ± SEM from six rabbits. *Different from control at p = 0.002 (25 min) and 0.003 (30 min).

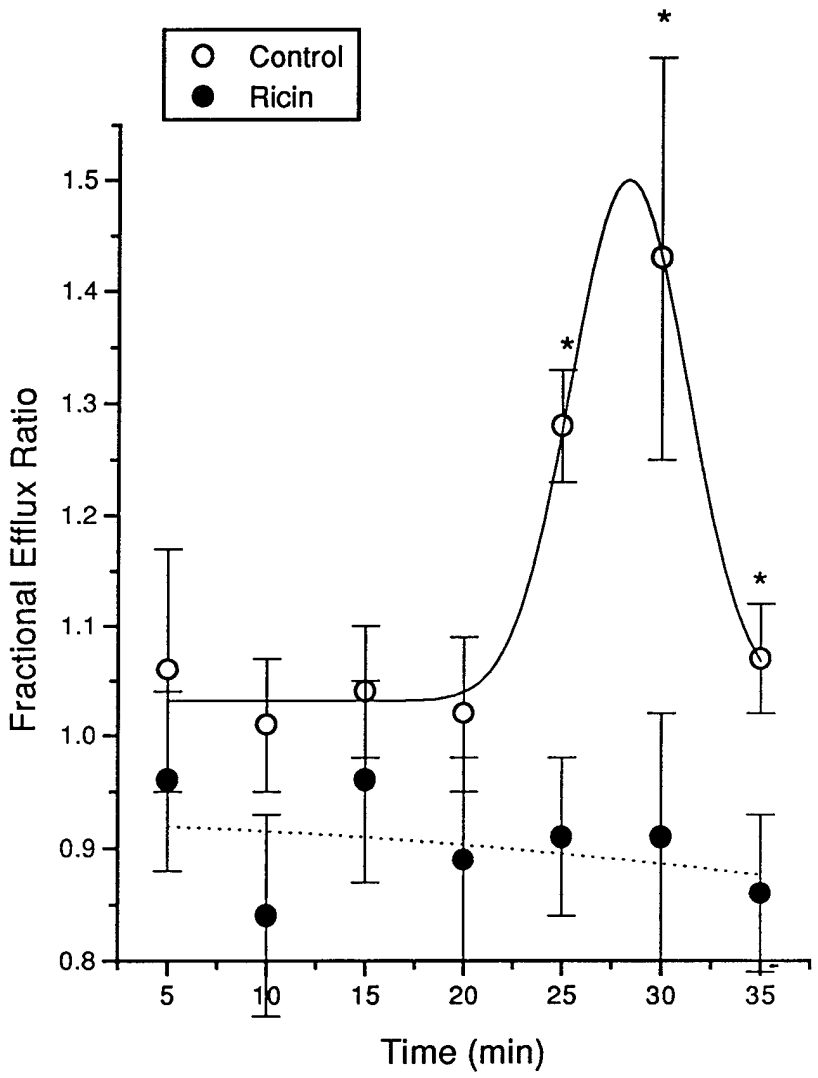

The effects of ricin administration to rabbits on basal ^{45}Ca uptake in isolated papillary muscles in 2.5 or 5 minutes are shown in figure 42. Ricin depressed basal calcium uptake into isolated papillary muscle at 5 min (mean ± SEM, μmol/g wet weight) (control: 3.68 ± 0.57; ricin: 2.31 ± 0.28, p = 0.045, n=6).

N. Effects of Ricin Administration on Calcium Uptake into Microsomes and Mitochondria in Isolated Rabbit Papillary Muscle from the Rabbit Heart.

The effects of ricin administration on calcium uptake into microsomes are shown in figure 43. Ricin administration significantly depressed calcium uptake into microsomes (mean ± SEM, μmol/g protein) (Control: 9.9 ± 1.9; Ricin: 3.1 ± 1.9, p = 0.025, n=6). The effects of ricin administration on calcium uptake into mitochondria are shown in figure 44. The calcium uptake into mitochondria was increased at the beginning (2 min, p = 0.048). Although, ricin administration did not significantly depress calcium uptake by mitochondria when compared to that of control rabbits, ricin administration did change the pattern of calcium uptake by mitochondria at 2 and 8 min.

Figure 42. Effects of ricin on calcium uptake into papillary muscles. Each bar is the mean ± SEM from six rabbits. *Different at p = 0.045 from control.

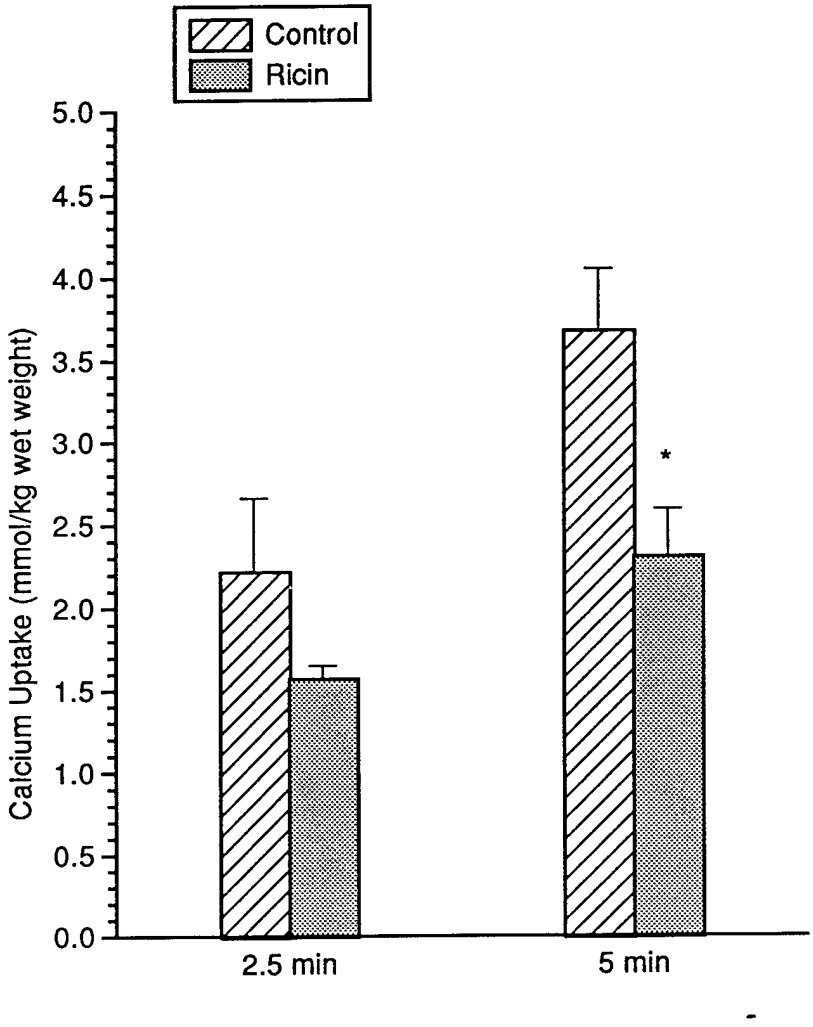

Figure 43. Effects of ricin on calcium uptake into microsomes. Each bar is the mean ± SEM from six rabbits. *Different at p = 0.025 from control.

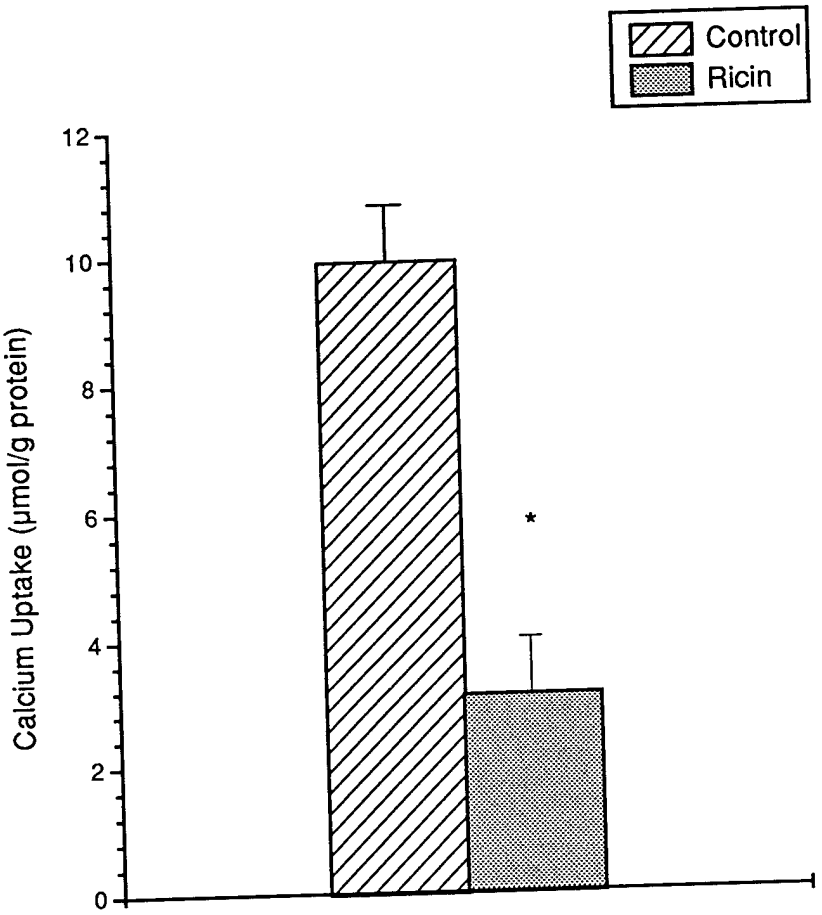

Figure 44. Effects of ricin on calcium uptake into mitochondria. Each point is the mean ± SEM from six rabbits. *Different at p = 0.048 from control.

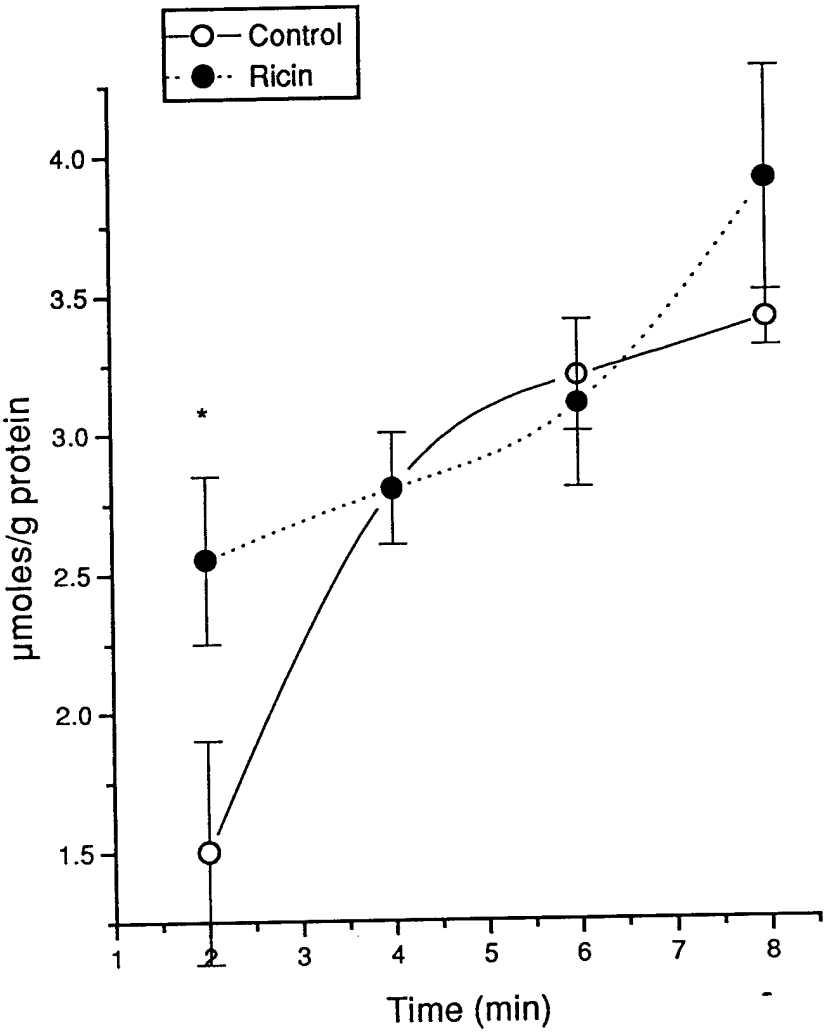

IV. DISCUSSION

The study of blood flow in rabbits with microspheres showed that ricin causes changes in both systemic and regional hemodynamics. Cardiac output was increased in all four ricin groups at both doses and both time points. Cardiac output is a very important systemic hemodynamic parameter. It, together with blood pressure, vascular resistance, and circulating blood volume maintains normal systemic hemodynamics. These are integrated to provide a sufficient blood supply to the body tissues. Ricin decreases rabbit blood pressure which starts to fall 20 hr after i.v. administration (Robinson *et al.*, 1992). The increased cardiac output observed in the present study can be simply an effort by the cardiovascular system to compensate for the falling blood pressure. Once the effort fails, blood pressure falls. That the higher dose of ricin causes the least increase in cardiac output at 18 hr may indicate the beginning of decompensation of the system.

Alterations of blood flow to individual tissues/organs following ricin administration varies markedly. In the four experimental groups, ricin administration increased blood flow to most tissues/organs examined in comparison with control. Blood flow to the heart, spleen, kidney and small intestines was markedly increased. Since cardiac output was increased before blood pressure fell (Christiansen *et al.*, 1992) and the heart rate was increased when blood pressure fell (Christiansen *et al.*, 1992), the central cardiovascular control system (such as the baroreceptor reflex) was functional. The decreased blood pressure was likely caused by reduced peripheral resistance which is largely controlled by vascular tone. Thus, the markedly increased blood flow to these organs may indicate that the vasculature in these organs was more readily affected by ricin.

The data on blood flow to the lungs reflect blood flow from bronchial arteries because the microspheres were injected into the left ventricle, so the only major source of microspheres available to the lungs was from bronchial arteries which originate in the systemic circulation. There may be a small number of microspheres from pulmonary

arteries if they fail to be stopped by capillaries or if they pass through A-V shunts. Even so, this blood flow determined with microspheres should be a reasonable representation of the circulation in the lungs. Changes in lung blood flow were inconsistent in different ricin-administered groups. The increased blood flow to the rabbit lungs in the toxic sublethal dose groups at 12 and 18 hours probably results from vasodilation and increased cardiac output. However, in the minimal lethal dose groups, blood flow to the lungs was at control levels at 12 hours, while blood flow at 18 hours was decreased by 50%. The pulmonary circulation is different from the systemic circulation. The differences are not only due to the fact that the pulmonary circulation is a low-pressure, low-resistance system but also may be due to its vascular architecture. Pulmonary vessels in general have thinner, more readily distensible walls containing less smooth muscle and elastin. Thus, the pulmonary blood flow should be more easily affected by changes in extravascular (outside the vessel or interstitial) pressure. If ricin damages blood vessels, the pulmonary vessels should be a vulnerable target for ricin toxicity. Pathological examination of rabbits that died earlier (approximately 22 hours after ricin intoxication) showed severe pulmonary congestion, edema and hemorrhage (Christiansen *et al.*, 1992). No doubt these changes increased the interstitial pressure in the lungs. It is also reasonable to believe that these changes could start much earlier than 22 hours after ricin administration and that the higher the dose of ricin the more severe and earlier these changes would occur. Asthmatic symptoms in a ricin intoxicated patient observed by Balint (1974) are indicative of the damage to lungs. Thus, the increased pulmonary circulatory resistance may be responsible for the decreased blood flow to the rabbit lungs in the minimal lethal dose groups.

Changes in blood flow to the total brain were found to be similar to changes in the lungs, but it is unlikely that they are caused by the same mechanism. Ricin seems not to affect the central nervous system and there are no observable pathological changes in the brain. The reason for this is unknown. Probably, the blood brain barrier plays a protective role. Anatomically, some characteristics of the cerebral circulation are opposite to those of

the lungs. The vessel walls are thicker and their permeability to substances is highly selective. The cranial cavity is filled with tissue and fluid which are incompressible, and thus, all of the blood vessels in the brain can not dilate at the same time. The increased blood flow to the brain in the toxic sublethal dose group at 12 hr may be due to the increased cardiac output. The decreased blood flow to the brain in the minimal lethal dose groups is more likely to have resulted from blood flow redistribution to the area with more dilatable arterioles and/or decreased compensation of cardiac output rather than from increased circulatory resistance.

The renal blood flow changes are also interesting to note. Ricin increased blood flow to the kidney in all ricin groups. The increased blood flow was largely accounted for by increased flow to the renal cortex. Blood flow to the medullary portion was just slightly increased in the minimal lethal dose groups and was at control levels or less in the minimal lethal dose groups. Kidney cortex contains the most important structures for renal function, glomeruli, which are tufts of capillary vessels and are responsible for filtration. In the normal situation, 90% of the renal blood flow is delivered to the cortex. Our data from control rabbits are in agreement with this conclusion. The increased blood flow especially to the cortex may reflect a more toxic effect of ricin on the vascular system of the cortex.

Thus, ricin affects both the systemic and regional hemodynamics in rabbits. If these changes are due to ricin-induced alterations in the vascular system, damage to the structurally vulnerable vessels would occur first.

In the study of contractions and relaxations of rabbit coronary rings ricin administration altered coronary artery responses to some vasoactive agents. Many of the patterns of these alterations are in agreement with our previous findings of the effects of ricin administration on responses of rabbit central ear arteries to NE (Christiansen *et al.*, 1994b), indicating that ricin seems to affect the coronary artery in the same way as it does the central ear artery. Maximal contractions to 5-HT and histamine in both control rabbits

and those receiving ricin were increased by removal of the endothelium which is consistent with reports by Griffith and co-workers (1984) in control rabbits. It has not yet been established whether this increase is mediated by evoked- or spontaneous-release of EDRF from the endothelium (Martin, 1988).

Although ricin administration increased the maximal contraction to 5-HT and histamine (Table 6), it decreased the sensitivity of coronary artery rings to them (Table 5), as was previously found in central ear artery responses to NE following ricin administration (Christiansen *et al.*, 1994b) (Although NE relaxes the rabbit coronary artery, it contracts the central ear artery). 5-HT and histamine cause vasoconstriction of vascular smooth muscle via stimulating G-protein coupled receptors and activating phospholipase C (de Chaffoy de Courcelles *et al.*, 1985) which converts phosphatidyl-inositol-4,5-diphosphate to 1,2-diacylglycerol and inositol-1,4,5-triphosphate (IP_3). The IP_3 stimulates release of Ca^{2+} from intracellular stores via an IP_3-receptor which is a type of Ca^{2+} channel (Hathaway *et al.*, 1991) and 1,2-diacylglycerol provides substrate for eicosanoid production and activates protein kinase C (Majerus *et al.*, 1986). The IP_3 is susceptible to several metabolic fates. One of these is hydrolysis by a specific phosphatase to inositol 1,4-bisphosphate, which in turn is hydrolyzed by an inositol 1-phosphatase to free inositol. The inositol 1-phosphatase is inhibited by Li^+ (Berridge *et al.*, 1982).

The basal IP_3 accumulation in coronary arteries from rabbits given ricin was significantly increased in the study of phosphatidylinositol hydrolysis. The basal IP_2 was also increased but not to a significant extent. Thus, the basal intracellular Ca^{2+} level should also be increased if the IP_3-Ca^{2+} channel coupling system is still functional. The ratio of basal IP_1/IP_2 in the ricin group is significantly lower than in the control group. This may indicate that the conversion from IP_2 to IP_1 was slowed by ricin and the increased IP_3 and IP_2 resulted from decreased hydrolysis from IP_2 to IP_1. Phospholipase C may be affected but since ricin inhibits protein synthesis there seems to be no reason to expect an increased enzyme activity.

The cGMP system is another signal transduction system that is involved in the regulation of the vascular smooth muscle. The cyclic-nucleotide assay showed that the basal cGMP content in the ricin group was significantly lower than that in the control group. The interactions between the synthesis of IP_3 and cGMP have been studied in a variety of cells (Takai *et al.*, 1982; Nakashima *et al.*, 1986) including rat and bovine vascular smooth muscle cells (Hirata *et al.*, 1990). In their reports, cGMP consistently inhibits the production of IP_3. Several mechanisms have been proposed in different cell types while in vascular smooth muscle the decreased IP_3 content seems to result from an inhibition of a guanine nucleotide regulatory protein activation and its interaction with phospholipase C which generates IP_3 (Hirata *et al.*, 1990). Thus, the decreased cGMP content in rabbit coronary arteries from rabbits in the ricin group may reduce its inhibition of the formation of IP_3 and result in an increased IP_3 level.

The cGMP also causes relaxation in vascular smooth muscle by reducing intracellular Ca^{2+} levels. Although the exact biochemical mechanism is not understood, it has been generally accepted that the activation of cGMP-dependent protein kinase is involved (Lincoln, 1989). Decreased cGMP levels will reduce the actions of the smooth muscle cells to lower intracellular Ca^{2+} ion concentrations and therefore may also result in an increased resting Ca^{2+} concentration. The mechanism of the changes in cGMP by ricin is not known. It could be either due to its decreased production or an increased degradation.

Histamine stimulation increases the IP_3, IP_2 and IP_1 levels in coronary arteries from rabbits in the control group. This is in agreement with a previous report (Shirinsky *et al.*, 1988). However, instead of an increase, 10^{-4} M histamine-stimulated IP_3, IP_2 and IP_1 levels were depressed in ricin group. This is very likely due to a decreased activity of phospholipase C because in this experiment inositol 1-phosphatase and related monophosphatase that can further hydrolyze different forms of inositol phosphate into inositol were inhibited by Li^{2+} (Berridge *et al.*, 1982; Majerus *et al.*, 1991). Thus, the ultimate outgoing

pathway of inositol phosphates was blocked and any change in inositol phosphate content should indicate a corresponding change in their production. Ricin may affect phospholipase C directly or indirectly. However, since the basal IP_3 levels were increased by ricin, this decrease in IP_3 concentration caused by 10^{-4} M histamine stimulation was likely due to some kind of inhibitory mechanism. The intracellular Ca^{2+} concentration after 10^{-4} M histamine is possibly much higher than the corresponding Ca^{2+} concentration in normal rabbits. This may induce a feedback inhibition on IP_3 production. Mobilization of Ca^{2+} and diacylglycerol can activate protein kinase C (Oishi *et al.*, 1988) which will inhibit synthesis of IP_3 (Itoh *et al.*, 1988). Thus, high intracellular Ca^{2+} concentrations may by a negative feedback system inhibit IP_3 production.

The phospholipase C/diacylglycerol/inositol-1,4,5-triphosphate-pathway is activated by *alpha*$_1$ agonists, angiotensin II, and endothelin. Angiotensin II and endothelin can cause positive inotropic effects in right atria (Davenport *et al.*, 1989; Schomisch Moravec Ch *et al.*, 1990; Urata *et al.*, 1989). The results of examination of IP_1, IP_2, and IP_3 showed that this pathway is not affected by ricin administration, which is consistent with the results of the functional study. However, alterations of cAMP and MAO were observed in ventricular tissues from rabbits given ricin. In addition to the *beta*- adrenergic system, the cAMP pathway is also connected to 5-HT, histamine, prostaglandin E_1 (PGE_1), vasoactive intestinal peptide (VIP), and glucagon receptors which can evoke positive inotropic effects. However, these receptors cause only submaximal activation of adenylate cyclase when compared with isoproterenol (Baumann *et al.*, 1983; Dumuis *et al.*, 1988; Hershberger *et al.*, 1989; Kaumann *et al.*, 1990). The depression of cAMP by ricin administration might be responsible for the decreased left ventricular systolic pressure. There are at least three receptor systems acting through inhibition of cAMP formation (G_i-protein coupled receptors) that exist in the human heart: muscarinic M_2, adenosine A_1, and somatostatin-receptors. Activation of M_2 and A_1 receptors causes negative inotropic effects in the heart. However, we did not observe negative inotropic effects in the contraction

studies. The depression of cAMP levels by ricin administration seems not to be caused by these receptor systems. It might be through an intracellular mechanism. The increased MAO activity is another piece of evidence that catecholamines were rapidly metabolized after ricin administration. Therefore, ricin administration reduces left ventricular systolic pressure probably by decreasing intracellular cAMP levels and by increasing the rate of catecholamine metabolism. In cardiac cells, activating a guanine nucleotide-binding protein (G_S) causes stimulation of adenylate cyclase and a resulting increase in the production of cAMP, which causes activation of cAMP-dependent protein kinases (Birnhaumer, 1990). This kinase causes phosphorylation of the *alpha*$_1$ subunit of the calcium channel, which increases calcium influx, and of phospholamban, which increases calcium uptake by the sarcoplasmic reticulum. These effects produce both an increase in the "trigger" Ca^{2+} entering the cell and an increase in releasable sarcoplasmic reticulum calcium. The results of decreased cAMP products in myocardium from rabbits receiving ricin is consistent with the reduced calcium movement observed in our calcium influx and efflux studies. The decreased calcium movement is probably caused by the depression of intracellular cAMP.

In the whole heart, cGMP antagonized the positive inotropic effects of catecholamines and cAMP. Cyclic GMP inhibits the L-type calcium channel current (ICa), which is the major source of Ca^{++} entry into heart cells, and which plays a predominant role in the initiation and regulation of cardiac electrical and contractile activities. However, the regulation of cGMP levels by a variety of agents was not always consistent with their effects on contractility (Lohmann *et al.*, 1991). Furthermore, experiments on isolated cardiac myocytes indicate that the mechanism of cGMP actions even in this single cell type can be multifaceted. Recent studies indicated that increased levels of cGMP is accompanied by a decrease in IP_3 (Rapoport *et al.*, 1986; Lang *et al.*, 1989) and by a decrease in calcium influx (Collins *et al.*, 1986). However, this relationship was not observed in this study. Depressing intracellular cGMP levels by ricin administration in this study did not show a corresponding response in contractility. It was evident from the depression of cAMP and

cGMP by ricin administration that ricin had a general inhibitory effect on intracellular second messengers.

The intracellular Ca^{2+} concentration is likely increased by ricin. In a parallel study on rabbit cardiac myocytes, ricin markedly increased the basal intracellular Ca^{2+} concentrations in cardiac myocytes observed with the fura-2 fluorescence method (unpublished data). Ricin may do the same in coronary arteries. In addition to mechanisms involving changes in second messengers, ricin may cause an intracellular Ca^{2+} increase through directly damaging calcium channels or Ca^{2+} pumps. These damaged pumps or channels could not efficiently maintain an intracellular low Ca^{2+} environment or efficiently remove excess intracellular Ca^{2+}. Thus, the increased intracellular Ca^{2+} may be responsible for the increased agonist-induced maximal contractions of coronary arteries. Another related piece of evidence is that a lower serum Ca^{2+} level was observed in rabbits after ricin administration (Robinson *et al.*, 1992). Although there are many factors involved in the regulation of the serum Ca^{2+} level, an increased Ca^{2+} influx into cells or a decreased efflux from cells are possible contributors to the low serum Ca^{2+} content.

The effects of cAMP on intracellular Ca^{2+} concentrations in vascular smooth muscle are complex. In physiological conditions a moderate rise in intracellular cAMP levels enhances inward current in Ca^{2+} channels whereas higher intracellular cAMP levels inhibit inward Ca^{2+} current (Ishikawa *et al.*, 1993). The cAMP enhances Ca^{2+}-influx by activating protein kinase A which phosphorylates L-type Ca^{2+} channels and increases their activity. The inhibitory effects of higher concentrations (ten times higher than basal level) of cAMP on Ca^{2+} channels is through the same pathway as that of cGMP (Lincoln *et al.*, 1990; Ishikawa, 1993). The cAMP has affinity for cGMP-dependent protein kinase and can activate it which leads to a decrease in Ca^{2+} channel activity. The cAMP concentration in rabbit coronary arteries was slightly increased in rabbits given ricin. This may increase Ca^{2+} influx and further contribute to the increased intracellular Ca^{2+} concentration.

Another important function of cAMP is to induce relaxation in vascular smooth muscle by activating cAMP-dependent protein kinase which phosphorylates smooth muscle myosin light chain kinase (Delanerolle *et al.*, 1984). Myosin light chain kinase mediates phosphorylation of the 20,000 dalton myosin light chain, which in the presence of actin will increase myosin-ATPase activity and promote cross-bridge cycling. Phosphorylation of myosin light chain kinase will reduce its affinity for the Ca^{2+}-camodulin complex and lead to dephosphorylation of the myosin light chain which breaks the above chain reaction and causes relaxation (Conti and Adelstein, 1981). The slightly increased cAMP concentration will probably maintain a low phosphorylation level of myosin light chain kinase. This may be a part of the mechanism of the desensitization of coronary arteries to stimulation by 5-HT and histamine and also of the low contractile response to low concentrations of histamine. Smooth muscle cells with high intracellular Ca^{2+} concentrations for a long period of time may become desensitized to calcium as an adaptive measure, because Ca^{2+}/calmodulin-dependent protein kinase II can also phosphorylate myosin light chain kinase (Ikebe *et al.*, 1990). By these mechanisms, smooth muscle may relax even in the presence of increasing levels of Ca^{2+} (Morgan and Morgan, 1984).

A fine regulation system in coronary arteries is indicated by the findings about basal and stimulated cyclic nucleotide levels. Histamine stimulation increased cAMP levels in coronary arteries from control rabbits. This is due to the activation of histamine H_2 receptors which are coupled to adenylate cyclase (Luchins *et al.*, 1980). The stimulated cGMP levels in coronary arteries from control rabbits were progressively reduced with increasing histamine concentrations but this depression was not observed in coronary arteries from rabbits given ricin. These varying responses of cyclic nucleotides to different concentrations of histamine in rabbit coronary arteries have not been previously reported. These different responses suggest a fine regulation by cyclic nucleotides in vascular smooth muscle cells. This regulatory system seems to be more effective when smooth muscle is exposed to lower concentrations of histamine, because with the lower concentration of

histamine the cAMP level is increased while cGMP is decreased. These two changes have opposite effects on contractions, one (cAMP) to desensitize contractions, the latter (cGMP) to promote contractions via increasing intracellular Ca^{2+} after reducing the actions of smooth muscle cells to lower intracellular Ca^{2+}. This delicate regulatory system may play an important role in physiological conditions since the normal histamine concentration in rabbit plasma is about 1.6×10^{-6} M (Waalkes *et al.*, 1957b) and histamine concentrations as high as 10^{-4} M are unlikely to be reached under normal physiological conditions.

The 10^{-6} M histamine-stimulated cAMP levels were increased in both control and ricin groups but 10^{-4} M histamine stimulated cAMP levels decreased slightly in the control group and decreased to even below the corresponding basal levels in the ricin group. With trend analysis the cAMP levels were usually increased in the control group after 10^{-4} M histamine stimulation but there was a greater inconsistency in the directional change in the ricin group. These findings indicate that the cAMP system of rabbit coronary arteries is still functional after ricin treatment but it may not function as well as that in the control group especially when it is under strong external stimulation. The differences in cyclic nucleotide basal concentrations and in their responses to stimulation in coronary arteries from rabbits given ricin suggests that not only the production of cyclic nucleotides but also their regulatory functions were affected by ricin. This may explain the increased maximum contractions of coronary arteries to contractile stimuli. The decreased cAMP level after a strong stimulation will reduce its inhibitory effect on contraction and result in an increased contraction.

Furthermore, ricin may directly alter contractile elements by actions such as by altering the phosphorylation of myosin light chain and actomyosin ATPase activity and thus affect muscle contraction.

The mechanisms involved in the changes in cyclic nucleotide concentrations induced by ricin administration are not clear. For cGMP, production was decreased, most likely by an inhibition of guanylate cyclase. Because the depression of cGMP by histamine

stimulation was not observed in coronary arteries from rabbits given ricin, the steps involved in this response were disrupted. In control rabbits depression of cGMP by histamine may be caused by the activation of histamine receptors inducing an inhibiting effect or by a feedback from the increased intracellular Ca^{2+} concentration. The cAMP system seems to be well preserved although there was a slight increase in basal cAMP in coronary arteries from rabbits given ricin, because there was still a response similar to that of coronary arteries from control rabbits present in the ricin group.

Norepinephrine caused relaxation in the rabbit coronary artery via *beta* adrenoceptors and endothelial removal did not increase the maximal response to NE (Corr *et al.*, 1991), in agreement with our results from control rabbits. This is because rabbit coronary arteries do not have endothelial *alpha*- and *beta*-adrenoceptors, at least no functional ones (Corr *et al.*, 1991). Stimulation of beta adrenoceptors increases intracellular cAMP concentrations and activates cAMP-dependent protein kinase which lowers the cytosolic free Ca^{2+} concentration via the phosphorylation cascade (Brown and Birnbaumer, 1988). The increased sensitivity to relaxing agents may be explained by increased basal cAMP levels plus an already desensitized contractile apparatus in smooth muscle. The better preserved cAMP response pathway in the coronary arteries from rabbits given ricin is essential for the normal functioning of *beta*-adrenoceptors.

Acetylcholine stimulates the endothelium to release EDRF which relaxes rabbit coronary artery via inducing production of cGMP in vascular smooth muscle. The lack of differences in ACh-induced relaxations between control rabbits and rabbits given ricin seems to indicate that ricin may not affect ACh-stimulated EDRF release from the coronary artery endothelium. However, the magnitude of agonist-induced relaxation has been shown to decrease when the level of initial smooth muscle tone rises (Cohen and Berkowitz,1974), so it is possible that an increase in the maximal relaxation of the coronary artery rings to NE or ACh would occur if contractions of the vessels to AEP in control rabbits was as high as those in rabbits receiving ricin. The basal cGMP levels were lower

in coronary arteries from rabbits given ricin, but the increased basal cAMP and well preserved cAMP pathway at the same time may have compensated for the decreased cGMP. This is because cAMP is capable of binding to cGMP-dependent protein kinase and reducing intracellular Ca^{2+} levels in smooth muscle by the same mechanism (Lincoln, 1990).

There are many factors involved in coronary blood flow regulation, including mechanical, neural and metabolic factors (Malindzak, 1982; Vatner and Murray, 1982). The receptors investigated in our experiments are only part of the coronary regulatory system, but the results provide information for better understanding the mechanism of ricin intoxication. The 5-HT from platelets in the blood can exert cardiovascular effects (Houston and Vanhoutte, 1986), usually being released in hemostasis or during an anaphylactic reaction (Hollenberg, 1988; Waalkes *et al.*, 1957a). Histamine is largely stored in basophils and mast cells which can be activated by many conditions, including immediate hypersensitivity reactions, trauma and nonspecific injuries (Beaven, 1976). The normal 5-HT and histamine concentrations in rabbit plasma are about 0.1 μg/ml (5.6×10^{-7} M) and 0.18 μg/ml (1.6×10^{-6} M) respectively, and in acute anaphylaxis they can rise to 0.5 μg/ml and 1.1 μg/ml, respectively, but rapidly return to normal (Waalkes *et al.*, 1957b). One injection of a minute amount of ricin does not produce an anaphylactic reaction and there were no other apparent factors to release 5-HT or histamine. So, in the early stages (12-18 hr) after ricin injection, plasma 5-HT and histamine concentrations should be approximately normal. At those concentrations, the contractile tension to 5-HT of coronary artery rings from rabbits receiving ricin was about 120 mg higher than that of rings from control rabbits and the contractile tension to histamine was lower by 200-300 mg compared with those of rings from control rabbits. Also, adding in the increased sensitivity of the coronary artery to relaxation by NE and the possible increased maximal relaxations to NE and ACh, the sum of the effects of circulating NE, ACh, histamine, and 5-HT seems likely to be a relaxation of coronary arteries.

Severe myocardial hemorrhage (Christiansen *et al.*, 1991) and a drop in systolic and diastolic blood pressure after intravenous administration of a sublethal dose of ricin have been observed in the rabbit (Christiansen *et al.*, 1994). In man, ricin intoxication produces signs and symptoms involving many organs including the heart (Balint, 1974).

In the studies on the heart, we intended to determine whether ricin affects cardiac function. If ricin affects heart function, we wanted to determine the mechanism of ricin's effects on the heart. Because calcium is very important in cardiotoxicity and cell intoxication, we also evaluated the role of calcium in the effects of ricin on the heart.

In the papillary muscle experiments, ricin administration did not show significantly positive inotropic or negative inotropic effects. Ricin administration did not alter the time to the peak tension or the contraction duration. An increase in frequency of stimulation is not accompanied by a significantly-altered force of contraction for the ricin treated rabbit papillary muscles. The V_{max} and the amplitude of action potential recorded from the right ventricular papillary muscles were not different between the control and ricin administration groups. The action potential duration was slightly prolonged and the effective refractory period was significantly increased by ricin administration. However no arrhythmias were observed in these studies, which is in agreement with our previous *in vivo* studies (Christiansen *et al.*, 1994a). These findings indicated that ricin did not significantly affect the contractility of the papillary muscles as assessed by contraction duration, time to peak tension and paired pacing, at least not at 48 hour after the administration of a minimum lethal dose of ricin. The lack of an alteration in either the resting membrane potential or in the overshoot potential indicated the fast channels were not affected by ricin administration. However, prolongation of the action potential duration and of the effective refractory period indicated that opening of the slow calcium channels was prolonged by ricin administration. In a previous study, Balint (1974) reported changes in the electrocardiogram in patients receiving ricin. Although we did not find changes in the electrocardiograms in these experiments, the alteration in action potential duration and effective refractory period is a

potential risk for arrhythmia development. The findings of increased intracellular calcium levels by ricin administration may be another potential risk factor for arrhythmia development in ricin toxicity. Steenbergen and his coworkers (1987) reported that arrhythmia occurred when the $[Ca^{2+}]_i$ concentration reached levels of 1 - 3 μM. The increased $[Ca^{2+}]_i$ by ricin can be followed by the onset of small $[Ca^{2+}]_i$ oscillations during systole, from which a spontaneous arrhthymia could occur. Elevation of $[Ca^{2+}]_i$ has been also proposed to cause cell-to-cell uncoupling (cells exposed to concentrations of $[Ca^{2+}]_o$ > 7 mM reportedly fail to transfer fluorescent dye between asynchronously beating cells, suggestive of cell-to-cell uncoupling), which is another mechanism that may mediate arrhythmia (Morgan et al., 1990). An increase of $[Ca^{2+}]_i$ by ricin may cause cell-to-cell uncoupling which would increase the risk for arrhythmia development. Procedures designed to inhibit Ca^{2+} flux across the sarcolemma and sarcoplasmic reticulum (Clusin et al., 1983; Opie et al., 1988) were found to reduce the incidence of ventricular arrhythmias in the heart during acute myocardial ischemia and on subsequent reperfusion. Elevation of $[Ca^{2+}]_i$ may play a role in arrhythmia development but not as the initiator of an arrhythmia. In our studies, the fact that increased intracellular calcium levels were not accompanied by the occurrence of arrhythmias is probably due to the inhibition of calcium flux.

The systolic pressure plotted against the balloon volume represents the capacity of the entire myocardium to generate systolic force (Weber *et al.*, 1976). Volume-induced increases in left ventricular contractility are mediated in part by an increase in calcium release from the sarcoplasmic reticulum (Lew, 1993). In the isolated heart experiments, the systolic developed pressure was decreased at a balloon volume of 0.3 to 1.5 ml in rabbits receiving ricin. Contractility, as assessed by changes in the maximal +dp/dt, differed between the two groups. These observations can be partially explained by the findings that calcium movements were depressed by ricin administration. Other possible mechanism for reduced systolic function will be discussed later in this chapter.

It is now generally accepted that there are many receptor systems involved in the regulation of heart rate and /or contractility. These are receptors acting via accumulation of intracellular cAMP (G_s-protein coupled), via inhibition of cAMP formation (G_i-protein coupled) or receptors acting independently of cAMP formation, possibly involving the phospholipase C/diacylglycerol/inositol-1,4,5,-triphosphate (PLC/DAG/IP_3-)-pathway. Among these receptor systems, the *beta*-adrenergic receptor-G_s-protein-adenylate cyclase complex is the most important physiological mechanism for regulating heart rate and contractility (Bristow *et al.*, 1989; 1990; Brodde, 1991).

Beta-adrenergic receptor stimulation increases active tension and contractility and accelerates active relaxation (Aoyagi *et al.*, 1991). The first effect is mainly a consequence of an increased slow inward calcium current, while the second results from activation of the Ca^{2+}-ATPase of the sarcoplasmic reticulum via phosphorylation of phospholamban. Phospholamban is a 6,080-d protein (Fujii *at al.*, 1987) that binds to and inhibits Ca^{2+} transport by the SR calcium ATPase. When it is phosphorylated by cAMP-dependent protein kinase, this inhibition is removed, resulting in a greater V_{max} and a lower K_{Ca} for calcium transport. Thus, it could be expected that, on an isolated heart, anything that can decrease the release of catecholamines, as well as block or damage *beta*-adrenergic receptors, would decrease the systolic pressure and relaxation velocity. In the experiment in which isoproterenol was administered to papillary muscle and in the isolated heart experiments, ricin did not significantly alter the isoproterenol-induced increase in contractility of papillary muscle and the left ventricular developed pressure in the heart. The contractility reflected by +dp/dt, and muscle relaxation reflected by -dp/dt were not affected either. Thus, overall, the *beta*-adrenergic system was not altered by the minimum lethal dose of ricin. To confirm these findings, radioligand binding studies were carried out. The results from the binding studies showed that ricin neither reduced *beta*-adrenergic receptor numbers nor altered its affinity. This indicated ricin did not damage the *beta*-

adrenergic receptor, which is consistent with the results from the functional studies of the contraction of the isolated papillary muscle and the isolated heart experiments.

The *alpha*-adrenergic system is another important system involved in regulation of heart function. Recent studies strongly support the view that, at least in ventricular tissue, a small proportion of *alpha*-adrenergic receptors exists that cause positive inotropic effects (Schmitz *et al.*, 1987). In the heart, the *alpha*-1 adrenergic receptors couple via a pertussis toxin-insensitive G-protein to the PLC/DAG/IP_3-pathway (Bristow *et al.*, 1988; Kohl *et al.*, 1989; Schmitz *et al.*, 1987). However, the number of *alpha*-adrenergic receptors (10-15 fmol/mg protein) and the maximal positive inotropic effect (about 10-15% of that of isoprenaline) is very small (Aass *et al.*, 1986; Bohm *et al.*, 1988; Bristo *et al.*, 1988; Bruckner *et al.*, 1984; Schmitz *et al.*, 1987). To determine whether ricin affects the *alpha*-adrenergic system, we tested the *alpha*- adrenergic function with phenylephrine in the rabbit isolated heart. The results were similar to those with the *beta*-adrenergic system. The *alpha*-adrenergic system was not altered by ricin administration.

Further studies were done on intracellular basal IPs, cAMP, cGMP levels and MAO and COMT activity to gain insight into the intracellular mechanism of the decreased systolic pressure caused by ricin administration.

Another major finding in these studies was that left ventricular diastolic function changed after ricin administration. The isolated heart perfused by the Langendorff procedure is particularly suitable for studying ventricular compliance (Jalil *et al.*, 1989). The diastolic stiffness of the chambers was increased by ricin administration. This reduction in diastolic compliance can be most easily explained by tissue edema or an increased amount of collagen. A previous study has shown severe hemorrhage in the myocardium following ricin administration (Christiansen *et al.*, 1991). Hemorrhage disrupts cellular function, resulting in a redistribution of fluids and electrolytes, which might cause cells to be swollen. However, whether or not myocardial hemorrhage causes the swelling of myocytes and diastolic dysfunction needs to be studied by electron

microscopy to see whether there are changes in cardiac myocyte vacuolization, myofibrillar loss, and necrosis, or ultrastructural alterations including swelling of endothelial cells, interstitial hemorrhage, and edema.

Calcium homeostasis in cardiac myocytes is of functional importance for at least three reasons. First, cardiac myocytes must achieve a resting cytosolic calcium ion concentration($[Ca^{2+}]_1$) of <200 nM if the contractile elements are to relax. Second, coupling of excitation to contraction (E-C coupling) in the heart involves a complex interaction of membrane electrical events mediated by specific ion channels in the sarcolemma. This results in calcium influx, the release of calcium from intracellular stores in the sarcoplasmic reticulum (SR) via Ca^{2+}-specific channels in the SR membrane, and subsequent extrusion of calcium. Third, the force of contraction in cardiac myocytes is modulated by variations in the magnitude of the calcium transient. The $[Ca^{2+}]_i$ is determined by a Ca^{2+} leak that is compensated for by an ATP-dependent sarcolemmal Ca^{2+} pump (sarcolemmal Ca^{2+}-ATPase) and the sarcolemmal Na^{+}-Ca^{2+} exchanger. This process is fundamental for maintaining steady-state calcium homeostasis. Calcium homeostasis in cardiac myocytes results from the integrated function of transsarcolemmal Ca^{2+} influx and efflux pathways modulated by membrane potential and from intracellular Ca^{2+} uptake and release caused predominantly by sarcoplasmic reticulum function. Alteration of these processes can cause significant changes in contraction and relaxation of the heart. Intracellular Ca^{2+} both regulates the cell and is regulated by the cell. The role of intracellular ion regulation, particularly that of intracellular ionized calcium($[Ca^{2+}]_i$) in toxin-induced cell injury, is very important. Ca^{2+} out of control is a lethal cell signal (Orrenius *et al.*, 1988; Chapman *et al.*, 1987). Some researchers have investigated the role of calcium in ricin toxicity. A deprivation of Ca^{2+} in the media can provide partial protection against ricin intoxication (Sandvig and Olsnes, 1982).

Previous studies have revealed that calcium is an important factor for ricin exerting its toxicity (Reid *et al.*, 1990; Jaffrezou *et al.*, 1992; Derbyshire *et al.*, 1992; Naseem *et al.*,

1992). Adding calcium blockers or changing the extracellular calcium concentration can alter ricin and/or ricin toxin A chain-immunotoxin activity *in vitro* and *in vivo*. In cultured macrophages, calcium plays a role in the expression of ricin toxicity. In Ca^{2+}-free medium, protein synthesis was inhibited only 19%. EGTA pretreatment (to deplete intracellular calcium) also partially protected cells from protein synthesis inhibition. Thus, calcium is required for ricin to exert its inhibitory effect on protein synthesis in cultured macrophages. These studies indicated that ricin administration affects intracellular calcium regulation.

Calcium homeostasis in cardiac myocytes results from the integrated function of trans-sarcolemmal Ca^{2+} influx and efflux pathways modulated by the membrane potential and from intracellular Ca^{2+} uptake and release caused predominantly by SR function. Based on studies of single myocardial cells, a cumulative increase in resting $[Ca^{2+}]_i$ can be influenced by Ca^{2+} handling by the sarcoplasmic reticulum (Hattori et al., 1991). The mechanism for this rise in $[Ca^{2+}]_i$ can be secondary to decreased calcium uptake by the sarcoplasmic reticula (Krause et al., 1985) or through Na^{+}-Ca^{2+} exchange (Lazdunski et al., 1985; Tani et al., 1989). Both these calcium movements were altered to an important extent by ricin administration. Ricin administration depresses calcium influx and efflux and calcium uptake into microsomes. The ricin-treated heart is no longer capable of maintaining calcium homeostasis. The inhibition of calcium flux results in a rise in the intracellular calcium concentration from 0.4 μM to 1.1 μM. Although calcium uptake into mitochondria is not very important under physiological conditions (McCormack, 1986), an abnormal uptake pattern was also observed in the ricin treated heart. Therefore, the total effects of ricin on intracellular calcium levels is interfering with calcium routing. It is assumed that the basic defect is the loss of control of the intracellular Ca^{2+} concentration.

An elevation of intracellular calcium may not be necessary to cause an increased contractility of the heart. It has been proposed that a decrease in the amount of calcium stored in the sarcoplasmic reticulum as a result of a reduction in the calcium pump activity

could diminish contractile protein activation through attenuated calcium release during systole (Krause et al., 1989). The concept of inadequate delivery of calcium to the contractile proteins secondary to sarcoplasmic reticulum dysfunction is an attractive hypothesis for excitation-contraction uncoupling. During systole, cytosolic calcium is released from the sarcoplasmic reticulum (cAMP independent) and there is an influx of extracellular calcium (cAMP dependent). We found that both these pathways for calcium accumulation in the cytoplasm were disturbed by ricin administration. This may be another mechanism involved in the depression of systolic function. Decreased sensitivity of myofilaments to calcium is the most likely reason for the depression of function. The dysfunction of the isolated heart receiving ricin is a result of reduced calcium sensitivity rather than reduced calcium availability. Increased cytosolic calcium can activate phospholipases and other degradative enzymes (Opie, 1989; Marban *et al.*, 1989). The excessive $[Ca^{2+}]_i$ levels could damage intracellular organelles concerned with contraction and thereby produce prolonged mechanical dysfunction. The changes of the pattern in which calcium is taken up into mitochondria may be a sign of dysfunction of mitochondria in ricin toxicity. If mitochondrial function was damaged by ricin administration, insufficient ATP synthesis might occur, which may decrease the systolic function of the heart receiving ricin. In addition, elevation of cytosolic calcium could trigger production of oxygen radicals via xanthine oxidase (McCord, 1985).

In our previous studies with the rabbit central ear artery (Christiansen *et al.*, 1994b), rabbits were sacrificed at three time points, 18 hr, 4 d, and 7 d. The effects of ricin on the dose response curve to NE at each time point were similar in direction, differing only in the magnitude of the effect. Thus, the effects of ricin on these rabbit arteries seem to be unidirectional and its effects at 48 hr may be representative of its effects on these arteries during the entire process of ricin intoxication. Thus, the results with coronary arteries may at least partially account for the decreased blood pressure (Robinson

et al., 1992) and increased blood flow (Zhang *et al.*, 1992) in rabbits after ricin intoxication.

Pathological studies of the rabbits that died from ricin demonstrated that the typical changes in heart, stomach, lungs and other organs are severe hemorrhage and necrosis (Christiansen *et al.*, 1991) which are similar to the pathological changes observed in disseminated intravascular coagulation (DIC). These changes should markedly increase the amount of histamine and 5-HT in the blood, at least locally (De Clerk *et al.*, 1984; Beaven, 1976). The increased contractions to the high concentrations of 5-HT and histamine may induce or facilitate spasms of coronary artery resulting from the DIC-like condition observed in the final stage of ricin intoxication and thus contribute to micro- and macro-circulatory collapse and death.

These studies also established that a minimum lethal dose of ricin affects both systolic and diastolic cardiac function, especially, diastolic function. Ricin did not cause the changes in the electrocardiogram. However, the alteration in action potential duration and effective refractory period may be a potential risk in arrhythmia development. The altered function of the heart by ricin administration is not caused by altering *alpha*- and *beta*- adrenergic receptors. The mechanism responsible for depressed cardiac function is probably due to a general inhibition of intracellular function by ricin. Inhibition of cAMP formation and disturbing intracellular calcium transients might directly alter the function of the heart. Knowing the effects of ricin on the heart is important for therapy of ricin intoxication.

Thus, ricin causes a significant decrease in both the systolic and diastolic function of the heart after a minimum lethal dose of ricin. Alterations of electrophysiological properties were observed. Ricin did not affect the *alpha*- and *beta*-adrenergic systems. The alteration of heart function is probably due to depression of intracellular cAMP concentrations and increased MAO activity and ricin-disturbed intracellular calcium homeostasis. Ricin causes a deregulation of intracellular mechanisms and calcium

homeostasis. Thus, the heart is a target organ for ricin, and ricin damages the heart by intracellular mechanisms.

V. CONCLUSIONS

This study investigated the effects of ricin on the distribution of blood flow to the various organs and tissues, its coronary arteries, and the rabbit heart. Both sublethal and minimal lethal doses caused changes in both the systemic and regional circulation in rabbits at 12 and 18 hours after ricin administration. Ricin increased cardiac output, and blood flow to most organs/tissues which may have resulted from decreased peripheral vascular resistance and compensatorily increased cardiac output. The organs or tissues with the largest increase in blood flow may indicate organs or tissues where the vessels are more sensitive to ricin's toxic actions. The decreased blood flow to the lungs at the higher ricin dose and longer periods of time is very likely due to severe damage to small vessels and to perivascular tissue in the lungs.

Ricin altered contractions and relaxations of rabbit coronary arteries to endogenous vasoactive agents. Ricin decreased the sensitivities of coronary arteries to 5-HT- and histamine-induced contractions but increased their sensitivity to NE-induced relaxation. The maximal contractions of rabbit coronary arteries were markedly increased by ricin administration. Ricin did not alter the ACh-induced relaxations in rabbit coronary arteries which seems to indicate that their endothelia still functioned well.

Ricin did not alter MAO activity in coronary arteries, but increased it in the heart. It reduced COMT activity in both the heart and its coronary arteries.

The intracellular messenger system in rabbit coronary arteries was affected by ricin administration. Basal cGMP levels were decreased while basal cAMP levels were increased. In the coronary arteries from rabbits given ricin, the responses of cGMP to external stimulation were inhibited, whereas the responses of the cAMP pathway were well preserved. Ricin increased the basal IP_3 levels, but the histamine stimulated IP_3 levels were depressed. The basal hydrolysis rate from IP_2 to form IP_1 were lowered by ricin administration. These intracellular alterations may explain the changed responses to

vasoactive agents observed in coronary arteries from rabbits given ricin. The decreased contractions of their coronary arteries to lower concentrations of histamine were due to the desensitization caused by an increased cAMP level and by an increased basal intracellular Ca^{2+} concentration. The increased maximum contractions were caused by increased intracellular Ca^{2+} and the decreased cGMP levels as well as the dysfunction of the cAMP regulatory system under excessive stimulations. All of the findings in rabbits concerning ricin-induced changes in hemodynamics and coronary arteries may underlay the mechanisms for the reduction of blood pressure and increased blood flow. They are also important for evaluation of the possible contribution of the lungs and heart in the lethality of ricin to rabbits.

In studies with rabbit myocardium, by examining the intracellular pharmacomechanical coupling system, it was observed that ricin depressed both cAMP and cGMP accumulation but not phosphoinositide hydrolysis. The 48-hour minimum lethal dose of ricin given i.v. (0.22 μg/kg) significantly altered the function of the heart. Heart rate, bipolar electrocardiograms, and action potentials were not altered. The contraction of papillary muscle from rabbits given ricin was increased initially by the addition of Bay K 8644, a calcium channel agonist. Ricin reduced left ventricular compliance and decreased left ventricular developed pressure per balloon volume. It did not alter the number or affinity of *beta* adrenergic receptors in the heart. An increase of intracellular calcium concentration was observed. Calcium movements in the heart were affected by ricin. Ricin depressed the calcium influx into papillary muscle and microsomes. Ricin also depressed NE-stimulated calcium efflux from papillary muscle. Ricin also altered the pattern of calcium uptake into mitochondria from the heart.

Thus, ricin increased cardiac output and increased blood flow to most tissues and reduced left ventricular compliance. It altered responses of coronary arteries to vasoactive agents and altered intracellular concentrations of cyclic nucleotides and inositol. It also altered calcium handling in isolated tissues and organelles.

VI. ACKNOWLEDGMENTS

The authors wish to thank:

- Donald Parker, Ph.D., University of Oklahoma, Department of Biostatistics and Epidemiology, for his help with statistical analyses.

- Paula Meder for typing this report.

- Eugene Patterson, Ph.D., Department of Pharmacology, for use of his facilities and equipment, help in planning and performing the experiments, and expertise in interpreting the results.

- Uhdo Thadani, M.D., Department of Cardiology, College of Medicine, University of Oklahoma, for assistance in interpreting the data.

- Bela Szabo, M.D., Ph.D., Department of Cardiology, College of Medicine, University of Oklahoma, for use of his facilities and assistance in recording action potentials.

- Benjamin Scherlag, Ph.D., Department of Cardiology, College of Medicine, University of Oklahoma, for use of his facilities.

VII. REFERENCES

1. Aass, H., Skomedal, T., Olsnes, J.B., Fjeld, N.B., Klingen, G., Langslet, A., Svennegig, J., and Semb, G. Noradrenaline evokes an alpha-adrenoceptor-mediated inotropic effect in human ventricular myocardium. Acta Pharmacol Toxicol 58:88-90, 1986.

2. Amlot, P.L., Stone, M.J., Cunningham, D., Fay, J., Newman, J., Collins, R., May, R., McCarthy, M., Richardson, J., and Ghetie, V. A phase I study of an anti-CD22-deglycosylated ricin A chain immunotoxin in the treatment of B-cell lymphomas resistant to conventional therapy. Blood 82:2624-2633, 1993.

3. Anderson, J.F. An illustrated history of the herbals. Columbia University Press. New York, 1977.

4. Angus, J.A., Cocks, T.M. Role of endothelium in vascular responses to norepinephrine, serotonin and acetylcholine. Bibl. Cardiol. 38:43-52, 1984.

5. Araki, T. and Funatsu, G. Revised amino acid sequence of the B-chain of ricin D due to loss of tryptophan in the cyanogen bromide cleavage. FEBS Letters 191:121-124, 1985.

6. Araki, T. and Funatsu, G. The complete amino acid sequence of the B-chain of ricin E isolated from small-grain castor bean seeds. Ricin E is a gene recombination product of ricin D and Ricinus communis agglutinin. Biochim.Biophys. Acta 911:191-200, 1987.

7. Araki, T., Yoshioka, Y. and Funatsu, G. The complete amino acid sequence of the B-chain of the Ricinus communis agglutinin isolated from large-grain castor bean seeds. Biochim. Biophys. Acta 872:277-285, 1986.

8. Axelrod, J. Catechol-O-methyltransferase from rat liver, in Methods in Enzymology (S.P. Colowick and N. O. Kaplan, eds.) Vol. 5, pp. 748-749, Academic Press, New York, 1962.

9. Axelrod, J. Methylation reactions in the formation and metabolism of catecholamines and other biogenic amines: the enzymatic conversion of norepinephrine (NE) to epinephrine (E). Pharmacol. Rev. 18:95-113, 1966.

10. Balint, G.A. Ricin: The toxic protein of castor oil seeds. Toxicol. 2:77-102, 1974.

11. Baenziger, J.U. and Fiete, D. Structural determinations of Ricinus communis agglutinin and toxin specificity of oligosaccharides. J Biol Chem 254:9795-9799, 1979.

12. Barbieri, L., Gasperi-Campani, A., Derenzini, M., Betts, C.M., and Stirpe, F. Selective lesions of acinar pancreatic cells in rats poisoned with ricin - morphological and biochemical study. Virchows Arch. B. Cell Path. 30:15-24, 1979.

13. Baumann, G., Mercader, D., Busch, U., Felix, S.B., Loher, U., Ludwig, L., Sebening, H., Heidecke, C.D., Hagl, S., Sevening, F., and Blomer, H. Effects

of the H_2-receptor agonist impromidine in human myocardium from patients with heart failure due to mitral and aortic valve disease. J Cardiovasc Pharmacol 5:618-625, 1983.

14. Bavari, S., Walters, D.M. and Creasia, D.A. Ricin and ricin B chain stimulate the release of tumor necrosis factor-alpha from alveolar macrophages. The Toxicologist 12:Abstract 1126, 1992.

15. Beaven, M.A. Histamine. N. Engl. J. Med. 294:30-36, 1976.

16. Berridge, M.J., Downes, C.P., Hanley, M.R. Lithium amplifies agonist dependent phosphatidylinositol responses in brain and salivary glands. Biochem. J. 206:587-595, 1982.

17. Berridge, M.J. Inositol and diacylglycerol: two interacting second messengers. Annu. Rev. Biochem. 56:159-193, 1987.

18. Berridge, M.J., Dawson, R.M.D., Downes, C.P., Heslop, J.P. and Irvine, R.F. Changes in the levels of inositol phosphates after agonist-dependent hydrolysis of membrane phosphoinositides. Biochem. J. 212:315-321, 1983.

19. Blakey, D. and Thorpe, P. Treatment of malignant disease and rheumatoid arthritis using ricin A-chain immunotoxins. Scand. J. Rheumatology Supp. 76:279-287, 1988.

20. Blakey, D., Watson, G., Knowles, P. and Thorpe, P. Effect of chemical deglycosylation of ricin A-chain on the in vivo fate and cytotoxic activity of an immunotoxin composed of ricin A-chain and anti-Thy 1.1 antibody. Cancer Res. 47:947-952, 1987.

21. Bohm, M., Diet, F., Feiler, G., Kemkes, B., and Erdmann, E. *Alpha*-adrenoceptors and *alpha*-adrenoceptor-mediated positive inotropic effects in failing human myocardium. J Cardiovasc Pharmacol 12:357-364, 1988.

22. Bourne, D.W.A. (1989). BOOMER, a simulation and modeling program for pharmacokinetic and pharmacodynamic data analysis. Computer Meth. Programs Biomed. 29:191-195, 1989.

23. Bourrie, B., Casellas, P., Blythman, H. and Jansen, F. Study of the plasma clearance of antibody-ricin A-chain immunotoxins. Evidence for specific recognition sites of the A-chain that mediate rapid clearance of the immunotoxin. Eur. J. Biochem. 155:1-10, 1986.

24. Bristow, M.R., Cubicciotti, R., Ginsburg, R., Stinson, E.B., and Johnson, C. Histamine-mediated adenylate cyclase stimulation in human myocardium. Mol Pharmacol 21:671-679, 1982.

25. Bristow, M.R., Hershberger, R.E., Port, J.D., Gilbert, E.M., Sandoval, A., Rasmussen, R., Cates, A.E., and Feldman, A.M. ß-adrenergic pathways in nonfailing and failing human ventricular myocardium. Circulation 82:I12-I25, 1990.

26. Bristow, M.R. Myocardial cell surface membrane receptors in heart failure. Heart Failure 5:47-50.

27. Bristow, M.R., Minobe, W., Rasmussen, R., Hershberger, R.E., and Hoffman, B.B. Alpha-1 adrenergic receptors in the nonfailing and failing human heart. J Pharmacol Exp Ther 247:1039-1045, 1988.

28. Brodde, O-E. Bisoprolol (EMD 33512), a highly selective β_1-adrenoceptor antagonist: in vitro and in vivo studies. J Cardiovasc Pharmacol 8 (suppl. 11):S29-S35.

29. Brown, A.M., and Birnbaumer, L. Direct G protein gating of ion channels. Am. J. Physiol. 254, H401-H410, 1988.

30. Brum, J.M., Sufan, Q., Lane, G., and Bove, A. Increased vasoconstrictor activity of proximal coronary arteries with endothelial damage in intact dogs. Circulation 70:1066-1703, 1984.

31. Burnstock, G. Nonadrenergic innervation of blood vessels-some historical perspectives and future directions. In Nonadrenergic Innervation of Blood Vessels Vol. 1. (G. Burnstock, and S. G. Griffiths, Ed.), pp. 1-14. CRC Press, Boca Raton, Florida, 1988.

32. Chapman, R.A. and Tunstall, J. The calcium paradox of the heart. Prog Biophys Mol Biol 50:67-96, 1987.

33. Chaudhary, V.K., Jinno, Y., Fitzgerald, D., and Pastan, I. *Pseudomonas* exotoxin contains a specific sequence at the carboxyterminus that is required for cytotoxicity. Proc. Natl. Acad. Sci. USA 87:308-312, 1990.

34. Christiansen, V.J., Hsu, C.-H., Kosanke, S.D. And Robinson C. P. Histological and laboratory value abnormalities following ricin administration to rabbits. The Pharmacologist. 33:210, 1991.

35. Christiansen, V.J., Hsu, C.-H., Dormer, K.J., and Robinson C.P. The cardiovascular effects of ricin in rabbits. J. Pharmacol. and Toxicol. 74:148-152, 1994a.

36. Christiansen, V.J., Hsu, C.-H. Zhang, L. and Robinson C.P. (1994b). The effects of ricin on the ability of rabbit arteries to contract and relax. J. Appl. Toxicol. In press, 1994b.

37. Clusin, W.T., Buchbinder, M., and Harrison, D.C. Calcium overload, injury current, and early ischemic cardiac arrhythmias: A direct connection. Lancet 2:272-274, 1983.

38. Cmiech, H.A., Morley, M., and Gee, D.J. Immunocytochemical detection of ricin. I Preliminary immunofluorescence studies. *Histochem. J* 17, 859-856, 1985.

39. Cohen, M.L., and Berkowitz, B.A. (1974). Age-related changes in vascular responsiveness to cyclic nucleotides and contractile agonists. J. Pharmacol. Exp. Ther. 191:147-155, 1974.

40. Collins, P., Griffith, T.M., Henderson, A.H., and Lewis, M.J. Endothelium-derived relaxing factor alters calcium fluxes in rabbit aorta: a cyclic guanosine monophosphate-mediated effect. J Physiol 381:427-437, 1986.

41. Conti, M.A., and Adelstein, R.S. The relationship between calmoldulin binding and phosphorylation of smooth muscle myosin kinase by the catalytic subunit of 3', 5' cAMP-dependent protein kinase in adipose, cardiac, and other tissues, J. Biol. Chem. 250:218-225, 1975.

42. Corr, L., Burnstock, G., and Poole-Wilson, P. Responses of the rabbit epicardial coronary artery to acetylcholine and adrenoceptor agonists. Cardiovascular Res. 25:256-262, 1991.

43. Creasia, D.A., Bavari, S., Bostian, K.A. and Walters, D.M. Broncho-alveolar lavage fluid enzymes after exposure of mice to ricin and ricin B chain aerosols. The Toxicologist 12 Abstract 1125, 1992.

44. Crompton, R. and Gall, D. Georgi Markov - Death in a pellet. Medico-Legal J. 48:51-62, 1980.

45. Cruz, G. Etude toxicologique de la ricine. Ann. Hyg. Pulb. Med. Leg., 10:344-359, 1898.

46. Cushny, A.R. Ueber das Ricinusgift. Arch. Exptl. Pathol. Pharmakol., 41:439-448, 1898.

47. Davenport, A.P., Hall, J.A., Nunez, D.J., and Brown, M.J. [^{125}I]-Endothelin binding in mammalian tissue: relation to human atrial inotropic effect and coronary contraction. Br J Pharmacol 96 (Suppl):102 P, 1989.

48. de Chaffoy de Courcelles, D., Leysen, J.E., De Clerck, F., Van Belle, H., and Janssen, P.A.J. (1985). Evidence that phospholipid turnover is the signal transducing system coupled to serotonin-S_2 receptor sites. J. Biol. Chem. 260: 7603-7608, 1985.

49. de Clerck, F., van Neuten, J.M., and Reneman, R.S. Platelet-vessel wall interactions: Implication of 5-hydroxytryptamine. A review. Agents and Actions 15:612-626, 1984.

50. Delanerolle, P., Nishikawa, M. Yost, D.A., and Adelstein, R.S. Increased phosphorylation of myosin light chain kinase after an increase in cyclic AMP in intact smooth muscle. Science 223:1415-1417, 1984.

51. Derbyshire, E.J. and Wawrzynczak, E.J. An anti-mucin immunotoxin BrE-3-ricin A-chain is potently and selectively toxic to human small-cell lung cancer. Int J Cancer 52:624-30, 1992.

52. Derenzini, M., Benetti, E., Marinozzi, V., and Stirpe, F. Toxic effects of ricin:Studies on the pathogenesis of liver lesions. Virchows Arch *B* 20:15-28, 1987.

53. Dhital, K.K., and Burnstock, G. Adrenergic and non-adrenergic neural control of the arterial wall. In Diseases of the Arterial Wall (J-P Camilleri, C. L. Berry, J-N. Fiessinger, and J. Bariety, Ed.), pp.97-126. Springer, London, 1989.

54. Dixon, T. *Ricinus communis*. Austral. Med. Gasette. 6 (1887) 137-155.

55. Duke, O., Panayi, G., Janossy, G., Poulter, L.W. An immunohistological analysis of lymphocyte subpopulations and their micro-environment in the synovial membranes of patients with rheumatoid arthritis using monoclonal antibodies. Clin. Exp. Immunol. 49:22-30, 1982

56. Dumuis, A., Bouhelal, R., Sebben, M., Cory, R., and Bockaert, J. A non-classical 5-hydroxytryptamine receptor positively coupled with adenylate cyclase in the central nervous system. Mol Pharmacol 34:880-887, 1988.

57. Ehrlich, P. The collected papers of Paul Ehrlich, Vol. 2. Pergamon: New York 1957, 21-44, 1957.

58. Eiklid, K., Olsnes, S., and Pihl, A. Entry of lethal doses of abrin, ricin, and modeccin into the cytosol of HeLa cells. Exp Cell Res 126:321-326, 1980.

59. Endo, Y., Kazuhiro, M., Motizuki, M., and Tsurugi, K. The mechanisms of action of ricin and related toxic lectins on eukaryotic ribosomes. The site and characteristics of the modification in 28S ribosomal RNA caused by the toxins. J Biol Chem 262:5908-5913, 1987.

60. Fiani, M.L., Blum, J.S., and Stahl, P.D. Endosomal proteolysis precedes ricin A-chain toxicity in macrophages. Arch Biochem Biophys 307:225-230, 1993.

61. Fodstad, O., Johannessen, J.V., Schjerven, L. and Pihl, A. Toxicity of abrin and ricin in mice and dogs. J. Toxicol. Environ. Health. 5:1073-1084, 1979.

62. Fodstad, O. and Pihl, A. Effect of ricin and abrin on survival of L1210 leukemic mice and on leukemic and normal bone marrow cells. Int. J. Cancer 22:558-563, 1978.

63. Fodstad, O., Olsnes, S. and Pihl, A. Toxicity, distribution and elimination of the cancerostatic lectins abrin and ricin after parenteral injection into mice. Br. J. Cancer. 34:418-425, 1976.

64. Foxwell, B.M.J., Detre, S.I., Donovan, T.A. and Thorpe, P.E. The use of anti-ricin antibodies to protect mice intoxicated with ricin. Toxicology 34:79-88, 1985.

65. Frankel, A., Welsh, P., Richardson, J., and Robertus, J.D. The role of arginine 180 and glutamic acid 177 of ricin toxin A chain in the enzymatic inactivation of ribosomes. Mol. Cell. Biol. 10:6257-6263, 1990.

66. Fujii J, Ueno A, Kitono K, Tanaka S, Kadoma M, and Tada M. Complete complementary DNA-derived amino acid sequence of canine cardiac phospholamban. J Clin Invest 79:301-304, 1987.

67. Funatsu, G., Kinura, M., and Funatsu, M. Primary structure of Ala chain of ricin D. Agric Biol Chem 43:2221-2224, 1979.

68. Funatsu, G., Yoshitake, S. and Funatsu, M. Primary structure of Ile chain of ricin D. Agric. Biol. Chem. 42:501-503, 1978.

69. Funatsu, M., Funatsu, G., Ishiguro, M., and Hara, K. Properties of subunits of ricin D. Jap J Med Sci Biol 26:30-32, 1973.

70. Funatsu, M., Funatsu, G., Ishiguro, S., Nanno, S. and Hara, K. Structure and toxic function of ricin. I. Purification procedures of ricin D. II. Subunit structure of ricin D. Proc. Jap. Acad. 47:713-723, 1971.

71. Godal, A., Fodstad, O., Ingebrigtsen, K., and Pihl, A. Pharmacological studies of ricin in mice and humans. Cancer Chemother Pharmacol 13:157-63, 1984.

72. Goldmacher, V.S., Lambert, J.M. and Blattler, W.A. The specific cytotoxicity of immunoconjugates containing blocked ricin is dependent on the residual binding capacity of blocked ricin: evidence that the membrane binding and A-chain translocation activities of ricin cannot be separated. Biochem. Biophys. Res. Comm. 183:758-766, 1992.

73. Gonatas, N. K., Stieber, A., Kim, S.U., Graham, D.I., and Avrameas, S. Internalization of neuronal plasma membrane ricin receptors into the Golgi apparatus. Exp Cell Res 94:426, 1975.

74. Gonatas, J., Stieber, A., Olsnes, S., and Gonatas, N.K. Pathways involved in fluid phase and absorptive endocytosis in neuroblastoma. J Cell Biol 87:579-583, 1980.

75. Gottstein, C., Winkler, U., Bohlen, H., Diehl,V., and Engert, A. Immunotoxins: is there a clinical value? Ann Oncol 1:S97-S103, 1994.

76. Grammas, P., Fugate, B., Botchlet, T., and Hanson-Painton, O. Alterations in calcium levels and calmodulin transcripts in endothelial cells in hypertensive rats. FASEB J 6:A1820, 1992.

77. Greco, M., Montanaro, L., Novello, F., Saccone, C., Sperti, S. and Stirpe, F. Inhibition of protein synthesis by ricin: experiments with rat liver mitochondria and nuclei and with ribosomes from Escherichia coli. Biochem. J. 142:695-697, 1974.

78. Griffith, T.M., Edwards, D.H., Jewis, M.J. and Henderson, A.H. Evidence that cyclic guanosine monophosphate (cMGP) mediates endothelium-dependent relaxation. European J. Pharmacol. 112:195-202, 1985.

79. Griffith, T.M., Henderson, A.H., Hughes Edwards, D., and Lewis, M.J. Isolated perfused rabbit coronary artery and aortic strip preparations: The role of endothelium-derived relaxant factor. J. Physiol. 351:13-24, 1984.

80. Griffith, T.M., and Henderson, A.H. The nature of endothleium-derived relaxing factor. In Relaxing and Contracting Factors (P. M. Vanhoutte, Ed), pp.159-178. The Humana Press Inc. Clifton, NJ., 1988.

81. Griffiths, G., Leek, M. and Gee, D. The toxic plant proteins ricin and abrin induce apoptotic changes in mammalian lymphoid tissues and intestine. J. Pathol. 151:221-229, 1987.

82. Griffiths, G.D., Leith, A.G., Leek, M.D., and Green, M.A. Demonstration of ricin within the mammalian para-aortic lymph node: I. Comparison of the localization, after intramuscular injection, with three immunocytochemical methods. Histochem J 21:380-386, 1989.

83. Griffiths, G.D., Leith, A.G., Leek, M.D., and Green, M.A. Distribution of ricin within the mammalian para-aortic lymph node: II. Comparison of the localization, after intramuscular dosage of colloidal gold-labelled ricin in vivo, with in vitro binding characteristics of the native toxin. Histochem J 21:387-392, 1989.

84. Griffiths, G.D., Newman, H.V., and Gee, D.J. Identification and quantification of ricin toxin in animal tissues using ELISA. J Forensic Sci Soc 26:349-358, 1986.

85. Griffiths, G.D., Newman, H.V., and Gee, D.J. Immunocytochemical detection of ricin.II. Further studies using the immunoperoxidase method. Histochem J 18:189-195, 1986.

86. Grossbard, M.L., Lambert, J.M., Goldmacher, V.S., Spector, N.L., Kinsella, J., Eliseo, L., Coral, F., Taylor, J.A., Blattler, W.A., and Epstein, C.L. Anti-B4-blocked ricin: a phase I trial of 7-day continuous infusion in patients with B-cell neoplasms. J Clin Oncol 11:726-737, 1993.

87. Hales, J.R.S. Radioactive microsphere techniques for studies of the circulation. Clin. Exper. Pharmacol. Physiol. Suppl. 1:31-46, 1974.

88. Hall-Craggs, E.C.B. The abdomen, in Anatomy as a Basis for Clinical Medicine. 2nd Edition, pp. 223-298, Urban & Schwarzenberg, Baltimore-Munich, 1990.

89. Hansen, S., Petersen, O., Sandvig, K., Olsnes, S., and van Deurs, B. Internalized ricin and the plasma membrane glycoprotein MAM-6 co-localize in the trans-golgi network of T47D human breast carcinoma cells. Exp Cell Res 185:373-386. 1989.

90. Haranghy, L. Deutung der Veranderungen der Milz bei Diphtherie auf Grund der Milzveranderungen nach Rizinvergiftung. Centralbl.f.aug.Path.u.Path.Anat. 60:161-168, 1934.

91. Harley, S.M., and Lord, J.M. *In vitro* endoproteolytic cleavage of castor bean lectin precursors. Plant Sci 41:111-119, 1985.

92. Harper, C.G., Gonatas, J.O., Mizutani, T., and Gonatas, N.K. Retrograde transport and effects of toxic ricin in the autonomic nervous system. Lab Invest 42:396-404, 1980.

93. Hatakeyama, T., Ohba, H., Yamasaki, N. and Funatsu, G. Binding of saccharides to ricin E isolated from small castor beans. J. Biochem. 105:444-448, 1989.

94. Hatakeyama, T., Yamasaki, N., and Funatsu, G. Further studies on the histidine residue located at the high affinity saccharide-binding site of ricin E. Agric Biol Chem 54:1085-1086, 1990.

95. Hathaway, D.R., March, K.L., Lash, J.A., Adam, L.P., and Wilensky, R.L. Vascular smooth muscle. A review of the molecular basis of contractility. Circulation 83:382-390, 1991.

96. Hattori, Y., Toyama, J., and Kodama, I. Cytosolic staircase in ventricular myocytes isolated from guinea pigs and rats. Cardiovasc Res 25:622-629, 1991.

97. Helke, C., Charlton, C., and Wiley, R. Suicide transport of ricin demonstrates the presence of substance P receptors on medullary somatic and autonomic motor neurons. Brain Res 328:190-195, 1985.

98. Hendren, W.G., Geffin, G.A., Love, T.R., Titus, J.S., Redonnett, B.E., O'Keefe, D.D., and Daggett, W.M. Oxygenation of cardioplegic solutions. Potential for the calcium paradox. J Thoracic & Cardiovas Surg. 94:614-625, 1987.

99. Hewetson, J.F., Rivera, V.R., Creasia, D.A., Lemley, P.V., Rippy, M.K., and Poli, M.A. Protection of mice from inhaled ricin by vaccination with ricin or by passive treatment with heterologous antibody. Vaccine 11:743-746,1993.

100. Hewetson, J.F., Rivera, V.R. Pitt, L.M. and Thompson, W.L. Protection of mice from inhaled ricin by vaccination with formalized ricin toxin. Toxicologist 31:138-139, 1993.

101. Hickey, W.F., Stieber, A., Hogue-Angeletti, R., Gonatas, J., and Gonatas, N.K. Nerve growth factor induced changes in the Golgi apparatus of PC-12 rat pheochromocytoma cells as studied by ligand endoctytosis, Cytochem Morphomet Meth. J Neurocytol 12:751-757, 1983.

102. Hirata, M., Kohse, K.P., Chang, C.H., Ikebe, T. and Murad, F. Mechanism of cyclic GMP inhibition of inositol phosphate formation in rat aorta segments and cultured bovine aortic smooth muscle cells. J. Biol. Chem. 265:1268-1273, 1990.

103. Hollenberg, N.K. Serotonin and vascular responses. Ann. Rev. Pharmacol. Toxicol. 28:41-59, 1988.

104. Houston, D.S., and Vanhoutte, P.M. Serotonin and the vascular system: role in health and disease, and implications for therapy. Drugs 31, 149-163, 1986.

105. Ikebe, M., and Reardon, S. Phosphorylation of smooth myosin light chain kinase by smooth muscle Ca^{2+}/calmodulin-dependent multifunctional protein kinase. J. Biol. Chem. 265:8975-8978, 1990.

106. Ishiguro, M., Nakashima, H., Tanabe, S. and Sakakibara, R. Interaction of toxic lectin ricin with epithelial cells of rat small intestine in vitro. Chem. Pharm. Bull. 40:441-445, 1992.

107. Ishiguro, M., Takahashi, T., Funatsu, G., Hayashi, K. and Funatsu, M. Biochemical studies on ricin I. Purification of ricin. J. Biochem. 55, 587-592. 1964.

108. Ishikawa, T., Hume, J.R., and Keef, K.D. Regulation of Ca^{2+} channels by cAMP and cGMP in vascular smooth muscle cells. Cir. Res. 73:1128-1137, 1993.

109. Jaffrezou, J.P., Levade, T., Thurneyssen, O., Chiron, M., Bordier, C., Attal, M., Chatelain, P., and Laurent, G. *In vitro* and *in vivo* enhancement of ricin-A chain immunotoxin activity by novel indolizine calcium channel blockers: delayed

intracellular degradation linked to lipidosis induction. Canc Res 52:1352-1359, 1992.

110. Janossy, G., Panayi, G., Duke, O., Bofill, M., Poulter, L. and Goldstein, G. Rheumatoid arthritis, a disease of LT-lymphocyte/macrophage immuno-regulation. Lancet ii:839-842, 1981.

111. Kanellos, J., MacKenzie, I. and Pietersz, G. Intratumour therapy of solid tumours with ricin-antibody conjugates. Immunol. Cell Biol. 67:89-99, 1989.

112. Kaumann, A.J., Sanders, L., Brown, A.M., Murray, K.J., and Brown, M.J. A 5-hydroxytryptamine receptor in human atrium. Br J Pharmacol 100:879-885, 1990.

113. Keef, K.D., Pasco, J.S., and Eckman, D.M. Purinergic relaxation and hyperpolarization in guinea pig and rabbit coronary artery: role of the endothelium. J. Pharmacol. Exp. Ther. 260:592-600, 1991.

114. Kerman, N.A., Byers, V., Scannon, P.J., Mischak, R.P., Brochstein, J., Flomenberg, N., Dupont, B., and O'Reilly, R.J. Treatment of steroid-resistant acute graft-vs-host disease by in vivo administration of an anti-T-cell ricin A chain immunotoxin. J Am Med Assoc 259:3154-3157, 1988.

115. Ko, T. and Kaji, A. Effect of ricin on biosynthesis of myeloma protein (IgA) and general cellular proteins in MOPC-315 cells. Biochim Biophys Acta 414:155-160, 1975.

116. Koga, M., Ohtsu, M., and Funatsu, G. Cytotoxic, cell agglutinating, and syncytium forming effect of purified lectins from Ricinus communis on cultured cells. Gann 70:585-591, 1979.

117. Kohl, C., Schmitz, W., Scholz, H., Scholz, J., Toth, M., Doring, V., and Kalimar, P. Evidence for $alpha_1$-adrenoceptor-mediated increase of inositol triphosphate in the human heart. J Cardiovasc Pharmacol 13:324-327, 1988.

118. Koja, N., Shibata, T., and Mochida, K. Enzyme-linked immunoassay of ricin. Toxicon 18:611-618, 1980.

119. Kopferschmitt, J., Flesch, F., Lugnier, A., Sauder, P.H., Jaeger, A., and Mantz, J.M. Acute voluntary intoxication by ricin. Human Toxicol 2: 239-242, 1983.

120. Krause, S.M. and Hess, M.L. Characterization of cardiac sarcoplasmic reticulum dysfuncton during short-term normothermic global ischemia. Circ Res 55:176-184,1985.

121. Lang, D. and Lewis, M.J. Endothelium-derived relaxing factor inhibits the formation of inositol trisphosphate by rabbit aorta. J Physiol 411:45-52, 1989.

122. Larkin J, Brown M, Goldstein J, and Anderson R. Depletion of intracellular potassium arrests coated pit formation and receptor-mediated endocytosis in fibroblasts. *Cell* 33:273-285, 1983.

123. Lazdunski, M., Frelin, C., and Vigue, P. The sodium/hydrogen exchange system in cardiac cells: Its biochemical and pharmacological properties and its role in regulating internal concentrations of sodium and internal pH. *J* Molec Cell Cardiol 17:1029-1042, 1985.

124. Leek, M., Griffiths, G. and Green, M. Intestinal pathology following intramuscular ricin poisoning. J. Pathol. 159:329-334, 1989.

125. Leek, M.D., Griffiths, G.D., and Green, M.A. Pathological aspects of ricin toxicity in mammalian lymph node and spleen. Med Sci Law 30:141-148, 1990.

126. Leith, A.G., Griffiths, G.D., and Green, M.A. Quantification of ricin toxin using a highly sensitive avidin/biotin enzyme-linked immunosorbent assay. J Forensic Sci Soc 28:227-236, 1988.

127. Lew, W.Y. Mechanisms of volume-induced increase in left ventricular contractility. Am J Physiol 265:H1778-H1786, 1993.

128. Lin, J., Tserng, K., Chen, C., Lin, L. and Tung, T. Abrin and ricin: New anti-tumour substances. Nature 227:292-293, 1970.

129. Lin, J., Liu, K., Chen, C. and Tung, T. Effect of crystalline ricin on the biosynthesis of protein, RNA and DNA in experimental tumor cells. Cancer Res. 31:921-924, 1971.

130. Lincoln, T.M., Cornwell, T.L. and Taylor, A.E. cGMP-dependent protein kinase mediates the reduction of Ca^{2+} by cAMP in vascular smooth muscle cells. Am. J. Physiol. 258 (Cell Physiol. 27):C399-C407, 1990.

131. Lincoln, T.M. Cyclic GMP and mechanisms of vasodilation. Pharmacol. Ther. 41:479-502, 1989

132. Lohmann, S.M., Fischmeister, R., and Walter, U. Signal transduction by cGMP in heart. Basic Res Cardiol 86:503-514, 1991.

133. Lord, J.M. Synthesis and intracellular transport of lectin and storage protein precursors in endosperm from castor bean, Eur J Biochem 146:403-412, 1985.

134. Lord, M.J., Roberts, L.M., and Robertus, J.D. Ricin: structure, mode of action, and some current applications. FASEB J. 8:201-208, 1994.

135. Luchins, A.R. and Makman, M.H. Presence of histamine and serotonin receptors associated with adenylate cyclase in cultured calf-aorta smooth muscle cells. Biochem. Pharmacol. 29:3155-3161, 1980.

136. Lugnier, A.A., Creppy, E.E., and Dirheimer, G. Ricin, the toxic protein of the castor-oil plant (Ricinus communis L). Structure and properties Pathologie Biologie 28:127-139, 1980.

137. Majerus, P.W., Bansal, V.S., Lips, D.L., Ross, T.A., Mitchell, C.A., Caldwell, K.K., and Cunningham, T.W. The phosphatidylinositol pathway of platelets and vascular cells. Ann. New York Acad. Sci. 614:44-50, 1991.

138. Majerus, P.W., Connolly, T.M., Deckmyn, H., Ross, T.S., Bross, T.E., Ishii, H., Bansal, V.S., and Wilson, D. B. The metabolism of phosphoinositide-derived messenger molecules. Science 234, 1519-1526.

139. Malindzak Jr., G.S. Differential segmental response characteristics of the coronary vasculature. In The Coronary Artery (S. Kalsner, Ed.), pp. 241-267. Oxford University Press, New York, 1982.

140. Marban, E., Koretsune, Y., Corretti, M., Chacko, V.P., and Kusoka, H. Calcium and its role in myocardial cell injury during ischemia and reperfusion. Circulation (suppl IV):IV-17-IV-22, 1989.

141. Martin, W. Basal release of endothelium-derived relaxing factor. In Relaxing and Contracting Factors (P. M. Vanhoutte, Ed), pp. 159-178. The Humana Press Inc. Clifton, NJ., 1988.

142. McCord, J.M. Oxygen-derived free radicals in postischemic tissue injury. N Engl J Med 312:159-163, 1985.

143. McCormack, J.G. and Denton, R.M. Ca^{2+} as a second messenger within itochondria. Trends Biochem Sci 11:258-262, 1986.

144. Mereish, K.A. and Fajer, A.B. The effect of antiviral agents on ricin toxicity in vitro. Toxicologist 31: Abstract 153, 1993.

145. Middlebrook, John L. Cell receptors for protein toxins. In Botulinum Neurotoxin and Tetanus Toxin (L. L. Simpson Ed.), pp. 95-119. Academic Press Inc. New York, 1989.

146. Milnor, W.R. Principles of hemodynamics. In Medical Physiology (Mountcastle, V. B. Ed), 14th Edition, pp.1017-1032, The C.V. Mosby Company, St. Louis, 1980.

147. Mise, T., Funatsu, G., Ishiguro, M. and Funatsu, M. Biochemical studies on ricin isolation and characterization of ricin E. Agric. Biol. Chem. 41, 2041-2046. 1977.

148. Mlsna, D., Monzingo, A.F., Katzin, B.J., Ernst, S., and Robertus, J.D. The structure of recombinant ricin A chain at 2.3 Å Prot. Sci. 2, 429-435, 1993.

149. Montfort, W., Villafranca, J.E., Monzingo, A.F., Ernst, S., Katzin, B., Rutenber, E., Xuong, N.H., Hamlin, R., and Robertus, J.D. The three-dimensional structure of ricin at 2.8 Å. *J Biol Chem* 262:5398-5403, 1987.

150. Monzingo, A.F., and Robertus, J.D. X-ray analysis of substrate analogs in the ricin A-chain active site. J. Mol. Biol. 227:1136-1145, 1992.

151. Morgan, J., Lal, R., Arnsdorf, M., and Cohen, L. Evidence that cell-cell uncoupling occurs during synchronous contractile behavior in the tissue culture model of calcium induced ventricular fibrillation. Clin Res 38:987a, 1990.

152. Mosinger, M. Effets necrosants ou clastiques exerces par la ricine sur divers organes et sur les sarcomes experimentaux. Compt. Rend. Soc. Biol. 145:412-415, 1951.

153. Moya, M., Dautry-Varsat, A., Goud, B., Louvard, D., and Boquet, P. Inhibition of coated pit formation in Hep_2 cell blocks the cytotoxicity of diphtheria toxin but not that of ricin toxin. J Cell Biol 101:548-559, 1985.

154. Muller, F. Beitrage zui Toxikologie des Ricins. Arch. Exptl. Pathol. Pharmakol., 42:301-322, 1899.

155. Nakashima, S., Tohmatsu, T., Hattori, H., Okano, Y. and Nozawa, Y. Inhibitory action of cyclic GMP on secretion polyphosphoinositide hydrolysis and calcium mobilization in thrombin-stimulated human platelets. Biochem. Biophys. Res. Commun., 135:305-312.

156. Nanno, S., Ishiguro, M., Funatsu, G and Funatsu M. Agric. Biol. Chem. 39:1651-1654, 1975.

157. Naseem, S.M. and Pace, J.G. Effects of ricin on macromolecular synthesis and arachidonic acid metabolism in cultured macrophages. FASEB J. 5:Abstract 5229, 1991.

158. Naseem, S.M., Wellner, R.B., and Pace, J.G. The role of calcium ions for the expression of ricin toxicity in cultured macrophages. J Biochem Toxicol 7:133-138, 1992.

159. Newton, D.L., Wales, R., Richardson, P.T., Walbridge, S., Saxena, S.K., Ackerman, E.J., Roberts, L.M., Lord, J.M., and Youle, R.J. Cell surface and intracellular functions for ricin galactose binding. J Biol Chem 267:11917-11922, 1992.

160. Nicolson, G. Ultrastructural analysis of toxin binding and entry into mammalian cells. Nature 251:628-630, 1974.

161. Nicolson, G.L., Lacorbiere, M. and Hunter, T.R. Mechanism of cell entry and toxicity of an affinity-purified lectin from Ricinus Communis and its differential effects on normal and virus-transformed fibroblasts. Cancer Res. 35:144-155, 1975.

162. Nielsen-Kudsk, F., Poulsen B, Ryon, C., and Nielsen-Kudsk, J.E. A strain-gauge myograph for isometric measurements of tension in isolated small blood vessels and other muscle preparations. J. Pharmacol. Meth. 16, 215-225, 1986.

163. Oda, T. and Funatsu, G. Cross-linking of the two constituent polypeptide chains of ricin D with N, N'-*O*-phenylenedinaleinide. Agric Biol Chem 43:547-554, 1979.

164. Oishi, K., Raynor, R.L., Charp, P.A., and Kuo, J.F. Regulation of protein kinase C by lysophospholipids. Potential role in signal transduction. J. Chem. 263:6865-6871, 1988.

165. Olsnes, S., Fernandez-Puentes, C., Carrasco, L., and Vasquez, D. Ribosome inactivation by the toxic lectins abrin and ricin. Kinetics of the enzymic activity of the toxin A-chains. Eur J Biochem 60:218-225, 1975.

166. Olsnes, S., Heiberg, R., and Pihl, A. Molec. Biol. Rep. 1:15-20, 1973.

167. Olsnes, S. and Pihl, A. Toxic lectins and related proteins, in *Molecular Action of 167Toxins and Viruses*, Cohen P, and van Heyningen S, Eds., Elsevier/North Holland, Amsterdam. 51-57, 1982.

168. Olsnes, S. and Pihl, A. Inhibition of peptide chain elongation. Nature 238:459-461, 1972.

169. Olsnes, S., Refsnes, K. and Pihl, A. Mechanism of action of the toxic lectins abrin and ricin. Nature 246:627-631, 1974.

170. Olsnes, S. and Sandvig, K. Entry of toxic proteins into cells, in *Receptor-mediated Endocytosis: Receptors and Recognition*, Series B, Vol. 15, Cuatrecasas P, and Toth TF, Eds., Chapman & Hall, London, 188-197, 1983.

171. Olsnes, S., and Sandvig, K. Entry of polypeptide toxins into animal cells, in *Endocytosis*, Pastan I, and Willingham MC, Eds., Plenum Press, New York, 195-199, 1985.

172. Olsnes, S., Sandvig, K., Moskaug, J.Ø., Stenmark, H., and van Deurs, B. Toxin translocation across membranes and intracellular mechanisms of action. Proc Int Symp Workshop Verocytotoxin, Toronto, 93-97, 1987.

173. Opie, L.H., Coetzee, W.T., Dennis, S.C., and Thandroyen, F.T. A potential role of calcium ions in early ischemic and reperfusion arrhythmias. Ann N Y Acad Sci 522:464-471, 1988

174. Orrenius, S., McConkey, D.J., Jones, D.P., and Nicofera, P. Ca^{2+}-activated mechanisms in toxicity and programmed cell death. ISI Atlas Sci Pharmacol 2:389-391, 1988.

175. Paulus, H., Machleder, H., Levine, S., Yu, D. and MacDonald, N. Lymphocyte involvement in rheumatoid arthritis. Studies during thoracic duct drainage. Arthritis Rheum. 20:1249-1262, 1977.

176. Pelham, H.R.B. The retention signal for soluble proteins of the endoplasmic reticulum. Trends Biochem. Sci. 15:483-486. 1990.

177. Porro, G., Bolognesi, A., Caretto, P., Gromo, G., Lento, P., Mistza, G., Sciumbata, T., Stirpe, F., and Modena, D. *In vitro* and *in vivo* properties of an anti-CD5-momordin immunotoxin on normal and neoplastic T lymphocytes. Cancer Immunol Immunother 36:346-350, 1993.

178. Rabkin, S.W. Mitochondrial and cytoplasmic aspartate aminotransferase enzyme release in the calcium paradox. Canad J Physiol & Pharmacol 64:602-608, 1986.

179. Rapoport, R.M., Schwartz, K., and Murad, F. Effect of sodium-potassium pump inhibitors and membrane-depolarizing agents on sodium nitroprusside-induced relaxation and cyclic guanosine monophosphate accumulation in rat aorta. Circ Res 57:164-170, 1985.

180. Rauber, A. and Heard, J. Castor bean toxicity re-examined: A new perspective. Vet. Hum Toxicol. 27:498-502, 1985.

181. Refsnes, K., Olsnes, S., and Pihl, A. On the toxic proteins abrin and ricin. J Biol Chem 249:3557-3562, 1974.

182. Reid, D.M., Friedel, U., Molday, R.S., and Cook, N.J. Identification of the sodium-calcium exchanger as the major ricin-binding glycoprotein of bovine rod outer segments and its localization to the plasma membrane. Biochemistry 29:1601-1607, 1990.

183. Ritthausen, H. Ueber die Eiweisskorper der Ricinus-samen der Proteinkorner, sowie der Krystalloide dieser same. Pfluegers Arch. Ges. Physiol. 19:15-53, 1878.

184. Robinson, C.P., Christiansen, V.J., Hsu, C.-H., Zhang, L. Effects of ricin on the vascular neuroeffector system. Final report, Department of Defense Contract DAMD-17-90-C-0109, 1992.

185. Roth, J.A. Presence of membrane-bound catechol-O-methyltransferase in human brain. Biochem. Pharmacol. 29:3119-3122, 1980.

186. Rutenber, E., Katzin, B.J., Collins, E.J., Mlsna, D., Ernst, S., Ready, M.P., and Robertus, J.D. The crystallographic refinement of ricin at 2.5 Å resolution. Proteins 10:240-250, 1991.

187. Sandvig, K. and Olsnes, S. Entry of toxic proteins abrin, modeccin, ricin, and diphtheria toxin into cells, II. Effect of pH, metabolic inhibitors and ionophores and evidence for penetration from endocytic vesicles. J Biol Chem. 257:7504-7513, 1982.

188. Sandvig, K., Olsnes, S., Petersen, O.W. and van Deurs, B. Acidification of the cytosol inhibits endocytosis from coated pits. J. Cell Biol. 105:679-689, 1987.

189. Sandvig, K., Olsnes, S., and Pihl, A. Binding, uptake and defraudation of the toxic proteins abrin and ricin by toxin resistant cells, Eur J Biochem 82:13-21, 1978.

190. Sandvig, K., Prydz, K., Hansen, S.H., and van Deurs, B. Ricin transport in brefeldin A-treated cells: correlation between Golgi structure and toxic effect. J. Cell Biol. 115:971-981, 1991.

191. Sandvig, K., Tonnessen, T., and Olsnes, S. Ability of inhibitors of glycosylation and protein synthesis to sensitize cells to abrin, ricin, Shigella toxin and Pseudomonas toxin. *Cancer Res* 46:6418-6422, 1986.

192. Sandvig, K. and van Deurs, B. Endocytosis without clathrine (a minireview). Cell Biol. Int. Rep. 15:3-8, 1991.

193. Schmitz, W., Scholz, H., Scholz, J., Steinfath, M., Lohse, M., Puurunen, J., and Schwabe, U. Pertussis toxin does not inhibit the alpha$_1$-adrenoceptor-mediated effect on inositol phosphate production in the heart. Eur J Pharmacol 134:377-378, 1988.

194. Schmitz, W., Scholz, H., and Erdmann, E. Effects of alpha and beta-adrenergic agonists, phosphodiesterase inhibitors and adenosine on isolated human heart muscle preparations. Trends Pharmacol Sci 8:447-450, 1989.

195. Schomisch Moravec, C.H., Schluchter, M.D., Paranandi, L., Czerska, B., Stewart, R.W., Rosenkranz, E., and Bond, M. Inotropic effects of angiotensin II on human cardiac muscle in vitro. Circulation 82:1973-1984, 1990.

196. Shirinsky, V.P., Sobolevsky, A.V., Grigorian, G.Y., Danilov, S.M., Tararak, E. M., and Tkachuk, V.A. Agonist-induced polyphosphoinositide breakdown in cultured human endothelial and vascular smooth muscle cells. Health Psychology 7(Suppl.):61-74, 1988).

197. Skilleter, D.N. and Foxwell, B.M.J. Selective uptake of ricin A-chain by hepatic non-parenchymal cells in vitro. FEBS 196:344-348, 1986.

198. Solis, D., Vallejo, M., and Diaz-Maurino, T. Reduction of ricin toxicity without impairing the saccharide-binding properties by chemical modification of the carboxyl groups. Analytic Biochem 209:117-122, 1993.

199. Steenbergen, C., Murphy, E., Levy, L., and London, R.E. Elevation in sytosolic free calcium concentration early in myocardial ischemia in perfused rat heart. Circ Res 60:700-707, 1987.

200. Stillmark, H. Uber Ricin, eines gifiges Ferment aus den Samen von *Ricinus Communis* L. und anderen Euphorbiacen. Inaugural Dissertation, University of Dorpat, Estonia. 1888.

201. Swauger, J.E., Pace, J.G., Glass, P.J., Rembish, S.J. and Trush, M.A. Effect of ricin on mitochrondrial function in alveolar macrophages. The Toxicologist, 12:Abstract 1089, 1992.

202. Takai, Y., Kikkawa, U., Kaibuchi, K., and Nishizuka, Y. Membrane phospholipid metabolism and signal transduction for protein phosphorylation. Adv. Cyclic Nucl. Prot. Phosphoryl. Res. 18:119-158, 1984.

203. Takai, Y., Kaibuchi, K., Sano, K. and Nishizuka, Y. counteraction of calcium-activated, phospholipid-dependent protein kinase activation by adenosine 3',5'-monophosphate and guanosine 3',5'-monophosphate in platelets. J. Biochem., 91:403-406, 1982.

204. Tani, M. and Neely, J.R. Role of intracellular Na^+ in Ca^{2+} overload and depressed recovery of ventricular function of reperfused ischemic rat hearts: Possible involvement of H^+-Na^+ and Na^+-Ca^{2+} exchange. Circ Res 65:1045-1056, 1989.

205. Thalley, B.S., Carroll, S.B., Lemley, P.V. and Stafford, D.C. Development of an avian ricin antitoxin. Toxicologist 31:174, 1993.

206. Thompson, W.L. and Pace, J.G. Studies on the use of brefeldin A and 3'-azido-3'-deoxythymidine to block the toxic effects of ricin *in vitro*. The Toxicologist 12:Abstract 1089,1992.

207. Thorpe, P.E., Wallace, P.M. Knowles P.P., Relf, M.G., Brown, A.N., Watson, G.J., Knyba, R E., Wawrzynczak, E.J. and Blakey, D.C. New coupling agents for the synthesis of immunotoxins containing a hindered disulphide bond with improved stability in vivo. Cancer Res. 47:5924-5931, 1987.

208. Urata, H., Healy, B., Stewart, R.W., Bumpus, F.M., and Husain, A. Angiotesin II receptors in normal and failing human hearts. J Clin Endocrinol Metab 69:54-66, 1989.

209. van Deurs, B., Hansen, S.H., Olsnes, S. and Sandvig, K. in: Biological Barriers to Protein Delivery (Audus, K.L. and Raub. T.J. ed.) pp. 71-104. Plenum, New York, 1993.

210. van Deurs, B., Pedersen, L.R., Sundan, A., Olsnes, S., and Sandvig, K. Receptor-mediated endocytosis of a ricin-colloidal gold conjugate in Vero cells, Intracellular routing to vacuolar and tubulo-vesicular portions of the endosomal system. Exp Cell Res 159:287, 1985.

211. van Deurs, B., Petersen, O.W., Olsnes, S., and Sandvig, K. Delivery of internalized ricin from endosomes to cisternal Golgi elements is a discontinuous, temperature sensitive process. Exp Cell Res 171:137-142, 1987.

212. van Deurs, B., Sandvig, K., Petersen, O.W., Olsnes, S., Simons, K., and Griffiths, G. Estimation of the amount of internalized ricin that reaches the trans Golgi network. J Cell Biol 106:253-267, 1988.

213. van Deurs, B., Tønnessen, T.I., Petersen, O.W., Sandvig, K., and Olsnes, S. Routing of internalized ricin and ricin conjugates to the Golgi complex. J Cell Biol 102:37-42, 1985.

214. Vatner, S.F., and Murray, P.A. Reflex control of coronary arteries. In The Coronary Artery (S. Kalsner, Ed.), pp. 216-240. Oxford University Press, New York, 1982.

215. Villafranca, J.E. and Robertus, J.D. Ricin B chain is a product of gene duplication. J Biol Chem 256:554-556, 1981.

216. Vitetta, E.S. and Thorpe, P.E. Immunotoxins containing ricin or its A chain. Sem. Cell Biol. 2:47-58, 1991.

217. Vulliemoz, Y., Verosky, M. and Triner, L. Effect of halothane on myocardial cyclic AMP and cyclic GMP content of mice. J. Pharmacol. Exp. Ther. 236:181-185, 1986.

218. Waalkes, T.P., Weissbach, H., Boricevich, J., and Udenfriend, S. Further studies on release of serotonin and histamine during anaphylaxis in the rabbit. Proc. Soc. Exp. Biol. Med. 95:479-482, 1957.

219. Waalkes, T.P., Weissbach, H., Boricevich, J., and Udenfriend, S. Serotonin and histamine release during anaphylaxis in the rabbit. J. Clin. Invest. 36:1115-1120, 1957.

220. Walters, D.M., Bostian, K.A., Creasia, D.A. Effects of vaccination and therapeutic agents on pulmonary inflammation induced by inhaled ricin aerosol. Toxicologist 13:Abstract 868, 1993.

221. Wannemacher Jr., R.W., Hewetson, J.F., Lemley, P.V., Poli, M.A., Interman, R.E., Thompson, W.L., and Franz, D.R. Comparison of detection of ricin in castor bean extracts by bioassays, immunoassays, and chemistry procedures, Recent Advances in Toxicol Res 3:108-119, 1992.

222. Wannemacher Jr., R.W., Thompson, W.L., Dinterman, R.E. and Grillo, F.G. In vivo treatment of ricin intoxication. The Toxicologist ll:Abstract 498, l991.

223. Wannemacher Jr., R.W., Thompson WL, and Dinterman RE. Use of lactulose for prophylaxis/treatment of ricin (RCA_{60}) intoxication. FASEB J 5:Abstract 2625, 1991.

224. Wei, C. H. and Koh, C. Crystallographic characterization of a principal non-toxic lectin from seeds of Ricinus communis. J. Mol. Biol. 123:707-711, 1978.

225. Wellner, R.B., Pless, D.D., and Thompson, W.L. Characterization of 3'-azido-3'-deoxythymidine inhibition of ricin and Pseudomonas exotoxin A toxicity in CHO and Vero cells. J Cell Physiol 159:495-505,1994.

226. Wikman-Coffelt, J., Stefenelli, T., Wu, S.T., Parmley, W.W., and Jasmin, G. $[Ca^{2+}]_i$ transients in the cardiomyopathic hamster heart. Circ Res 68:45-51, 1991a.

227. Wikman-Coffelt, J., Stefenelli, T., Wu, S.T., Parmley, W.W., and Mason, D.T. Angiotensin II and phorbol esters depress cardiac performance and decrease diastolic and systolic $[Ca^{2+}]_i$ in isolated perfused rat hearts. Am Heart J 122:786-794, 1991b.

228. Wiley, R.G., Blessing, W.W., and Reis, D.J. Suicide transport-destruction of neurons by retrograde transport of ricin, abrin and modeccin. Science 216:889-890, 1982.

229. Winkler, U., Gottstein, C., Schon, G., Kapp, U., Wolf, J., Hansmann, M.L., Bohlen, H., Thorpe, P., Diehl, V., and Engert, A. Successful treatment of disseminated human Hodgkin's disease in SCID mice with deglycosylated ricin A-chain immunotoxins. Blood 83:466-475, 1994.

230. Wrenn, S., Homcy, C. and Haber, E. Evidence for the a-adrenergic receptor regulation of membrane-bound catechol-O-methyltransferase activity in myocardium. J. Biol. Chem. 254:5708-5712, 1979.

231. Wurtman, R.J. and Axelrod, J. A sensitive and specific assay for the estimation of monoamine oxidase. Biochem. Pharmacol. 12:1439- 1440, 1963.

232. Yoshida, T., Chen, C., Zhang, M. and Wu, H.C. Brefeldin A which disrupts the membrane recycling between ER and Golgi reduces cytotoxicity of ricin in vero and CHO cells. Cell Biology Meeting, November, Abstract 1118, 1989.

233. Yoshida, T., Chen, C., Ahang, M., and Wu H.C. Disruption of the Golgi apparatus by brefeldin A inhibits the cytotoxicity of ricin, modeccin and Pseudomonas toxin. Exp. Cell Res. 192:389-395, 1991.

234. Youle, R.J. and Huang, A.H.C. Protein bodies from the endosperm of castor beans. Subfractionation, protein components, lectins, and changes during germination. Plant Physiol 58:703-711, 1976.

235. Zentz, C., Frenoy, J.P., and Bourrillon, R. Binding of galactose and lactose to ricin. Equilibrium studies. Biochem Biophys Acta 536:18-21, 1978.

236. Zhang, L., Hsu, C-H. and Robinson, C.P. Effects of ricin administration to rabbits on the ability of their coronary arteries to contract and relax *in vitro*. Toxicol. Appl. Pharmacol. 129,(in press), 1994

237. Zhang, L., Mills, S., Basmadjian, G.P. and Robinson, C.P. Effects of ricin on blood flow in the rabbit. The Pharmacologist, 34:156, 1992.